

**NADPH oxidase (NOX) in the heart:**

**The interplay of NOX-derived ROS in  $\beta_1$ -integrin-induced survival signalling**

**Inauguraldissertation**

zur

Erlangung der Würde eines Doktors der Philosophie  
vorgelegt der  
Philosophisch-Naturwissenschaftlichen Fakultät  
der Universität Basel

von

**Berit Ines Rosc-Schlüter**

aus

**Österreich (AT)**

**Basel, 2011**

Genehmigt von der Philosophisch-Naturwissenschaftlichen Fakultät  
auf Antrag von

Dr. Gabriela M. Kuster

Prof. Dr. Markus A. Rüegg

Prof. Dr. Karl G Hofbauer

Basel, den 22. Februar 2011

Prof. Dr. Martin Spiess

# INDEX

1.) Abbreviations, acronyms and synonyms .....	6
2.) Abstract .....	9
3.) Introduction .....	10
3.1.) General Introduction .....	10
3.1.1) Classification of heart cells .....	12
3.1.2.) The cardiac interstitium .....	12
3.2.) Cell adhesion receptors .....	16
3.2.1.) Integrins .....	16
3.2.1.1.) Integrin structure .....	18
3.2.1.2.) Integrin signalling .....	20
3.2.1.3.) $\beta_1$ -integrin (CD29) .....	23
3.2.1.3.1.) $\beta_1$ integrin-induced survival and signalling .....	23
3.2.1.3.2.) Effects of CD29 engagement on JNK/SAPK .....	24
3.2.1.3.3.) Src family kinase and protein kinase C are likely upstream partners in CD29- induced survival signalling .....	25
3.3.) Reactive Oxygen Species (ROS) .....	26
3.4.) NADPH oxidase .....	29
3.5.) ROS, NOX and signalling .....	31
3.5.1.) ROS generation and NOX in cardiomyocytes .....	31
3.6.) Aims of this study .....	33
4.) Materials & Methods .....	34
4.1.) Reagents .....	34
4.2.) Cell culture .....	37
4.2.1.) Isolation of neonatal rat ventricular myocytes (NRVM) .....	37
4.2.2.) Isolation of neonatal mouse ventricular myocytes (NMVM) .....	38
4.2.3.) Cell line: H9C2 .....	38
4.2.3.1.) Defreezing .....	38
4.2.3.2.) Passaging .....	39
4.2.3.3.) Cryopreservation .....	39
4.3.) Treatments .....	40
4.4.) Viral infection .....	41
4.5.) Sample preparation .....	41
4.6.) Sodium dodecyl sulfate-polyacrylamide gelelectrophoresis (SDS-PAGE) .....	41

4.6.1.) Western blotting .....	41
4.6.2.) Stripping for reprobing.....	42
4.7.) Flow Cytometry .....	43
4.8.) RNA.....	44
4.8.1.) RNA isolation.....	44
4.8.2.) Deoxyribonuclease I (DNase I) treatment of RNA and cDNA synthesis .....	45
4.8.3.) Primers .....	45
4.8.4.) Gradient PCR .....	46
4.8.5.) Optimization of PCR cycles.....	47
4.8.6.) Semi-quantitative PCR.....	47
4.9.) Statistical analyses .....	48
5.) Results .....	49
5.1.) CD29 activation induces phosphorylation of ERK1/2 (Thr202/Tyr204), Akt (Ser473) and GSK-3 $\beta$ (Ser9) in newborn cardiomyocytes .....	49
5.2.) CD29 activation induces a time-dependent oxidative burst.....	51
5.2.1.) The CD29-induced oxidative burst is impaired by apocynin and diphenylene iodonium in cardiomyocytes .....	52
5.3.) CD29-induced pro-survival signalling is ROS-dependent .....	53
5.4.) CD29-induced pro-survival signalling is inhibited by apocynin and DPI .....	55
5.5.) gp91 <sup>phox</sup> - and p47 <sup>phox</sup> -deficient cardiomyocytes show loss of $\alpha$ -CD29-induced pro-survival signals.....	56
5.6.) The CD29-induced oxidative burst is impaired in p47 <sup>phox</sup> LOF, but not in NOX2 knock-out cardiomyocytes .....	58
5.7.) Effects of CD29 activation on SAPK/JNK phosphorylation.....	60
5.7.1.) Localization of SAPK/JNK1/2 in CD29-induced signalling.....	60
5.7.2.) Effect of JNK inhibition on GSK-3 $\beta$ phosphorylation.....	61
5.7.3.) Effect of apocynin and the flavoenzyme inhibitor DPI on SAPK/JNK phosphorylation .....	62
5.8.) Src tyrosine kinase is upstream of both MEK/ERK and PI3K/PKB .....	62
5.8.1.) Src family kinase is ROS dependent .....	65
5.8.2.) Protein kinase C inhibits CD29-induced GSK-3 $\beta$ phosphorylation.....	66
5.8.3.) Effects of the Src kinase inhibitor PP2, SU and PKC inhibitor on ROS generation .....	66
5.9.) Preliminary gene expression data.....	68
5.9.1.) NOX expression .....	68
5.9.2.) Expression patterns of stress responsive and anti-apoptotic genes .....	69
6.) Discussion.....	71
6.1.) CD29 and the oxidative burst.....	71

6.2.) CD29-induced signalling depends on NOX2-derived ROS .....	72
6.3.) Kinases potentially up- and downstream of NOX .....	75
6.4.) NOX and NOX-derived ROS in the heart .....	76
6.5.) The physiological relevance of NOX and ROS .....	79
6.6.) The spatiotemporal distribution and subcellular localization of NOX .....	80
6.7.) Conclusions .....	82
7.) References.....	83
8.) Acknowledgements.....	94
9.) Curriculum Vitae.....	96

# 1.) ABBREVIATIONS, ACRONYMS AND SYNONYMS

ANF: atrial natriuretic factor  
ang II: angiotensin II  
AMI: acute myocardial infarction  
aPKC: atypical PKC  
apo: apocynin  
AT<sub>1</sub>R: angiotensin II type 1 receptor  
Bcl-2: B-cell lymphoma 2  
BrdU: 5-bromo-2-deoxyuridine  
BSA: bovine serum albumin  
CAM: cell adhesion molecules  
cat: catalase  
CD29:  $\beta_1$ -integrin  
CHD: congenital heart disease  
CGD: chronic granulomatous disease  
CMC: cardiomyocytes  
CM-H<sub>2</sub>DCF-DA: dichlorodihydrofluorescein diacetate acetyl ester  
CVD: cardiovascular disease  
cPKC: Classical PKC  
CR: counter-receptors  
DCF: dihydrodichlorofluorescein diacetate  
ddH<sub>2</sub>O: double distilled H<sub>2</sub>O  
DDR2: discoidin domain receptor 2  
DEPC: diethylpyrocarbonate  
DMEM: Dulbecco's modified Eagle's medium  
DMSO: dimethylsulfoxide  
dNTP: deoxyribonucleotide  
DPI: diphenylene iodonium  
EC: endothelial cells  
EDTA: ethylenediaminetetraacetic acid  
ECL: enhanced chemiluminescence  
EGF(R): epidermal growth factor (receptor)  
ECM: extracellular matrix  
ER: endoplasmic reticulum  
FACS: Fluorescence Activated Cell Sorter  
FAK: focal adhesion kinase  
FB: fibroblasts  
FLIM: fluorescence lifetime imaging microscopy  
FN: fibronectin  
FRET: fluorescence resonance energy transfer  
FCS-DMEM: fetal calf serum- Dulbecco's modified Eagle's medium

GAPs: GTPase activating proteins  
GEFs: eight guanine-nucleotide exchange factors  
GPCR: G-protein coupled receptor  
GPX: glutathione peroxidase  
GR: glutathione reductase  
GSH/GSSG: glutathione  
GSK: glycogen synthase kinase  
HBSS: Hank's Buffered Salt Solution  
HO-1: haem oxygenase 1  
HRP: horseradish peroxidase  
Ig: immunoglobulin  
Ig-CAM: immunoglobulin-cell adhesion molecule  
IL-1 $\beta$ : interleukin-1  $\beta$   
ILK: integrin linked kinase  
JNK/SAPK: c Jun terminal kinase/stress activated protein kinase  
k.o.: knock-out  
LN: laminin  
LOF: loss of function  
LOX: lipoxygenase  
MAPKKKK: mitogen activated protein kinase kinase kinase kinase  
MAPK: mitogen-activated protein kinase  
MEK: mitogen-activated protein kinase/extracellular signal- regulated kinase  
MMP: metalloproteinases  
MHC: myosin heavy chain  
MIDAS: metal-ion-dependent adhesive site  
MnT: manganese(III) tetrakis(1-methyl-4-pyridyl)porphyrin  
MST2 Mammalian sterile 20-like kinase  
NF $\kappa$ B: nuclear factor kappa B  
NMVM: neonatal mouse ventricular myocytes  
NOX: NADPH oxidase  
NADP<sup>+</sup>/NADPH: nicotinamide adenine dinucleotide phosphate  
NGF: nerve growth factor  
nPKC: novel PKCs  
NRVM: neonatal rat ventricular myocytes  
PBS: phosphate buffered saline  
PKB: protein kinase B (also known as Akt)  
phox: phagocytic oxidase  
PI3K: phosphoinositide (PI)-3-OH kinase  
PKC: protein kinase C  
PKN: PKC related kinases  
PMA: phorbol myrestate acetate  
prf-DMEM: phenolred free- Dulbecco's modified Eagle's medium  
PSI: plexin-semaphorin-integrin domain  
redox: reduction/oxidation  
ROI: reactive oxygen intermediates  
ROS: reactive oxygen species

ROM: reactive oxygen mediators  
RT-PCR: reverse transcriptase-polymerase chain reaction  
PP2: pyrazolopyrimidin  
P/S: penicillin/streptomycin  
PVDF: polyvinylethen fluoride  
RSK: ribosomal S6 kinase  
S6K: S6 protein kinase  
SDS-PAGE sodiumdodecylsulfate-polyacrylamide gelelectrophoresis  
SF-DMEM: serum free- Dulbecco's modified Eagle's medium  
SH2: Src homology 2 domain  
SOD: superoxide dismutase  
SOO: superoxide oxidase  
SOR: superoxide reductase  
STAT3: signal transducer and activator of transcription 3  
SU: SU6656  
SU: subunit  
TAE: Tris-acetate EDTA  
TBS: Tris-buffered saline  
TBST: Tris-buffered saline and Tween 20  
TNF $\alpha$ : tumour necrosis factor  $\alpha$   
TM: transmembrane  
UV: ultraviolet  
VLA: very late antigen  
VSMC: vascular smooth muscle cells  
wt: wild-type



## 2.) ABSTRACT

Moderate levels of reactive oxygen species (ROS) act as mediators in cellular signalling processes. An important source of cardiac ROS is the highly expressed NADPH oxidase (NOX) family isoform NOX2. However, little is known about whether NOX-derived ROS are protective in the heart.

In this study we show that CD29 ( $\beta_1$ -integrin), a cell adhesion receptor highly expressed on cardiac muscle cells, induces NOX-dependent ROS. CD29 is known to be mandatory in cell growth and survival, and non-functional CD29 causes severe heart disease. We demonstrate that NOX2-derived ROS are essential for CD29-induced survival signalling, including the PI3K/PKB and MEK/ERK pathways. Furthermore, CD29-induced NOX-derived ROS are indispensable in the inhibition of the pro-apoptotic kinase GSK-3 $\beta$ , which we uncovered as a downstream target of both the ERK and PKB survival pathways in cardiac muscle cells. These findings clearly add to the growing body of evidence suggesting that moderate ROS levels are beneficial to the cell and highlight the crucial role of NOX2-derived ROS for cell survival in the heart.

## 3.) INTRODUCTION

### 3.1.) General Introduction

Cardiovascular disease (CVD) is the leading cause of death globally with estimated 17.1 million people dying per year according to the WHO<sup>1</sup>. About 80% of these deaths occurred in the developing countries [Smith Jr., Jackson et al. 2004]. CVD encompass hypertensive heart disease (due to high blood pressure), coronary heart disease (including myocardial infarction), valvular heart disease, congenital heart disease and idiopathic cardiomyopathies, cerebrovascular (including stroke) and peripheral-vascular diseases, most of which occur with no geographic, gender or socio-economic boundaries<sup>2</sup>.

The heart is the first organ formed in the embryo [Olson 2004]. It requires precise functionality and is responsible for blood circulation, thereby supplying the organism with the required oxygen and nutrients. Heart formation is closely regulated, and any subtle perturbation of this process might have devastating consequences such as congenital heart disease (CHD) [Srivastava and Olson 2000]. Here, cardiac malformation or abnormalities occur due to mutations in control genes involved in heart development. Besides the developing heart, also the adult heart is prone to malfunction. Conditions of haemodynamic stress such as myocardial infarction, hypertension, aortic stenosis and valvular dysfunction, cause injury of the heart. This leads to the development of adaptive (compensatory or pathological) hypertrophy (figure 1), which is characterized by an increase in myocardial mass (both cell size and interstitial content) [Dorn II and Diwan 2008; Hill and Olson 2008]. It results in ventricular wall thickening to compensate wall stress and to preserve contractile function. Continuing stress leads to ventricular dilation and failure, which may or may not be accompanied by arrhythmia. All these processes are accompanied with the death of cardiomyocytes.

---

<sup>1</sup> [http://www.who.int/cardiovascular\\_diseases](http://www.who.int/cardiovascular_diseases)

<sup>2</sup> [http://www.who.int/cardiovascular\\_diseases](http://www.who.int/cardiovascular_diseases)

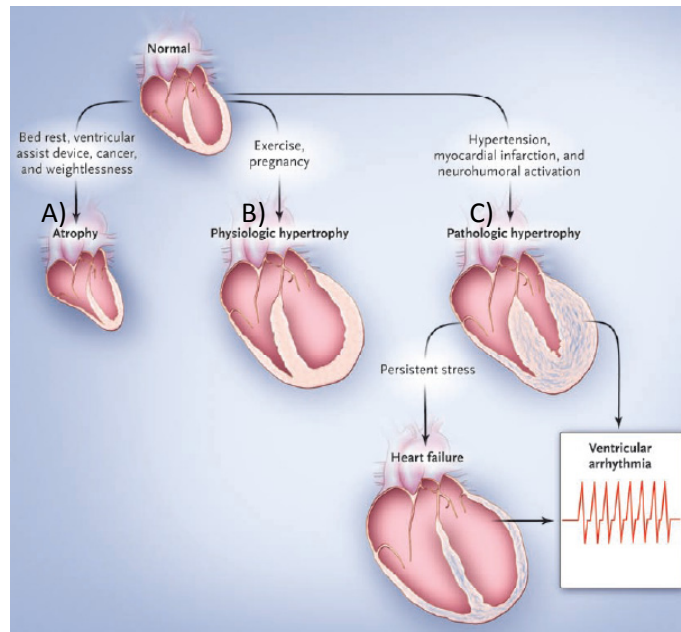


**Figure 1. Cardiac remodelling due to environmental stimuli.** The heart adapts (remodels) in response to environmental conditions causing the heart to shrink (A; Atrophy) or grow (B and C; hypertrophy). While normal remodelling occurs during exercise, pregnancy, and postnatal growth (physiological hypertrophy), pathologic remodelling due to neurohumoral activation, hypertension, and myocardial injury lead to pathologic hypertrophy. The initial adaptation in pathologic hypertrophy is also known as compensated (adaptive) hypertrophy which will develop to decompensated (maladaptive) hypertrophy in response to continuous stress. This adverse cardiac remodelling leads to heart failure. Figure was taken and adapted from [Hill and Olson 2008]

### **3.1.1) Classification of heart cells**

The main cell types in the myocardium (figure 2) are cardiomyocytes (CMC) and non-myocytes including cardiac fibroblasts (FB), vascular smooth muscle cells (VSMC) and endothelial cells (EC). In the past, CMC and FB were thought to account for 30% and 70% of the heart, respectively [Weber 1989; Baudino, Carver et al. 2006]. This view has changed in the last couple of years, because more specific markers are now available for the identification of FB. These markers include the discoidin domain receptor (DDR2, FB) or  $\alpha$ -MHC (CMC). DDR2, which belongs to the family of collagen-specific receptor tyrosine kinases, is capable of transmitting extracellular signals into the cell [Schlessinger 1997; Goldsmith, Hoffman et al. 2004]. Using FACS analysis, Banerjee and colleagues recently confirmed that the number and type of cardiac cells in the heart varies depending on the developmental stage, the physiological or pathophysiological conditions and also the species. Neonatal murine hearts (day 1) were composed of 10 % FB versus 70% CMC compared to neonatal rat hearts (day 1) with 30% FB and 62 % CMC [Banerjee, Yekkala et al. 2006; Banerjee, Fuseler et al. 2007]. Cardiac FB produce various proteins found in the extracellular matrix (ECM) including collagen fibres of type I and III, elastin, growth factors and matrix metalloproteinases (MMP) [Weber and Brilla 1991; MacKenna, Summerour et al. 2000; Spinale 2002; Bowers, Banerjee et al. 2010]. Type I collagen, which accounts for 85% of the collagen matrix, mainly forms thick fibres that have substantial strength; in contrast, type III collagen fibres (11%) that maintain structural integrity and distensibility of the 3-dimensional network are thin and resilient [Weber 1989].

### **3.1.2.) The cardiac interstitium**

The cardiac interstitium (extracellular matrix, ECM) consists of the collagen network that envelopes and connects muscle cells and the vasculature. A functional network of cells and their ECM is characterized by a) direct or b) indirect cell adhesions. In a) cells adhere to one another by cell-cell adhesion through so-called cell adhesion molecules (CAM). These cluster in cell junctions such as tight junctions, gap junctions or desmosomes. In case b) cells

connect to surrounding components of the ECM through plasma membrane adhesion receptors. These include polysaccharides and proteins, which are secretion products of the present cells [Lodish, Berk et al. 2008]. The cell adhesion receptor classes involved in group a) are cadherins and immunoglobulin (Ig)-superfamily CAM, both of which generate homophilic (self) interactions. The receptors of group b) include integrins which bind to multiadhesive ECM proteins such as laminin (LN), and selectins which bind to carbohydrates of the counter-receptors (glycoproteins) [Hynes 1999; Juliano 2002]. Collagens, proteoglycans and structural glycoproteins (also known as multiadhesive matrix proteins) are the three classes of ECM components distinguished in vertebrates. Collagens are highly abundant structural components forming fibres of type I, II and III, or sheets and networks like basement collagen type IV [Aumailley and Gayraud 1998]. The multiadhesive matrix proteins LN and fibronectin (FN), due to their structural flexibility, bind to various collagen-types, ECM or signalling proteins, polysaccharides, and cell adhesion receptors. By doing so, these matrix proteins control, regulate and organize cell adhesion processes, migration, and cell shape [Martin and Timpl 1987; Lodish, Berk et al. 2008]

Overall, the heart's interstitium (figure 2) can be subdivided into three parts: epimysium, perimysium, and endomysium. The epimysium surrounds the entire muscle and is located along the epicardial and endocardial surfaces. The perimysial collagen fibres cover groups of cardiomyocytes, organized in laminae of two to five myocytes in thickness. Further, permysial strands are located between muscle bundles to connect to adjacent collagen weaves. Endomysial collagen fibres which are formed from the perimysium either surround individual cardiomyocytes, or connect adjoining myocytes to another or to capillaries by perpendicular attachments [Weber 1989; Goldsmith and Borg 2002; Pope, Sands et al. 2008]. FBs lie near or between cardiomyocytes; connecting either with them or with one another, enmeshed in the connective collagen tissue network [Goldsmith, Hoffman et al. 2004].

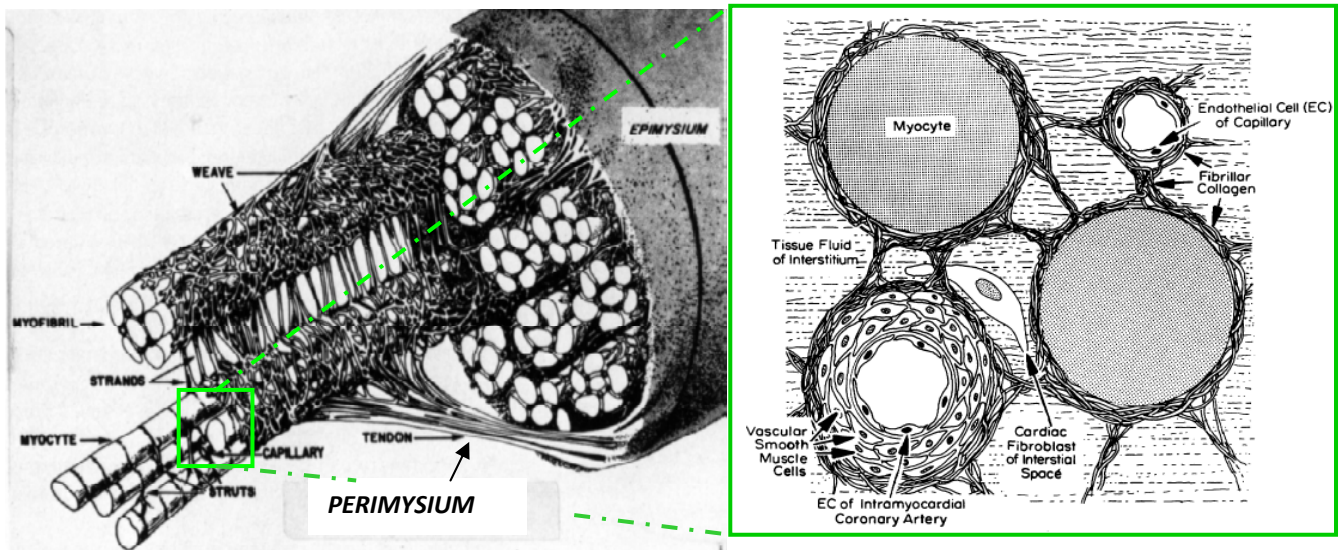


**Figure 2. The cardiac interstitium.** The interstitium connects cardiac myocytes, intramyocardial coronary arteries, arterioles, capillaries and veins and thereby provides a structure that is important for contractility and viability of the myocardium. Moreover, it also maintains defence mechanisms (against invading foreign proteins, bacteria or viruses), and facilitates the exchange of nutrients between myocytes and capillaries [Weber 1989]. The lateral surfaces of myocytes are connected by endomysial collagen fibres (struts), gap junctions and slender filaments [Robinson, Factor et al. 1987]. Struts lie between mammalian cardiomyocytes, myocytes and capillaries, myocytes and collagen fibres. They are mostly orientated perpendicular to the long axes of myocytes. The figure was adapted from Weber [Weber 1989] and [Weber and Brilla 1991].

These collagen fibres fulfil various functions:

*“1) they provide a scaffolding that supports muscle cells and blood vessels; 2) they act as lateral connections between cells and muscle bundles to govern architecture while coordinating the delivery of force, generated by myocytes, to the ventricular chamber, and 3) their respective tensile strength and resilience are important determinants of diastolic and systolic myocardial stiffness and serve to resist myocardial deformation, maintain shape and wall thickness and prevent ventricular aneurysm and rupture”* [Weber 1989].

However, if the physiological conditions of heart cells change, the form and function of the ECM has to adapt, a process which known as remodelling [Weber, Sun et al. 1994; Goldsmith and Borg 2002]. It has become evident that not only cardiac myocytes and the coronary

vasculature are mandatory for the contractility and viability of the myocardium, but so is the ECM, too. Alterations of the interstitium results in loss of normal structural support and changes in myocardial geometry and function [Spinale 2002], which plays an important role in the progression to heart failure [Miner and Miller 2006]. Indeed, Gustafsson *et al.* (2003) pointed out that:

*“changes in the ECM components which are constantly being remodelled, degraded, and resynthesized locally, can modulate their interactions of a cell with its environment. The matrix also serves as a reservoir for many extracellular signalling molecules that control cell growth and differentiation. In addition the matrix provides a lattice through or on which cells can move, particularly in the early stage of tissue assembly. Morphogenesis - the stage of embryonic development in which tissues, organs and body parts are formed by cell movements and re-arrangements - also is critically dependent on cell matrix adhesion as well as cell-cell adhesion. [...] Disruption in cell-matrix or cell-cell interactions can have devastating consequences for the development of tissues, as is seen in the dramatic changes in the skeletal system of embryonic mice when the genes of either the two key ECM molecules, collagen II or perlecan, are inactivated.”* [Gustafsson, Aszódi *et al.* 2003]

Depletion of hormones or growth factors from the ECM leads to apoptosis [Meredith, Fazeli *et al.* 1993; Schwartz 2010]. When mouse strains with null mutations in the FN gene (which is recessive and embryonic-lethal) were intercrossed, the resulting strains had embryonic defects such as a deficit in mesoderm or neuronal tube formation [George, George-Labouesse *et al.* 1993], as well as defects in heart and blood vessel development. It was observed that embryos developed either no primitive hearts or abnormal hearts, dependent on the genetic background of the mice used to create FN null strains. [George, Baldwin *et al.* 1997]. These and further studies (reviewed by Hynes 1996) clearly show that *per se*, the ECM represents a survival signal [Hynes 1996]. Furthermore, disruption of the connection between cells and the ECM leads to cell detachment-induced apoptosis (also referred to as anoikis) [Frisch and Francis 1994].

### **3.2.) Cell adhesion receptors**

Receptors that maintain connections a) among cells and b) between cells and the ECM represent the large family of cell adhesion receptors. Integrins, cadherins, selectins and IgG superfamily (immunoglobulin-cell adhesion molecules: Ig-CAMs) are members of this family (figure 3) [Aplin, Howe et al. 1998; Hynes 1999; Juliano 2002]. Among these, integrins represent the major receptor group in the ECM in cardiomyocytes [Ross and Borg 2001]. Early studies in neonatal rat ventricular myocytes (NRVM) showed a tight binding of this cell type to collagen IV, LN, collagen I and III, all of which are found in the interstitium [Borg, Rubin et al. 1984].

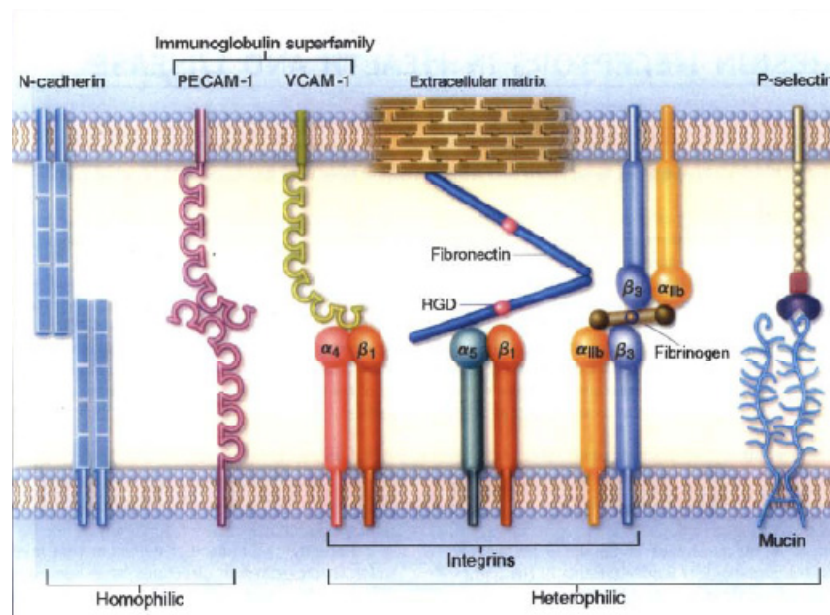


**Figure 3. Families of cell adhesion receptors associated with their typical binding partner.** While integrins normally bind components of the ECM, they can also bind counter-receptors (CR) such as Ig CAMs or selectins. Figure taken from [Rojas and Ahmed 1999].

#### **3.2.1.) Integrins**

Integrins have been identified from sponges to chicken to mammals, but are absent from plants, fungi or bacteria [Hynes and Zhao 2000; Takada, Ye et al. 2007]. In mammals, connections to ECM components are essential for the survival and the structural and



functional integrity of CMC [Meredith, Fazeli et al. 1993; Hynes 1996]. In particular, these transmembrane cell surface adhesion receptors bind ECM proteins such as LN, collagen and FN [Hynes 1992; Ross and Borg 2001]. Integrins are heterodimeric transmembrane receptors composed of different  $\alpha$ - and  $\beta$ -subunits, which can form 24 distinct receptors; these receptors are in a bent conformation in quiescent and in an extended conformation in activated adherent cells [Askari, Tynan et al. 2010].

Based on their binding affinity, the integrin family can be grouped (figure 4, for an informative review see [Barczyk, Carracedo et al. 2010]) into RGD-binding, LN-binding, collagen binding-receptors, and leukocyte specific receptors [Hynes 1987; Hynes 2002]. As their name implies, the RGD binding group binds to the short tripeptide sequence Arg-Gly-Asp, one or more of which are found in many ECM proteins such as FN, fibrinogen or vitronectin [Hynes 1987; Hynes 2002]. Although many integrin ligands have a RGD binding sequence, not all of them are actually involved in binding.

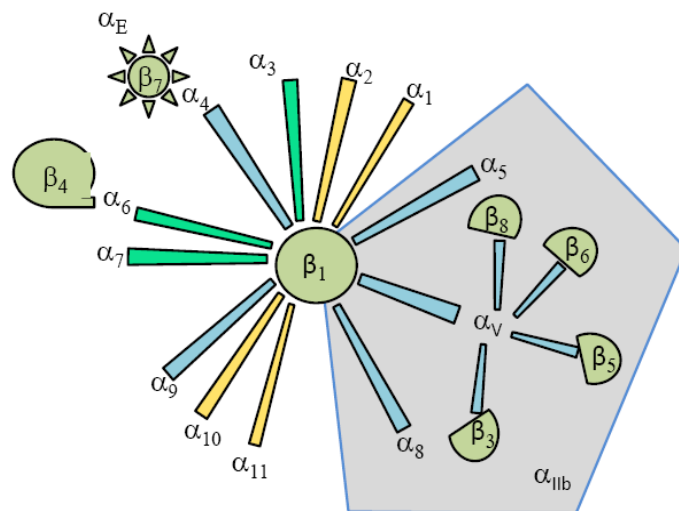


**Figure 4. Integrin subunits and their binding partners.** The coloured  $\alpha$  bars represent the ligand specificity: where  $\alpha_3$ ,  $\alpha_6$  and  $\alpha_7$  represent LN binding receptors (turquoise),  $\alpha_1$ ,  $\alpha_2$ ,  $\alpha_{10}$ , and  $\alpha_{11}$  are collagen binding (yellow),  $\alpha_5$ ,  $\alpha_v$  and  $\alpha_8$  (grey pentagon) represent RGD binding receptors.  $\beta_7$  (green sun) and  $\beta_2$  integrins (not depicted here; pairs with  $\alpha_L$ ,  $\alpha_M$ ,  $\alpha_X$ , and  $\alpha_D$ ) are restricted to leukocytes [Hynes 2002]. A given  $\beta$ -subunit (SU) binds several  $\alpha$  SUs, and some  $\alpha$ -SU can bind several  $\beta$ -SU.  $\alpha$  and  $\beta$  form non-covalently linked receptors.  $\beta_1$  integrin, for instance, pairs with 10 different  $\alpha$  SU, whereas  $\beta_3$  has  $\alpha_v$  as a partner and  $\alpha_v$  combines with 4 different  $\beta$  SU. Adapted from [Hynes 2002; Brakebusch, Hirsch et al. 1997]

Also, different RGD binding integrins have different affinities to the RGD sequence [Hynes 1992]. While  $\alpha_5\beta_1$ ,  $\alpha_{1b}\beta_3$  and  $\alpha_v\beta$  integrins recognize RGD,  $\alpha_{11b}\beta_3$  integrins additionally recognize the sequence KQAGDV in fibrinogen;  $\alpha_2\beta_1$  binds the sequence DGEA in type I collagen;  $\alpha_4\beta_1$  binds EILDV in alternatively spliced FN; and  $\alpha_v\beta_2$  binds GPRP in fibrinogen [Loike, Sodeik et al. 1991]. Ligand binding by integrins requires divalent cations [D'Souza, Ginsberg et al. 1991]. Collagen-binding integrins recognize the sequence GFP\*GER (where P\* stands for hydroxyproline) [Knight, Morton et al. 1998]. These findings clearly indicate that integrin binding to RGD sequences is not sufficient to explain the specificity of ligand binding. It is likely that integrin splice variants in the extracellular and cytosolic part add to the binding specificity of integrins (reviewed by Melker 1999). For example, the cytoplasmic domain is essential in integrin heterodimerization and membrane expression [de Melker and Sonnenberg 1999]. Five splice variants of  $\beta_1$  integrin were found in the cytoplasmic domain ( $\beta_{1A}$ ,  $\beta_{1B}$ ,  $\beta_{1C}$ ,  $\beta_{1C-2}$  and  $\beta_{1D}$ ), which can activate different signalling cascades resulting in different cellular responses.  $\beta_{1A}$  and  $\beta_{1D}$  splice variants differ only by 13 amino acids in their cytoplasmic domain.  $\beta_{1D}$  for instance is specifically found in adult skeletal muscle and strongly expressed in the heart (adult and postnatal) [Van der Flier, Gaspar et al. 1997].  $\beta_{1D}$  integrins show a high affinity to the actin cytoskeleton and extracellular ligands [de Melker and Sonnenberg 1999].  $\beta_{1A}$  is downregulated during myoblast differentiation as compared to  $\beta_{1D}$  and binds actin less tightly than  $\beta_{1D}$ . Baudoin (1998) reported that  $\beta_{1A}$  is more efficient in transducing mechanical signals to the cell than  $\beta_{1D}$  [Baudoin, Goumans et al. 1998].

### ***3.2.1.1.) Integrin structure***

Both,  $\alpha$  and  $\beta$  subunits are comprised of a large extracellular domain (700-1100 amino acids) followed by a hydrophobic membrane spanning part and a short cytosolic domain (20-60 amino acids) [Ruoslahti and Pierschbacher 1987]. Integrins bind to an array of distinct proteins [McDonald 1989; Plow, Haas et al. 2000; Van der Flier and Sonnenberg 2001], and can be bound by anti-integrin antibodies [Diamond and Springer 1994]. The  $\alpha$ - and  $\beta$ -integrin subunits consist of several characteristic domains as illustrated in figure 5A and B. The extracellular part of the integrin subunits can be divided into "head" and "leg" parts. The "head" of  $\alpha$  integrin is composed of two domains: the  $\beta$  propeller domain, and in some cases

an  $\alpha$ A domain. This  $\alpha$ A domain is also known as I domain and is located between the  $\beta$ -sheets 2 and 3 of the  $\beta$  propeller domain; it contains a metal-ion-dependent adhesive site (MIDAS, occupied by a divalent cation) for binding of negatively charged ligand residues. The “leg” domain consists of the Ig-like “thigh” domain, the “knee” domain (genu) and 2  $\beta$  sandwiches known as “calf” domains.

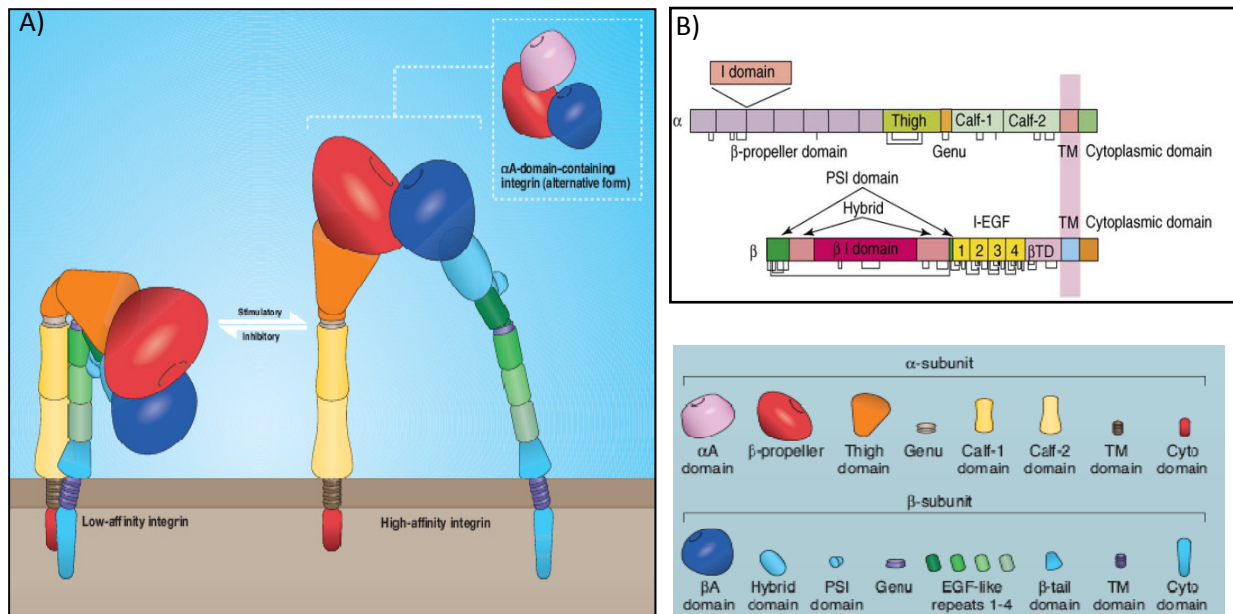


**Figure 5. Common integrin structure with organized regions.** TM: transmembrane domain; cyto: cytoplasmic domain; genu: knee; PSI: Plexin-semaphorin-integrin domain. The head part contains the I domain or van Willebrand factor A domain, which is also referred to as A domain. Figures were taken from [Luo and Springer 2006; Byron, Humphries et al. 2009].

The  $\beta$ -integrin subunit contains 11 domains which can be also subdivided into “head” and “leg”. The head is composed of the  $\beta$ A domain (or  $\beta$  I-like domain) which is inserted in the hybrid domain and the PSI domain. Additionally the top face of the  $\beta$ A domain has also a MIDAS site. The leg of  $\beta$  integrin is comprised of a hybrid, a PSI and a knee domain, followed by four EGF-like domains and a  $\beta$  tail domain.

The RGD binding site is located between the  $\beta$  propeller of the  $\alpha$  subunit and the A domain of the  $\beta$  subunit [Shimaoka, Takagi et al. 2002; Luo and Springer 2006; Arnaout, Goodman et al. 2007; Takada, Ye et al. 2007; Byron, Humphries et al. 2009]. Activation of integrins and

their associated conformational changes have been studied extensively. Several models have been developed to describe signalling, including data from the investigation of the localization of integrin transmembrane and cytoplasmic domains [Xiong, Stehle et al. 2003; Arnaout, Goodman et al. 2007].

Integrins are not constitutively active, persisting in an inactive, bent conformation. It is hypothesised that this closed conformation embodies a low affinity state for ligand binding [Arnaout, Goodman et al. 2007]. The knee region keeps the integrin receptors of quiescent, non-activated cells in the bent conformation. Upon activation, the conformation of the receptor changes and the “leg” swings open into a state primed for activation [Luo and Springer 2006], and then an activated, extended state with an open headpiece, finally resulting in integrin clustering with high apparent affinity (or avidity) [Rocco, Rosano et al. 2008; Byron, Humphries et al. 2009]. Some models imply a separation of the transmembrane and cytosolic domains [Wegener and Campbell 2008], whereas Rocco *et al.* (2009) proposes that tail domains stay in contact [Rocco, Rosano et al. 2008] during inside-out signalling, whereas outside-in signalling may be independent of this separation.

Recently, Askari *et al.* (2010) showed that  $\alpha_5\beta_1$  integrin can be directly activated at focal adhesions of adherent cells in response to binding of stimulating anti- $\beta_1$  and anti- $\alpha_5$  monoclonal antibodies directed to several epitopes of the extracellular part of a mutated  $\alpha_5\beta_1$  integrin receptor [Askari, Tynan et al. 2010]. In that study, the integrin  $\alpha$ -subunit and  $\beta$ -subunit were locked together through a disulphide bond. By use of the FLIM (fluorescence lifetime imaging microscopy) based FRET (fluorescence resonance energy transfer) technology,  $\alpha_5\beta_1$  conformational changes were observed in human foreskin FB.

### ***3.2.1.2.) Integrin signalling***

Integrins can signal in two directions: a) from the outside into the cell (outside-in signalling) and b) from inside to the outside (inside-out signalling). They signal in combination with growth factor receptors, cytokine receptors or G-protein coupled receptors, and in an array

of different cell types, including cardiac cells [Arnaout, Mahalingam et al. 2005]. Outside-in signalling happens synergistically with co-stimulators, ligands, and/or cations ( $Mn^{2+}$ ), however, it can be also triggered experimentally by so-called activating antibodies [Bazzoni, Ma et al. 1998]. Since cytosolic integrin domains do not have kinase activity, they have to recruit functional proteins to focal adhesion sites in order for signalling to occur [Giancotti and Ruoslahti 1999]. Integrin signalling is a complex matter, because these receptors bind to an array of proteins and lipids. Zaidel-Bar *et al.* (2007) illustrated the complex network of integrins and their interconnected partners [Zaidel-Bar, Itzkovitz et al. 2007] derived from published experimental studies from different cell types. Their model revealed a signalling interaction network of 690 links of which 213 were activating and 98 were inhibitory (figure 6).

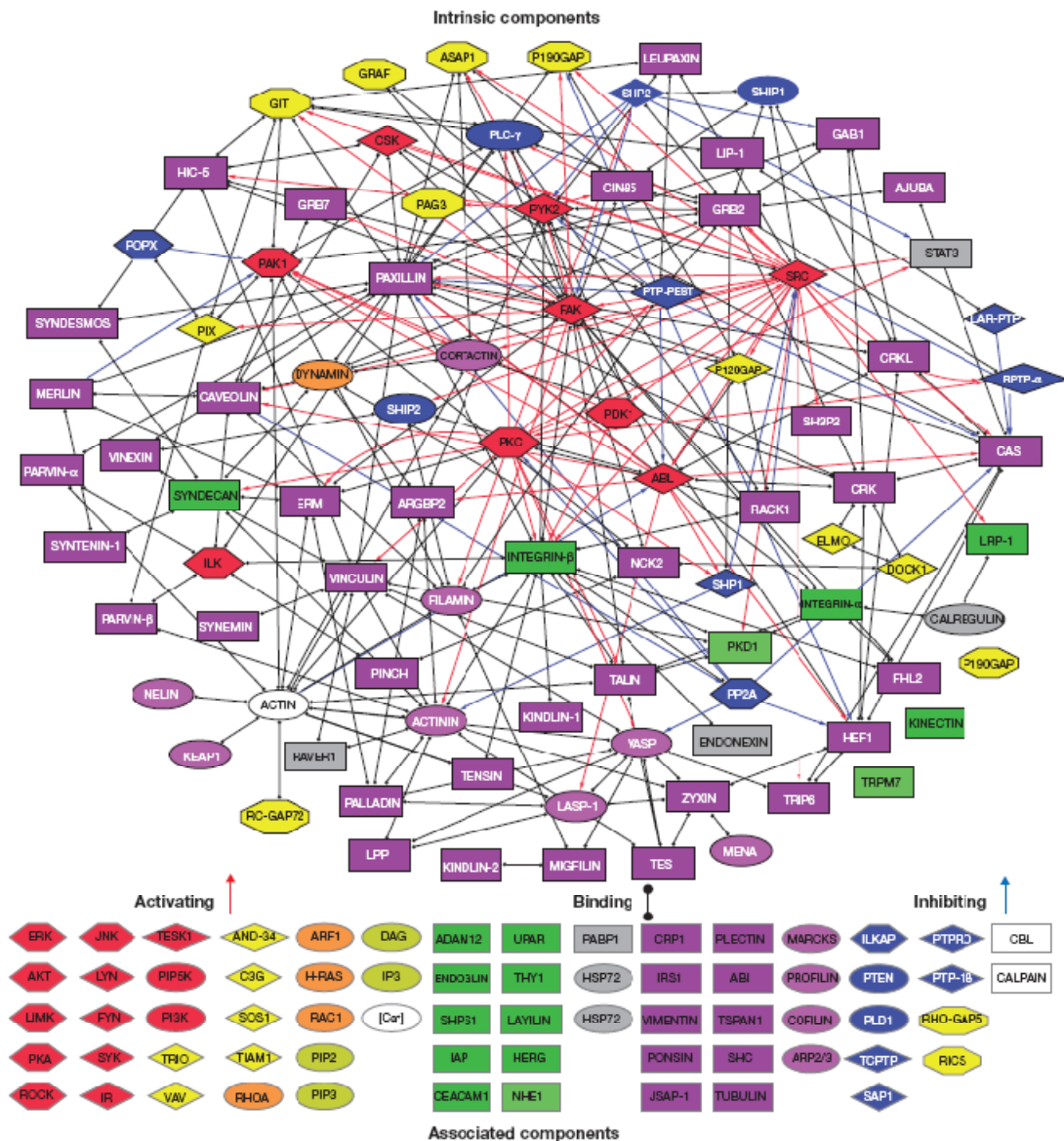


**Figure 6. The integrin signalling network.** This network consists of 156 components that can be divided into different functional groups: 25 adaptor proteins, 24 cytoskeletal proteins, nine actin binding proteins, ten serine/threonine protein kinases, three serine/threonine phosphatases, nine tyrosine phosphatases, eight tyrosine kinases, eight GTPase activating proteins (GAPs), eight guanine-nucleotide exchange factors (GEFs) seven transmembrane receptors, six adhesion proteins, five GTPases and 32 others. Taken from Zaidel-Bar *et al.* (2007).

Integrins bind to cytoskeletal proteins including talin, paxilin and  $\alpha$ -actinin, vinculin, and actin microfilaments, predominantly via their cytosolic  $\beta$ -domain [Clark and Brugge 1995; Giancotti and Ruoslahti 1999]. These scaffold proteins provide stability in cell adhesion, morphology and motility of the cell, and likewise tether signalling kinases. Activation of

various kinases upon integrin engagement has been reported. Among the first kinases that are recruited are the tyrosine kinase Src, focal adhesion kinase (FAK), and integrin linked kinase (ILK). The latter was shown to bind to the cytosolic  $\beta$  integrin domain, activating GSK-3 $\beta$ , mTOR or NF $\kappa$ B as substrates, besides other kinases [Legate, Montañez et al. 2006]. But also serine/threonine kinase families (such as protein kinase C, PKC and MAPK) are recruited [Clark and Brugge 1995]. The lipid kinase phosphoinositide (PI)-3-OH kinase (PI3K) phosphorylates its substrate, the protein kinase B (PKB, also known as Akt) either in a FAK-Src dependent or independent manner [Giancotti 1997]. The latter case was described by Velling (2004) in a  $\beta_{1B}$  integrin transfected cell line (GD25) that lacks endogenous  $\beta_1$  integrin expression [Velling, Nilsson et al. 2004].

### **3.2.1.3.) $\beta_1$ -integrin (CD29)**

#### 3.2.1.3.1.) $\beta_1$ integrin-induced survival and signalling

The  $\beta_1$  integrin subunit (also known as CD29, very late antigen or VLA in humans) [Hemler, Huang et al. 1987; Hynes 1987], represents the most abundant isoform expressed in foetal and postnatal rat heart [Carver, Price et al. 1994; de Melker and Sonnenberg 1999], where it can dimerize with different  $\alpha$  subunits [Ross 2002]. The expression of the  $\alpha$  integrins is altered in neonatal development and hypertrophied hearts [Terracio, Rubin et al. 1991; Ross 2002]. Neonatal cardiomyocytes mainly interact with the subunits  $\alpha_1$ ,  $\alpha_3$ ,  $\alpha_5$  and  $\alpha_6$  [Terracio, Rubin et al. 1991; Maitra, Flink et al. 2000; Ross 2002]. Integrin expression and signalling are of tremendous importance to myocyte growth and survival [Kuppuswamy 2002], as well as in cardiomyocyte remodelling [Ross 2002].

For instance, a Chinese ovary hamster cell line that expressed  $\alpha_5\beta_1$  integrin was protected from apoptosis by Bcl-2 upregulation [Zhang, Vuori et al. 1995]. Lei *et al.* (2008) showed that endothelial CD29 expression is needed for postnatal vascular remodelling. Homozygous deletion of CD29 in the endothelium led to embryonic death whereas heterozygous endothelial CD29 deletion did not diminish foetal or postnatal survival but reduced CD29 expression in endothelial cells of adult mice [Lei, Liu et al. 2008]. Deletions of CD29 are embryonic lethal [Fässler and Meyer 1995; Fässler, Rohwedel et al. 1996; Keller, Shai et al.

2001]. Moreover, cardiac-specific knock-outs or inhibition lead to disturbed cardiac function, impaired cardiac differentiation, fibrosis and heart failure [Fässler and Meyer 1995; Shai, Harpf et al. 2002]. Deficiency in CD29 is reported to cause increased myocardial dysfunction after myocardial infarction in mice [Krishnamurthy, Subramanian et al. 2006].

*In vitro*, CD29 is directly activated by the binding of ECM components or activating antibodies [Diamond and Springer 1994], which causes the rearrangement of the actin cytoskeleton and recruitment of signalling kinases such as FAK, PI3K, PKB, MEK1/2, ERK1/2 or talin to the cytosolic part of the integrin receptor [Hynes 1992; Clark and Brugge 1995]. Besides activating anti-CD29 antibodies also inhibiting anti-CD29 antibodies were developed [Byron, Humphries et al. 2009]. Through activation of above signalling kinases, CD29 participates in the regulation of CMC growth and survival [Ross and Borg 2001]. Specifically, CD29 mediates  $\alpha$ -adrenergic receptor-stimulated hypertrophy [Ross, Pham et al. 1998] and inhibits  $\beta$ -adrenergic receptor-induced apoptosis [Communal, Singh et al. 2003; Menon, Singh et al. 2005].

#### 3.2.1.3.2.) Effects of CD29 engagement on JNK/SAPK

The JNK (c-Jun N-terminal kinase) /SAPK (stress-activated protein kinase) belongs to the MAPK (mitogen-activated protein kinase) superfamily, besides ERK and the p38 MAP kinases [Davis 2000]. Stress and inflammatory signals activate JNK and p38 MAPK. The JNK family includes; JNK1 (four isoforms), JNK2 (four isoforms), and JNK3 (two isoforms). JNK has been implicated in both survival [Dougherty, Kubasiak et al. 2002; Scuteri, Galimberti et al. 2010] and death pathways [Lin 2002]. Its involvement in cell survival is context-dependent, varying according to stimulus, tissue and environmental factors. It has been observed that persistent but not transient activation of JNK is linked to apoptosis [Andreka, Zang et al. 2001; Lin 2002]. ROS have been assumed to cause sensitive and permanent activation of JNK [Nakano, Nakajima et al. 2006]. Reinhard *et al.* (1997) showed that TNF $\alpha$ -induced JNK activation occurred independently of the death pathway [Reinhard, Shamon et al. 1997]. Whereas insulin-like growth factor protects human neuroblastoma cells from apoptosis through the PI3K/PKB/GSK-3 $\beta$  pathway by inhibiting JNK [Wang, Yang et al. 2010]; integrin induced



survival signalling was shown to be mediated by FAK and JNK activation in rabbit synovial FB [Almeida, Ilić et al. 2000].

#### 3.2.1.3.3.) Src family kinase and protein kinase C are likely upstream partners in CD29-induced survival signalling

Integrin engagement results in the recruitment of several protein kinases to propagate signals, including upstream protein tyrosine kinases such as Src (Src family kinases), FAK, as well as a serine/threonine kinase ILK [Giancotti 1997; Giancotti and Ruoslahti 1999]. Upon auto-phosphorylation of FAK at residue Tyr397, a binding site for Src's Src homology 2 domain (SH2) is created in chicken embryo cells [Schaller, Hildebrand et al. 1994]. Based on reports that inhibition of PI3K by Wortmannin or Ly inhibited phosphorylation of the regulatory NADPH oxidase (NOX) subunit p47<sup>phox</sup>, and hence suppressing NOX activity in neutrophils [Ding, Vlahos et al. 1995], Chen *et al.* (2003) showed that PKB is capable of activating and phosphorylating p47<sup>phox</sup>; it therefore regulates human gp91<sup>phox</sup> [Chen, Powell et al. 2003]. Beside PKB and ERK [Dewas, Fay et al. 2000], also PKC, specifically PKCζ, has been implicated in the independent activation of the NADPH oxidase by phosphorylation of p47<sup>phox</sup>, [Dang, Fontayne et al. 2001]. and gp91<sup>phox</sup> [Raad, Paclet et al. 2009]. Protein kinases C can be subdivided into 4 distinct groups, namely atypical, classical, novel, and PKC related kinases. PKCζ belongs to the subclass of atypical or aPKC, together with PKCι (also known as PKCλ in mice) [Rosse, Linch et al. 2010]. Classical PKC (cPKC) proteins including PKCα, PKCβ, PKCγ, novel PKCs (nPKC) PKCδ, PKCε, PKCη, PKCθ and PKC related kinases (PKN) include PKN1, PKN2 and PKN3. It is of note that Src kinase interacts with PKCζ in nerve growth factor (NGF)-stimulated PC12 cells (a cell line derived from a pheochromocytoma - a neuroendocrine tumour - of the rat adrenal medulla) [Greene and Tischler 1976]. Tyrosine residues of PKCζ were shown to be only phosphorylated in the presence of Src kinase in PC12 cells [Seibenhener, Roehm et al. 1999]. Also, PKCδ was shown to be a target of Src tyrosine kinase phosphorylation [Gschwendt, Kielbasse et al. 1994]. In 2009, Gupte and co-workers showed that Src kinase mediated PKC-induced NOX2 activation and peroxide production upon phorbol 12, 13-butyrate treatment in coronary artery smooth muscle cells [Gupte, Kaminski et al. 2009]. Moreover, intracellular lipoxygenase (LOX)-derived ROS activated Src kinase during cell adhesion [Giannoni, Buricchi et al. 2005] upstream of

epidermal growth factor receptor (EGFR), ERK, PKB and Bim [Giannoni, Buricchi et al. 2008] in mouse embryonic FB (NIH-3T3 cell line).

### 3.3.) Reactive Oxygen Species (ROS)

The term ROS or oxygen-derived species comprises radicals (superoxide anion,  $O_2^{\bullet-}$ ; hydroxyl radicals, etc.) and non-radicals (hydrogen peroxide,  $H_2O_2$ ). However, other terms, such as reactive oxygen intermediates (ROI) or reactive oxygen mediators (ROM), are also used in the literature. Radicals are defined as any molecule species having one or more unpaired electrons, and participating in one-electron transfer reactions [Halliwell and Gutteridge 1985]. ROS are generated as by-products in many metabolic processes, or as products of enzymatically catalysed processes.

The ground state of molecular oxygen ( $O_2$ ) bears two unpaired electrons with parallel spins in the  $2\pi^*$  molecular orbitals (figure 7). Two different singlet oxygen states exist, both of which contain two electrons of anti-parallel spins in their  $2\pi^*$  orbitals. These states of molecular oxygen easily interconvert by photoreactions or radiation. By transfer of one electron to singlet oxygen, superoxide anion ( $O_2^{\bullet-}$ ) is formed, a process that occurs in almost all aerobic cells [Halliwell and Gutteridge 1985].

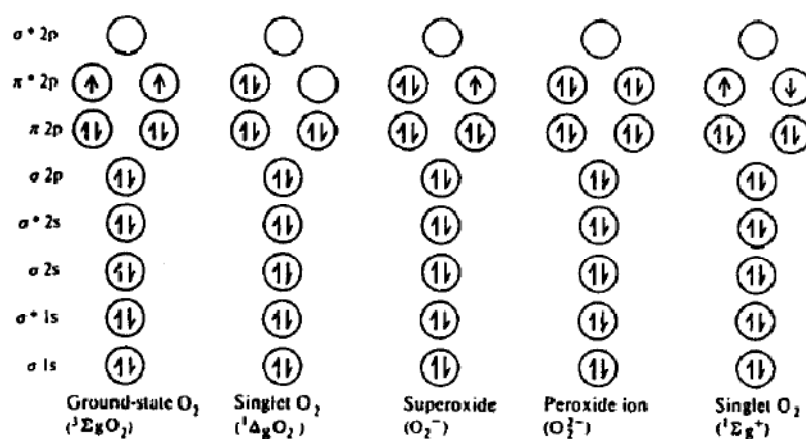


**Figure 7. Electron spins in molecular oxygen and oxygen radicals.** Taken from Halliwell & Gutteridge (1985).

For instance, superoxide is formed by one-electron transfer from the electron transport chains of mitochondria, chloroplasts or the endoplasmic reticulum (ER), but also by the respiratory (oxidative) burst oxidase in phagocytes [Hancock, Desikan et al. 2001] and xanthine oxidase [Halliwell and Gutteridge 1985].  $H_2O_2$  has no unpaired electrons and is either spontaneously formed at low pH or in a reaction catalysed by the enzyme superoxide dismutase (SOD), which was uncovered by McCord & Fridovich in 1969 [McCord and Fridovich 1969]. The enzyme catalase (cat) subsequently reduces  $H_2O_2$  to  $H_2O$ . Other detoxification mechanisms include glutathione peroxidase (GPX), as well as non enzymatic compounds like ascorbic acid,  $\alpha$ -tocopherol or glutathione [Dröge 2002].

Four classes of SOD enzymes can be distinguished, containing either divalent Cu/Zn ions or Mn, nickel (Ni) or iron (Fe) ions. In humans, three SOD subtypes can be distinguished, a) extracellular SOD (ecSOD or SOD3, homotetrameric and glycosylated, and heparin binding), b) intracellular, homodimeric SOD (Cu/Zn-SOD or SOD1, found in the cytosol, nucleolus, lysosomes and the intermembrane space of mitochondria) and c) homotetrameric SOD (Mn-SOD or SOD2, in the mitochondrial matrix) [Fridovich March 2009]. Mn-SOD obtains its main superoxide anions from the mitochondrial respiratory chain. Lack of Mn-SOD results in dilated cardiomyopathy and neonatal lethality in knock-out mice [Matés 2000]. TNF application in mice “selectively induces Mn-SOD expression and human Mn-SOD expressed in transgenic mice protects against oxygen induced pulmonary injury and adriamycin-induced cardiac toxicity” [Matés 2000]. Molecular oxygen induces SOD in prokaryotes such as *Escherichia coli* and *Streptococcus faecalis*, as well as in eukaryotes [Gregory and Fridovich 1973; Gregory, Goscin et al. 1974]. Notably, Cu/Zn-SOD can be inactivated by  $H_2O_2$ , due to reduction/oxidation processes of the cofactor  $Cu^{2+}$  at the active site of the enzyme [Liochev and Fridovich 2002]. Aside from having a dismutase activity, Cu/Zn-SOD also displays superoxide reductase (SOR) and a superoxide oxidase (SOO) activities [Liochev and Fridovich 2000]. By contrast, human Mn-SOD does not seem to have any additional activities [Liochev and Fridovich 2000].

Although oxygen is inherently toxic to aerobic organisms, efficient systems have evolved to handle oxygen in living systems ranging from bacteria to mammals. Irrespective of ROS-induced toxic effects including lipid-peroxidation, DNA damage (strand breaks), and damaging effects on phospholipids, peptides, nucleotides, carbohydrates, also beneficial

effects of ROS have been investigated [Hensley, Robinson et al. 2000; Bochkov, Kadl et al. 2002; Blüml, Rosc et al. 2008]. High levels of ROS are damaging and are often referred to as oxidative stress, whereas low level of ROS may act as second messengers in redox signalling [Rhee 2006], activating signalling cascades that have been implicated in cell survival and growth. Sources of such ROS (figure 8) include xanthine oxidase, mitochondria, 5-lipoxygenase, and NOX, the latter having been implicated as an important source of cardiac ROS, generating ROS in a highly regulated fashion [Dröge 2002; Sawyer, Siwik et al. 2002; Lambeth 2004; Cave, Brewer et al. 2006; Chiarugi and Fiaschi 2007].

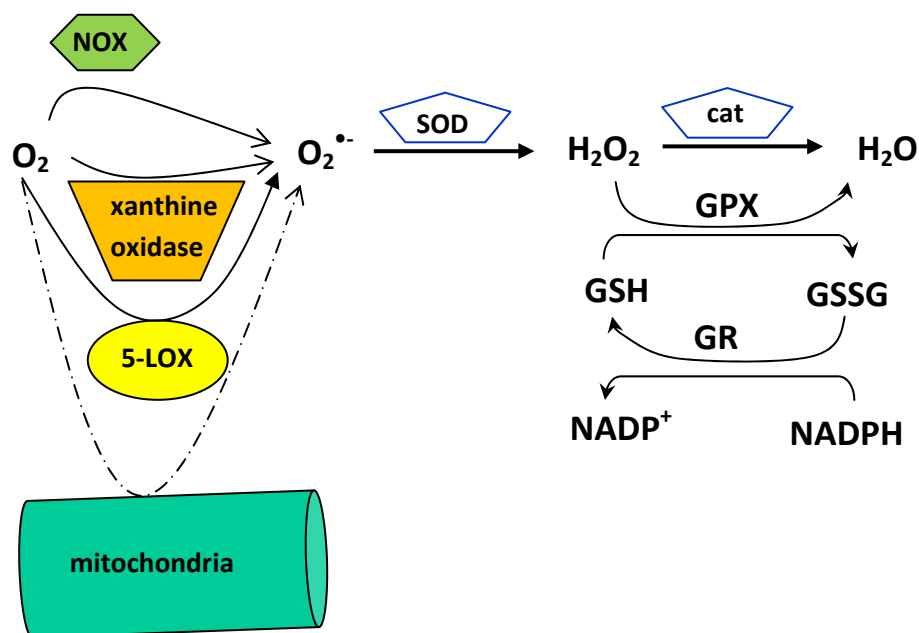


**Figure 8. Generation and clearance of ROS.** glutathione peroxidase (GPX), glutathione reductase (GR); 5-lipoxygenase (5-LOX). Adapted from Dröge (2002).

### 3.4.) NADPH oxidase

The NADPH oxidase is a transmembrane, multi-component protein that produces a surge of ROS upon stimulation [Petry, Weitnauer et al. 2010]. Initially, this enzyme was referred to as “O<sub>2</sub><sup>-</sup> generating enzyme” [Babior, Curnutte et al. 1976] or phox (phagocytic oxidase) [Babior 1999], but in the recent literature it is termed NOX (NADPH oxidase). NOX generates oxygen radicals radicals in what is termed a respiratory or oxidative burst. This phenomenon was first observed in phagocytes by Sbarra and Karnovsky [Sbarra and Karnovsky 1959; Karnovsky and Sbarra 1960]. The catalytic entity of NOX is comprised of gp91<sup>phox</sup> and p22<sup>phox</sup>. These are also referred to as cytochrome b<sub>558</sub>, and lie embedded in the plasma membrane [De Leo, Ulman et al. 1996; Vignais 2002]. p47<sup>phox</sup>, p67<sup>phox</sup>, p40<sup>phox</sup> and rac1/2 make up the regulatory subunits. Studies from patients suffering from inherent chronic granulomatous disease (CGD) showed their incapability to deal with bacterial infections due to loss of functional NOX. In most cases (66.6%), CGD could explained by a defective *CYBB* (gp91<sup>phox</sup>) gene, followed by defective *CYBA* (p22<sup>phox</sup>), *NCF1* (p47<sup>phox</sup>) or *NCF2* (p67<sup>phox</sup>) genes [Segal and Shatwell 1997]. NOX is not restricted to leukocytes; several NOX homologues have been identified in non-phagocytes including NOX1-5 and, DUOX1-2 [Geiszt and Leto 2004], and a NOX2 splice variant NOX2S [Heidari, Shah et al. 2004] in various tissues and species [Lambeth, Cheng et al. 2000; Geiszt and Leto 2004; Kawahara, Quinn et al. 2007]. In the heart, NOX2 has been reported as the predominant isoform, but also NOX4 and NOX1 have been shown to be expressed in rat CMC [Hingtgen, Tian et al. 2006]. NOX2 and NOX1 both depend on regulatory subunits such as the NOX organizers p47<sup>phox</sup> (for NOX2) and its equivalent NOXO1 (for NOX1). NOX4 is active even in the absence of regulatory subunits, as depicted in figure 9 [Brown and Griendling 2009].

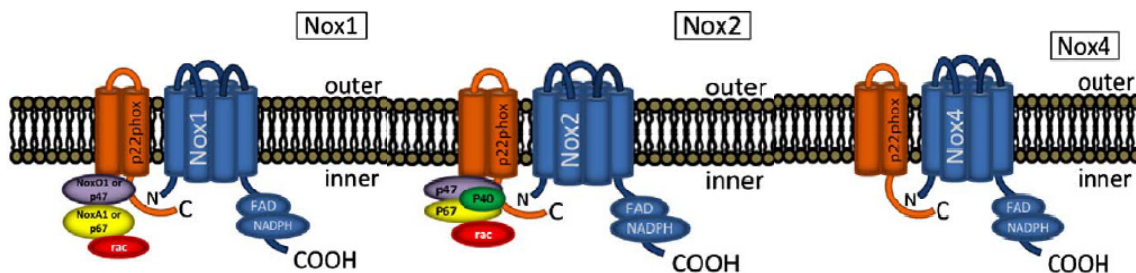


**Figure 9. NOX1, NOX2 and NOX4**, with and without regulatory subunits. Taken and adapted from [Brown and Griendling 2009]

Early studies in phagocytes showed that phosphorylations of the cytosolic NOX subunits (including p47<sup>phox</sup> and p67<sup>phox</sup>) regulate NOX [Heyworth, Shrimpton et al. 1989; Okamura, Babior et al. 1990; Uhlinger, Taylor et al. 1994]. Upon phosphorylation these proteins, together with rac1/2 and p40<sup>phox</sup>, translocate to the transmembrane gp91<sup>phox</sup> and p22<sup>phox</sup> [De Leo, Ulman et al. 1996; Vignais 2002], followed by a conformational change in p47<sup>phox</sup> and p40<sup>phox</sup>, both of which bind to the membrane [Ueyama, Kusakabe et al. 2008]. After assembly (figure 10) the functional enzymes reduces molecular oxygen to O<sub>2</sub><sup>•-</sup> at the expense of NADPH. ( $2O_2 + NADPH \rightarrow 2O_2^{\bullet-} + NADP^+ + H^+$ ) [Lambeth 2004].

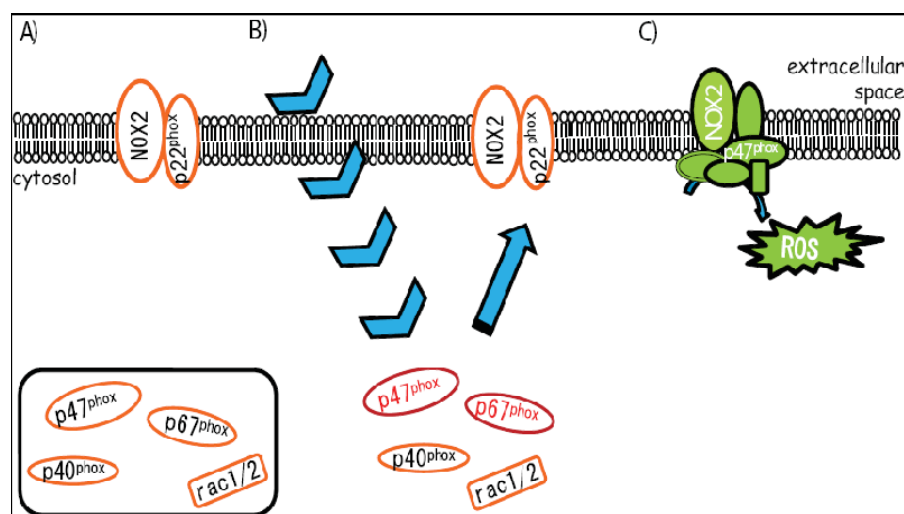


**Figure 10. Assembly of NOX.** The catalytic NOX subunits, gp91<sup>phox</sup> and p22<sup>phox</sup>, are embedded in the plasma membrane. In dormant cells (A) the regulatory subunits are located in the cytosol but translocate to gp91<sup>phox</sup> and p22<sup>phox</sup> upon activation (B), whether receptor or non-receptor mediated, to form an active enzyme (C) Figure drawn based on information from [Babior 1999; Lambeth, Cheng et al. 2000; Nauseef 2004].

The phenomenon of the oxidative burst [Vowells, Sekhsaria et al. 1995] was also shown in various cell types in response to growth factors, G-proteincoupled receptor agonists [Finkel 1999; Amin, Xiao et al. 2001; Xiao, Pimentel et al. 2002], as well as by anchorage dependent processes [Chiarugi and Fiaschi 2007]. NOX is essential in innate immunity, because it produces large amounts of ROS, which are elicited as a defence mechanism against invading microorganisms upon binding of bacterial components such as lipopolysaccharide [De Leo, Renee et al. 1998]. However, phagocytic ROS also underlie destructive “bystander effects”

that can damage surrounding tissue (rheumatoid arthritis). For every tissue expressing NOX - including heart, lung and the central nervous system - NOX-derived ROS have been implicated in physiological as well as pathophysiological processes [Quinn, Ammons et al. 2006].

### **3.5.) ROS, NOX and signalling**

NOX-derived H<sub>2</sub>O<sub>2</sub> is typically thought to be the most likely ROS-derived signalling molecule in physiological processes, promoting normal physiological processes, which although some authors only attribute a minor role to NOX [Chiarugi and Fiaschi 2007; Forman, Maiorino et al. 2010] Cells use H<sub>2</sub>O<sub>2</sub> as signalling modulators regulating peroxyredoxin signalling [Toledano, Planson et al. 2010] and activating protein tyrosine kinases. Gianonni *et al.* (2005) showed that in NIH 3T3 cells, Src is activated through H<sub>2</sub>O<sub>2</sub>-mediated oxidation of cysteine residues and subsequent phosphorylation upon cell adhesion [Giannoni, Buricchi et al. 2005]. In CMC survival was determined by activation of ERK through Src and Ras as well as by activation of the PI3K/PKB pathway in response to H<sub>2</sub>O<sub>2</sub> [Aikawa, Komuro et al. 1997; Aikawa, Nawano et al. 2000]. ROS have also been implicated as mandatory mediators during cell adhesion [Chiarugi, Pani et al. 2003]. Further, increased ROS levels have been observed upon excessive exercise [Ristow, Zarse et al. 2009]. If those ROS are scavenged by antioxidants, the beneficial effects of exercise-induced ROS are lost [Ristow, Zarse et al. 2009].

#### ***3.5.1.) ROS generation and NOX in cardiomyocytes***

Various stimuli including growth factors and G-protein coupled receptor (GPCR) agonists induce intracellular ROS [Finkel 1998; Finkel 1999; Xiao, Pimentel et al. 2002]. NOX plays a decisive role in myocardial ROS formation [Bendall, Cave et al. 2002; Sawyer, Siwik et al. 2002]. By contrast, previous studies (Chirugi, 2003; Giannoni, 2008) concluded that the integrin requirement for growth factor signalling depends mainly on lipoxygenase-derived ROS, based on the use of synthetic inhibitors. As noted before, at moderate levels, NOX-

derived ROS act as second messengers in redox-signalling, activating several signalling kinases implicated in cell survival and growth [Sawyer, Siwik et al. 2002; Rhee 2006].

Although NOX or NOX-derived ROS are generally implicated in physiological and pathophysiological processes [Bedard and Krause 2007], they are mainly associated with pro-apoptotic processes in the heart [Akki, Zhang et al. 2009], which may be due to the lack of studies in morphologically normal CMC, of comprehensive studies, and the choice of stimulus and working model. NOX was implicated as a mediator of ischaemia and GPCR-induced apoptosis in H9C2 cells based on the use of synthetic inhibitors [Qin, Patel et al. 2006]. Likewise, NOX was shown to be involved in cardiac hypertrophy and fibrosis. While NOX2 was reported to be involved in GPCR-dependent myocardial hypertrophy, it is dispensable in pressure overload-induced hypertrophy [Maytin, Siwik et al. 2004]. On the other hand, the lack of NOX2 in ischaemic preconditioning prevented NOX-associated pro-survival signalling and protection against ischaemia and reperfusion injury [Bell, Cave et al. 2005]. Irrespective of the number of studies performed to elucidate the role of cardiac NOX or NOX-derived ROS, the respective protective pathways involved in CMCs remain poorly characterized.



### **3.6.) Aims of this study**

The highly abundant cell adhesion receptor CD29 is essential for CMC growth and survival. Its deletion is embryonic lethal and its loss of function or disruption causes severe heart diseases. CD29-induced survival signalling cascades in healthy, morphologically normal cardiomyocytes are barely investigated. Further, several lines of evidence suggest a potential role of ROS in the regulation of cell survival, with NOX having been reported to act as a source of ROS in the heart. Due to the emerging role of ROS as regulators of cell survival, and the crucial role of NOX as a potent source of ROS in the heart, we addressed the question if CD29-induced pro-survival signalling depends on NOX-derived ROS in neonatal CMC.

Therefore, the involvement of ROS in the survival signalling hierarchy was dissected, with a special focus on the PI3K/PKB and the MAPK pathways. It was also investigated whether GSK-3 $\beta$ , which is reported to be a direct substrate of PKB, could be involved in pro-survival signalling. Further, likely upstream kinases of PI3K/PKB, MAPK and/or NOX were investigated. Additionally we wanted to explore whether CD29 induces ROS formation in newborn rat CMC, and in mouse CMC deficient in functional NOX subunits.

A minor aim was to investigate which *NOX* gene homologues are expressed in neonatal rat cardiomyocytes in response to CD29 stimulation, and whether the genes encoding the ROS sensor NF $\kappa$ B, the O<sub>2</sub><sup>•-</sup> converting enzyme SOD, or the anti-apoptotic protein Bcl2 were expressed upon CD29 engagement.

## 4.) MATERIALS & METHODS

### 4.1.) Reagents

**Materials for cell culture:** Reagents from GIBCO/Invitrogen: Dubelco's Modified Eagles Medium (DMEM) for cardiomyocytes; low glucose, 1g/L, for cell line; high glucose, 4.5g/L; phenol red free (prf)-DMEM, low glucose, 1 g/L (cardiac myocytes); high glucose, 4.5 g/L (H9c2), HBSS, Hepes, 0.05% trypsin-EDTA, PBS, D-PBS (+ Ca<sup>2+</sup>), L-glutamine (GlutaMAX), penicillin (P, 100 U/mL), streptomycin (S, 100 µg/mL) and FCS; 5-bromo-2-deoxyuridine (BrdU, 200 mmol/L) and trypan blue were purchased from Sigma Aldrich, Collagenase was from Worthington, Accutase from PAA Laboratories (The cell culture company). Culture flasks T75 and T25, as well as sterile 5 mL, 10 mL and 25 mL serological plastic pipettes, 1.5 mL and 2.0 mL micro tubes, syringe filter (Filtropour S; nonpyrogenic/sterile 0.20µM; No.: 83.1286.001) were purchased from Sarstedt Cell culture dishes easy grip (standard tissue culture) 35 × 10 mm and 60 × 15 mm, cell strainer (100µM; Ref. No.: 353260) were from BD Falcon™. 50 mL tubes were from both suppliers Sarstedt and BD Falcon.

**Treatments:** Wortmannin (#W1628), U0126 (#U120), apocynin ([4'-hydroxy-3'-methoxyacetophenone], acetovanillone, #W508454) DPI (diphenyleneiodonium chloride, #D2926), PMA [12-O-tetradecanoylphorbol 13-acetate, 4β,9α,12β,13α,20-pentahydroxytiglic-1,6-dien-3-one 12-tetradecanoate 13-acetate, #P1585], phenylephrine (PE, phenylephrine hydrochloride, #P6126) were purchased from Sigma-Aldrich; LY294002 (LY, [2-(4-morpholinyl) 8-phenyl-4H-1-benzopyran-4-one], #440202-5MG ) Akti1/2 (PKB inhibitor VIII; isozyme selective, [1,3-dihydro-1-((4-(6-phenyl-1H-imidazo[4,5-g]quinoxalin-7-yl)phenyl)methyl)-4-piperidinyl)-2H-benzimidazol-2-on]; #124018-1MG), PP2 ([4-amino-5-(4-chlorophenyl)-7-(t-butyl)pyrazol[3,4-d]pyrimidine], #529573-1MG), SU6656 (Src family kinase inhibitor, #572635-1MG) and MnTMPyP ([Mn(III)tetrakis(1-methyl-4-pyridyl) porphyrin pentachloride], #475872-25MG was stored desiccated in Drierite® from Fluka at -20°C) were purchased from Merck. H3232 (PKC inhibitor; 19-31, #H-3232.0001) was from Bachem. Activating anti-β<sub>1</sub>-integrin (α-CD29, #610468) antibody was from BD Biosciences, inhibitory α-CD29 from BioLegend (#102209) and rabbit IgG from Sigma Aldrich.

**Viral infection:** The following viral constructs were purchased from the Gene Transfer Vector Core, University of Iowa: Ad5CMVCatalase, Ad5CMVSOD1 and Ad5CMVcytoLacZ.

**Flow cytometry:** 5-(and-6)-chloromethyl-2',7'-DCF-DA (dichlorodihydrofluorescein diacetate acetyl ester, CM-H<sub>2</sub>DCFDA, # C6827) was purchased from Invitrogen.

**Sample preparation:** Cell lysis buffer (Cell Signaling Technology, Inc., Danvers, MA, USA): 10×; 20 mM Tris-HCl (pH 7.5), 150 mmol/L NaCl, 1 mmol/L Na<sub>2</sub>EDTA, 1 mmol/L EGTA, 1% Triton-X100, 2.5 mmol/L sodium pyrophosphate, 1 mmol/L β-glycerophosphate, 1 mmol/L Na<sub>3</sub>VO<sub>4</sub>, 1 μg/mL leupeptin; 1 mmol/L Pefabloc SC Plus (Roche Diagnostics GmbH, Mannheim, Germany) and 100 × phosphatase inhibitor cocktail 1 (Sigma-Aldrich).

**Sodium dodecylsulfate polyacrylamide gel electrophoresis (SDS-PAGE) and Western Blotting**

	company	Product #
Acrylamide / Bis-acrylamide 30% solution	Sigma	A3699-100G
Acrylamide / Bis-acrylamide 37.5:1 (Rotiophere gel 30)	Roth	3029.1 (1 litre)
ammonium persulfate (APS)	Sigma	A3678-25G
blotting paper; pure cellulose; extra thick, size 7x10cm	Whatman/Sigma	P7796-100EA
bovine serum albumin (BSA)	Sigma Aldrich	A7906
enhanced chemiluminescence Western Lightening Plus glycine	Perkin Elmer	
	Fluka	50050 (5kg)
HCl (fuming) 37%	Fluka	84422 (1 ltr.)
Dual colour protein loading buffer pack	Fermentas	R1011
Methanol (CHROMASOLV <sup>®</sup> for HPLC; ≥99.9%)	Sigma	34860-2.5L-R
milk-powder; low fat	Migros or COOP	
PVDF (polyvinyliden fluoride)-membrane (Hybond <sup>™</sup> - P)	Amersham/GE Healthcare	RPN303F
NaCl	Fluka	7138 (1kg)
sodium dodecyl sulphate (SDS)	Fluka	05030 (500ml)
TEMED	Fluka	87689
Tris base, Trizma <sup>®</sup> base	Sigma	T1503-1KG
Tween 20	Qbiogene, Sigma	TWEEN201 (500ml)
loading tips	Costar to order via Vitaris	4853 (2 boxes/ cardboard box)
Blue X-ray films	ThermoFischer Scientific	

**Table 1 Compounds for Western blot**

Dual Color Protein Loading Buffer Pack (4 × Loading Buffer: 0.25 M Tris-HCl (pH 8.5), 8% SDS, 1.6 M EDTA, 0.024% pyronin Y, 0.04% bromophenol blue and 40% glycerol; 20 × Reducing Agent: 2 M DTT; stored at -20°C), and Page Ruler™ Prestained Protein Ladder (SM0671) from Fermentas were used.<sup>3</sup>

**Antibodies:** Anti-phospho-ERK1/2 [p44/42-MAPK, (Thr202/Tyr204)], anti-phospho-MEK1/2 (Ser217/221), monoclonal anti-phospho-Akt [(Ser437) (193H12)], anti-phospho-GSK-3β (Ser9), phospho-src tyrosine kinase (Tyr416), non-phospho src (Tyr 527), phospho PKCζ/λ/δ (Thr410/403) and corresponding anti-total p44/42 MAP kinase, MEK1/2, Akt, monoclonal GSK-3β, Src, PKCζ rabbit antibodies were from Cell Signaling. Secondary antibody [horseradish peroxidase (HRP)-conjugated AffiniPure goat α-rabbit-IgG] was purchased from Jackson Immuno Research Laboratories.

**Stripping buffer:** For one litre abcam® buffer 15 g glycine and 1 g SDS dissolved in 900 mL ddH<sub>2</sub>O. 10 mL Tween 20 were added and pH adjusted to 2.2. Restore™ Plus Western Blot stripping Buffer (# 46430) from Thermo Scientific was used.

**RNA-isolation:** TRIzol or TRI reagent was purchased from Invitrogen or Sigma, respectively. Chloroform and isopropanol (2-propanol) were from Fluka, nuclease-free water (#R0582), RNA loading dye from Fermentas. EtOH absolute (96%) was from Sigma. Equipment needed a cooling centrifuge (Hettich), a chemical hood, a thermoblock (Eppendorf), a Nanodrop ND-1000 spectrophotometer, an agarose gel apparatus and power supply both from Biorad, a balance, a Gel documentation system (Gel doc).

**DNase I treatment:** DNase I, RNase-free (#EN0521) supplied with 10× reaction buffer with MgCl<sub>2</sub> (100mM Tris, pH 7.5 at 25°C, 25mM MgCl<sub>2</sub>, 1 mM CaCl<sub>2</sub>) and RNase inhibitor (RiboLock™; #EO0381) were from Fermentas. EDTA was from Fluka.

**cDNA synthesis:** Oligo dT-primer were purchased from Microsynth. dNTP (10 mM), RNase inhibitor (Riboblock; # EO0381), reverse transcriptase (RevertAid™ H Minus M-MuLV RT; #EP0452), Reverse Transcriptase/RevertAid 5x buffer Buffer were from Fermentas. Equipment: Thermal cycler/PCR machine.

**PCR:** Nuclease free water (Fermentas, #R0582), Sigma REDTaq® ReadyMix™ PCR reaction mix with MgCl<sub>2</sub> (#R2523) and DreamTaq™ Green PCR Master Mix (2X; #K1081) from Fermentas were used; Equipment: Thermal cycler/PCR machine.

---

<sup>3</sup> [www.thermofischer.com/fermentas](http://www.thermofischer.com/fermentas)

## **4.2.) Cell culture**

### ***4.2.1.) Isolation of neonatal rat ventricular myocytes (NRVM)***

NRVM were isolated from 1-3 day old pup hearts as previously described [Thaik, Calderone et al. 1995; Lim, Zuppinger et al. 2004]. Hearts were removed from Wistar rat pups sacrificed by decapitation. After ventricles were dissected from the heart, they were washed in HBSS and cut in equal pieces. Ventricle pieces were digested in 0.05% trypsin-EDTA in a 50 mL tube (Sarstedt) for 14 hours with gentle agitation in a square box at 4°C, to ensure controlled rolling of the tube. The following day trypsin-EDTA was removed and pieces were washed once with 10 mL 7% FCS-DMEM (low glucose) by shaking gently in a pre-warmed water bath at 37°C for 4 minutes. After having removed the FCS-containing DMEM, a step-wise digestion with 7 mL 0.07% (w/v) collagenase in 50 mL HBSS followed for 1 to 8 minutes, in which the first step lasted 5 minutes. Each digestion step was stopped when the collagenase-cell suspension turned cloudy. Aliquots were collected in 50 mL tubes containing 10 mL 7% FCS-DMEM that were kept on ice. Since with each digestion step (7 mL collagenase-HBSS) the ventricle pieces release cardiomyocytes and non-myocytes, the ventricular tissue left gets slurry and its transfer to the collected cells must be avoided. After the 7<sup>th</sup> digestion step, first the collected cell suspension and second the tissue left in collagenase-HBSS solution were filtered with a 100 µm cell strainer to remove tissue parts, the tubes rinsed with 7% FCS-DMEM, equilibrated in volume and centrifuged for 8 minutes at 800 rpm and 4°C. Pellets were resuspended in 10 mL 7%-FCS-DMEM. Cell suspensions were pre-cultured at 37°C, 5% CO<sub>2</sub> in T75 culture flasks (Sarstedt) for 2 hours to allow FB to attach, and after 1 hour of incubation the cell suspension was transferred to new T75 culture flasks.

The cell number was estimated using a Neubauer haemocytometer counting chamber with trypan blue as an exclusion dye for dead cells. The yield of viable cells was estimated as follows: Mean (total number of cells in 4 grids/ 4) × 2 × 10<sup>4</sup> × (cell suspension volume). 2x10<sup>6</sup> cells were plated in 7% FCS-DMEM (with P/S, 25 mM Hepes and 100 µM BrdU; BrdU was used to prevent proliferation of non-myocytes) on a 60 mm plastic dish (P60, BD Falcon). NRVM were kept for 24 hours at 37 °C and 5% CO<sub>2</sub> before changing to serum-free (SF)-DMEM (without FCS, but with Hepes and P/S) for an additional 16 hours.

#### **4.2.2.) Isolation of neonatal mouse ventricular myocytes (NMVM)**

NMVM were isolated from 1-2 days old pup hearts of wild-type (C57/BL6), p47<sup>phox</sup> loss-of-function (LOF, homozygous *Ncf1<sup>m1j</sup>*) and NOX2 (gp91<sup>phox</sup>, homozygous *Cybb<sup>tm1Din</sup>*) knock-out strains as described previously [Springhorn and Claycomb 1989; Xiang, Sakata et al. 2006]. Collected ventricular heart pieces were digested in 0.05% trypsin-EDTA for 45 minutes with gentle agitation at 4°C, followed by a wash step with 10% FCS-DMEM, and serial digestions with 0.0686% (w/v) collagenase in HBSS, 6 mL at each step for 4 to 8 minutes. As soon as the solution turned cloudy, cells were collected in pre-cooled 10 mL 10%-FCS-DMEM. The cell suspension was filtered through a 100 µm filter strainer. After centrifugation at 800 rpm at room temperature for 5 minutes, the pellet was resuspended in 12 mL 10% FCS-DMEM and transferred to T75 Sarstedt-flasks. Non-myocytes were removed by pre-plating of these flasks at 37 °C and 5% CO<sub>2</sub> for 2 h. The cell number was estimated using a Neubauer haemocytometer counting chamber [yield= Mean (total number of cells in 4 grids/ 4) × 10<sup>4</sup> × (cell suspension volume)]. 10% FCS-DMEM (with P/S, Hepes and BrdU) was used to plate cells of each strain on LN pre-coated (70 µg/mL) 35 mm dishes (P35) or 12-well plates. Cardiomyocytes were seeded at a density of 0.9x10<sup>6</sup> (12-well plate) or 1.8x10<sup>6</sup> (P35) and kept at 37°C and 5% CO<sub>2</sub> for 24 h. The serum containing medium was replaced by SF-DMEM 16 to 18 hours prior to treatment.

#### **4.2.3.) Cell line: H9C2**

H9c2 are cardiac myoblasts from rat [Kimes and Brandt 1976; Hescheler, Meyer et al. 1991] and were handled as described previously [Masters and Stacey 2007]. Passages 12-20 were used.

##### **4.2.3.1.) Defreezing**

Cells were thawed at room temperature, and transferred to a Sarstedt tube containing 19 mL pre-warmed FCS-DMEM (4.5g/L glucose) supplemented with 10% FCS. The cell

suspension was centrifuged for 5 minutes at 1300 rpm and room temperature. The pellet was resuspended in 7 mL 10% FCS-DMEM (high glucose), transferred to T25 culture flasks and incubated at 37°C with 5 % CO<sub>2</sub>.

#### ***4.2.3.2.) Passaging***

Cells were split 1:4 to 1:6 twice a week when sub-confluent (70-80%). After having removed the medium, cells were washed twice with 5 mL pre-warmed HBSS. For detaching cells 5 mL 0.05% Trypsin-EDTA were used and cells incubated for about 2 minutes at 37°C and 5 CO<sub>2</sub>. While incubating, a 50 ml tube supplemented with 3 mL 10% FCS high glucose DMEM was prepared. Cells were transferred from the T75 flasks to the 50 mL tubes and rinsed with a few mL 10% FCS DMEM (4.5g/L glucose) and cells centrifuged at 1300 rpm for 5 minutes. Resuspend pellets in 25 mL 10% high glucose DMEM, in case of 1:5 splitting. 5 mL cell suspension were mixed with 15 mL high glucose medium and transferred to new T75 flasks and kept at 37°C and 5% CO<sub>2</sub>. The cell density was controlled after 74 h. If cells were sub-confluent, they were split again to new T75 flasks or seeded on P60s for experiments, with 300000 cells per P60 (used within the next 48 h) and 200000 cells (for experiments in the following 74 h). For estimating the cell number, a Neubauer counting chamber with trypan blue as an exclusion dye for dead cells was used.

#### ***4.2.2.3.) Cryopreservation***

The total volume of the cell suspension to be frozen was estimated; cells were collected, counted and re-suspended in 10% FCS-DMEM supplemented with 10% FCS and 20% DMSO; one T75 flask equals 4 cryotubes with 1 mL volume each. A cryofreezing container "Mr.Frosty"<sup>4</sup> was used, supplemented with 100% isopropyl alcohol to guarantee cryopreservation with 1°C/min.

---

<sup>4</sup> [http://www.nalgenelabware.com/products/productDetail.asp?product\\_id=405](http://www.nalgenelabware.com/products/productDetail.asp?product_id=405)

### **4.3.) Treatments**

NRVM were treated with the following compounds: W, LY, Akti1/2, U, DPI, PP2, SU6656, H3232 or MnTMPyP with final concentrations as indicated for 45 minutes or in case of apocynin (apo) for 16 to 18 hours prior to  $\alpha$ -CD29 administration for 15 min, except for time course experiments.

Abbr.	Drug	[stock]	[target]	dilution	remarks
Apo	apocynin acetovanillon	10mM 1.66mg/mL	500 $\mu$ g/mL	1:20	dissolved in DMSO; droplet-wise application
Akti	Akt inhibitor VIII, Akti 1/2			1:1000	dissolved in DMSO
BrdU		200mM	100 $\mu$ M	1:2000	
DPI		10mM	10 $\mu$ M	1:1000	dissolved in DMSO
H3232	PKC-inhibitor	1 mM	10 $\mu$ M	1:100	dissolved in 5% acetic acid
CD29	$\beta_1$ -integrin		10 $\mu$ g/mL	1: 50	40 $\mu$ L/2 mL
			15 $\mu$ g /mL	1:33.3*	60 $\mu$ L/2 mL
LN	Laminin	1 mg/mL	70 $\mu$ g/mL	1:14.3	500 $\mu$ l/ well of a 12 well plate 1 mL/P35
LY	PI3K-Inhibitor	1mM	1 $\mu$ M	1:1000	dissolved in DMSO
MnT	MnTMPyP	5mM	5 $\mu$ M	1:1000	dissolved in water; keep desiccated
PP2	Src-Inhibitor	10 mM	10 $\mu$ M	1:1000	dissolved in DMSO
SU6656	Src-inhibitor	10 mM	10 $\mu$ M	1:1000	dissolved in DMSO;
U	MEK-Inhibitor	10 mM	10 $\mu$ M	1:1000	dissolved in DMSO
W	Wortmannin, PI3K-Inhibitor	100 mM	100 nM	1:100 000	dilute in DMSO

**Table 2 Dilution scheme of inhibitors and treatments applied**



#### **4.4.) Viral infection**

After cardiomyocytes were changed to SF-DMEM, they were infected with viral constructs bearing either SOD (Ad5CMVSOD1) [Zwacka, Zhou et al. 1998], catalase (Ad5CMVCatalase) [Lam, Zwacka et al. 1999] or  $\beta$ -galactosidase (Ad5CMVcytoLacZ) [Davidson, Allen et al. 1993] for 36 h. Cardiomyocytes were washed twice with SF-DMEM before supplemented with SF-DMEM for additional 14-16 h, followed by CD29 treatment for 15 minutes.

#### **4.5.) Sample preparation**

All signalling samples were washed twice with ice-cold PBS and scraped in 70  $\mu$ L (P35) or 120  $\mu$ L (P60) cell lysis buffer, centrifuged at 15000 rpm for 15 min at 4 °C, supernatants were collected in new micro tubes (Eppendorf). Cell lysis buffer (1:10 in ddH<sub>2</sub>O) was supplemented with 1 mM Pefabloc SC Plus and phosphatase cocktail 1 (1:100). Sample protein concentrations were estimated using a Pierce protein BCA kit (Thermo Fischer Scientific) [Kurien and Scofield 2003]. 10 $\mu$ g (ERK), 25 $\mu$ g (PKB) and 35 $\mu$ g (GSK-3 $\beta$ , Src, PKC) protein were prepared according to Fermentas DualColor protein loading buffer pack instructions (1  $\mu$ L DTT and 5  $\mu$ L loading buffer per 20 $\mu$ L total volume including protein sample and ddH<sub>2</sub>O; incubated for 5 minutes at 95-100 °C with 300 rpm mixing on a thermo-block; spun a few seconds in a microcentrifuge).

#### **4.6.) Sodium dodecyl sulfate-polyacrylamide gelelectrophoresis (SDS-PAGE)**

SDS-PAGE was performed as previously described [Rehm 2002]. Briefly, a 12% resolving gel was prepared. Gels polymerized within 30 minutes. To obtain an even gel a thin layer of 70% ethanol (300-500  $\mu$ L) covered the top of the gel, which was removed before the 5% stacking gel was prepared.

##### ***4.6.1.) Western blotting***

Western blotting was performed as previously described [Kurien and Scofield 2006]. The gel apparatus was set up (Mini-PROTEAN<sup>®</sup> Tetra Electrophoresis System, Bio-Rad) and filled with pre-cooled running buffer. Protein samples and prestained protein ladder ran with constant

Volts (90 V) till the tracking dye reached the bottom of the gel. Next, fibre pads, blotting paper (Whatmann, extra thick, pure cellulose) and PVDF- membranes were soaked in 1× used transfer buffer, whereas PVDF- membranes were first activated for 10 second in methanol (Chromasolv<sup>®</sup>, Sigma) and 5 minutes in ddH<sub>2</sub>O. The transfer apparatus was assembled (electrophoresis blotting module, 2 gel holder cassettes and the Bio-Ice<sup>™</sup> cooling unit; pre-cooled transfer buffer; Bio-Rad), placed in a styrofoam box surrounded with ice cubes (a stir bar inside the buffer tank). The tank transfer system was plugged to a BioRad Power Pac 3000 for 2 hours with constant Volts (100 V). After transfer, membranes were reactivated in methanol and blocked in 5% milk/TBST (TBS with 0.1% Tween-20, Sigma) for GSK-3β (Ser9) or 4% BSA/TBST for 30 to 60 minutes. Effectiveness of protein transfer was checked by either staining gels with Coomassie Blue R (Sigma) or staining the membranes with Ponceau S solution (Sigma).

Membranes were incubated with the primary antibody overnight, while gently shaking at 4°C (phospho and total ERK 1:5000, phospho and total PKB, total GSK3β 1:2500, phospho-GSK-3β, phospho-Src, phospho-PKCζ dilutions 1:1500,). Membranes were washed 3 times with TBST for 15 minutes. HRP-conjugated secondary antibody (in 4% BSA/TBST) was added and left for 45 min with gentle shaking at room temperature. Finally membranes were washed 3 × with TBST for 15 min, ECL was prepared according to the manufacturer's protocols (Perkin Elmer Biosciences; Oxidizing Reagent Plus and Enhanced Luminol Reagent Plus in ratio 1:1) to detect immunoreactive bands with a blue X-ray film (Fisher Thermo Scientific) and a Curix Developer. The bands were analysed using Image J v1.372<sup>5</sup> [Burger and Burge 2007].

#### **4.6.2.) Stripping for reprobing**

Membranes that were re-used to probe for different antibodies were stripped either with mild stripping buffer protocol provided by abcam<sup>®6</sup> or by use of Restore<sup>™</sup> Plus Western Blot stripping buffer according to manufacturers' instructions.

---

<sup>5</sup> <http://rsb.info.nih.gov/ij/>

<sup>6</sup> [www.abcam.com/index.html?pageconfig=resource&rid=11353](http://www.abcam.com/index.html?pageconfig=resource&rid=11353)

## 4.7.) Flow Cytometry

The method was adapted from those described previously [Bass, Parce et al. 1983; Vowells, Sekhsaria et al. 1995]. 25 mM CM-H<sub>2</sub>DCFDA (figure 11) in DMSO was diluted to a 12.5 μM working solution in pre-warmed (37°C) prf-DMEM with L-glutamine (4 mM) and Hepes (25mM). CMC were treated with apocynin and diphenylene iodonium as described above and medium was exchanged for DCF working solution (2 mL/P60) for 20 min in the dark at 37°C and 5 % CO<sub>2</sub>. Cells were washed once with 7% FCS prf-DMEM and twice with ice-cold PBS prior to detachment with accutase. Accutase was incubated 5 to 10 min at 37°C and 5% CO<sub>2</sub>. Cells were transferred to polystyrene FACS tubes (BD Falcon), filtered through a 40 μm cell strainer cap and centrifuged at 700 rpm at room temperature for 7 minutes. Pellets were re-suspended in 500μL prf-DMEM and kept on ice. CD29 (10 μg/mL for NRVM, 15 μg/mL for NMVM), H<sub>2</sub>O<sub>2</sub> (100 μM) and PMA (1 μM) were supplemented prior to measurement at defined time points. The oxidative burst was measured with FL-1, 488nm excitation and 530 nm emission on a DAKO flow cytometer and DAKO Summit v.4.3 software.

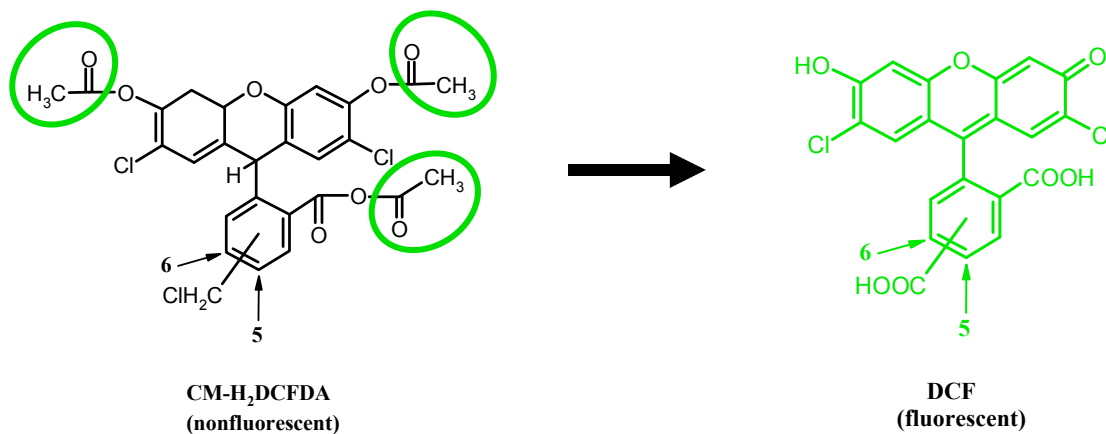


**Figure 11. ROS detection reagent chloromethyl-dihydrodichlorofluorescein diacetate (CM-H<sub>2</sub>DCFDA).** CM-H<sub>2</sub>DCFDA is a nonfluorescent, reduced cell-permeant probe that becomes fluorescent upon cleavage of acetate-groups (indicated by green circles) by intracellular esterases and oxidation within the cell. CM-H<sub>2</sub>DCFDA is reportedly retained longer in cells due the thiol reactive chloromethyl group, which can bind to intracellular components<sup>7</sup>.

<sup>7</sup> <http://probes.invitrogen.com/media/pis/mp36103.pdf>

## **4.8.) RNA**

### ***4.8.1.) RNA isolation***

RNA isolation using Trizol reagent was performed as recommended by manufacturer (Invitrogen)<sup>8</sup>

Total RNA was extracted from tissue cultured cells (NRVM). Cells were washed with ice-cold PBS prior to lysing with 1.4 mL Trizol (Invitrogen) or TRI<sup>®</sup> reagent (Sigma) on each P60 culture dish. Cell lysates were passed several times through a pipette, scraped with a cell scraper and collected in 2 mL microtubes (Sarstedt). Homogenised cells (NRVM) were stored at -80°C.

Trizol samples were centrifuged for 10 min at 12000 *g* and 4°C in a precooled centrifuge (Hettich MIKRO 22R). 1000 µL were transferred to fresh, sterilized 1.5 microtube, 200 µL ice-cold chloroform was applied. The two solutions were mixed by inversion, left at room temperature for 5 minutes and centrifuged for 15 min at 12000 *g* and 4°C. The aqueous phase (containing RNA) was transferred to new micro tubes. RNA was precipitated by adding the same volume ice-cold 2-propanol, and left at room temperature for 10 minutes, followed by a centrifugation step for 15 min at 12000 *g* and 4°C.

After discarding the supernatant the RNA pellet was washed with 75% ethanol in RNase-free (DEPC-treated) water, and centrifuged for 5 minutes at 7400 *g* and 4°C. Ethanol was discarded and the pellet was air dried at room temperature for 10 minutes.

Pellets were re-suspended in 50 µL RNase-free water and dissolved for 10 min at 60°C with gentle mixing (Eppendorf Thermoblock, 300 rpm). Afterwards, RNA was chilled on ice.

Total RNA concentrations were measured with a NanoDrop<sup>9</sup> UV/VIS spectrophotometer ND-1000 according to the manufacturer's protocol, loaded with 1.2 to 1.5 µL total RNA extract on the lower measurement pedestal. RNA quality was assessed by loading an RNA : loading dye mix on 1% agarose gel, which ran for 30 minutes at 100 V. Visualization under UV revealed two strong rRNA bands on the gel.

---

<sup>8</sup> <http://products.invitrogen.com/ivgn/product/15596026>

<sup>9</sup> <http://www.peqlab.de/wcms/nanodrop/nanodrop-service.php>

#### **4.8.2.) Deoxyribonuclease I (DNase I) treatment of RNA and cDNA synthesis**

DNase I treatment and cDNA synthesis were performed as described by the supplier (Fermentas)<sup>10</sup>.

1.5 µg total RNA were supplemented with 0.25 µL 40u/µL RNase inhibitor, 1 µL 10x DNase I buffer with MgCl<sub>2</sub> and 1 u DNase I in a final volume of 10 µL. Samples incubated for 30 min at 37°C followed by application of 25 mM EDTA and incubation at 65°C for 10 minutes. Samples were kept on ice until use for cDNA synthesis.

RevertAid™ H Minus Reverse Transcriptase (Fermentas) was used, which is a genetically modified Moloney Murine Leukaemia Virus reverse transcriptase, with a mutated and non-functional RNase H. Briefly, 1.5 µg total RNA was used, pre-mixed with 1 µL 100µM dT<sub>18</sub> primer (~0.5 µg/µL) and incubated for 5 min at 70°C. Further, 4 µL 5x RevertAid Buffer, 2 µL 10 mM (each) dNTP, 0.5 µL 40 u/µL RNase Inhibitor, and finally 1 µL 200 u/µL RevertAid H<sup>-</sup> M-MuLV RT t were added. RNA was incubated for 5 min at 37°C followed by 1.5 h at 42°C and 10 min at 70°C. cDNA samples were stored at 4°C for use in RT-PCR to avoid freeze thaw damage.

#### **4.8.3.) Primers**

Primer pairs (Table 2) were designed using the NCBI primer-BLAST<sup>11</sup> tool, except for primers marked \* and <sup>§</sup>.

\*primers were taken from [Cao, Dai et al. 2007]; <sup>§</sup> primer was taken from [Kutty, Kutty et al. 1995].

---

<sup>10</sup> <http://www.fermentas.com/en/products/all/modifying-enzymes>

<sup>11</sup> <http://www.ncbi.nlm.nih.gov/tools/primer-blast/index.cgi>

Gene	NCBI accession #	Primer	Sequence (5' → 3')	Product length
<i>NCF1</i>	NM_053734.2	RnNCF1-1f	ACCTATCGCCGCAACAGCGT	954
<i>NCF1</i>		RnNCF1-1r	CGCCAGATGTTGGAACACGGA	954
<i>NOX1*</i>	AF152963	RnNOX1-1f	TGAACAACAGCACTCACCAATGCC	245
<i>NOX1*</i>		RnNOX1-1r	AGTTGTTGAACCAGGCAAAGGCAC	245
<i>CYBB*</i>	AF298656	RnCYBB-1f	GTGGAGTGGTGTGTGAATGC	324
<i>CYBB*</i>		RnCYBB-1r	TCCACGTACAATTCGCTCAG	324
<i>NOX4</i>	NM_053524.1	RnNOX4-1f	TTCCGTCCCAAGCACCGAGC	431
<i>NOX4</i>		RnNOX4-1r	CAGGGCGTTACCAAGTGGGC	431
<i>ITGB1</i>	NM_017022.2	RnITGB1-1f	GCAGGCGTGGTTGCCGGAAT	951
<i>ITGB1</i>		RnITGB1-1r	GCAGAACAGGCCCTGCTCC	951
<i>GAPDH</i>	NM_017008.3	RnGAPDH-1f	CAAGAAGGTGGTGAAGCAGGCGGC	317
<i>GAPDH</i>		RnGAPDH-1r	AGTTGGGATGGGGACTCCTCAGC	317
<i>SOD1</i>	NM_017050.1	RnSOD1-1f	GCGGCTTCTGTCTCTCCTTGC	506
<i>SOD1</i>		RnSOD1-1r	CCAAGCGGCTTCCAGCATTTCCA	506
<i>NFKB1</i>	XM_342346.4	RnNFKB1-1f	TGCACTTGGCCGTGATCACCA	364
<i>NFKB1</i>		RnNFKB1-1r	TCCAGGAGCAGGCAGCCGG	364
<i>STAT3</i>	NM_012747.2	RnSTAT3-1f	AACATGGCCGGCAAGGGCT	440
<i>STAT3</i>		RnSTAT3-1r	GGGTCAGCTTCAGGGTGCTCCT	440
<i>BCL2</i>	NM_016993.1	RnBCL2-1f	AGGACGTCGCCTCTACGGCC	354
<i>BCL2</i>		RnBCL2-1r	CCAGGTGTGCAGATGCCGGTT	354
<i>HO-1<sup>§</sup></i>	NM_012580	RnHmox1-1f	AAGGAGGTGCACATCCGTGCA	568
<i>HO-1<sup>§</sup></i>		Rn Hmox1-1r	ATGTTGAGCAGGAAGGCGGTC	568

**Table 3 Primers.**

#### 4.8.4.) Gradient PCR

Primer annealing temperature was optimized in a preliminary gradient PCR [Mülhardt 2008] experiment (e.g., figure 12) with annealing temperature points ranging from 51°C to 62°C. All set of experiments of NRVM were pooled to test whether the primers were suitable for RT-PCR amplification at temperature points 51°C, 52.1°C, 53.4°C, 56.3°C, 59.1°C and 61.9°C



**Figure 12.** *NOX1*, *NOX2* and *HO-1* PCR products at different annealing temperatures, loaded on a 1% agarose gel with a 1 kbp ladder.

#### 4.8.5.) Optimization of PCR cycles

Primers were optimized for the number (21, 27, 33, 39, 45) of cycles to be used in semi-quantitative PCR and cycle numbers chosen so as to avoid PCR signal saturation.

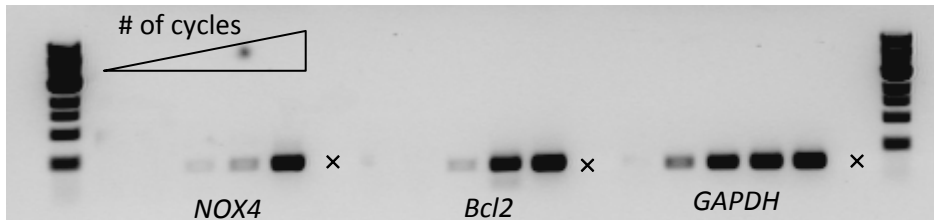


**Figure 13.** *NOX4*, *Bcl2* and *GAPDH* PCR products with different cycles, loaded on a 1% agarose gel with a 1 kbp ladder. While *NOX4*'s optimal detection cycle number lies between 39 and 45 cycles, *GAPDH* is already present at 27 cycles.

#### 4.8.6.) Semi-quantitative PCR

PCR reaction mixes were scaled to 8  $\mu$ L final volume containing 1.2  $\mu$ L cDNA (equivalent to 15 ng total RNA), 0.32  $\mu$ L 5  $\mu$ M forward and reverse primers, 4  $\mu$ L RedTaq Ready Mix (Sigma) and 2.16  $\mu$ L nuclease-free water. Reaction mixes were prepared for each primer pair with defined cycling number and temperature. PCR cycling parameters were 94°C 3 min,  $N \times$  (94°C 30 s,  $T_A$  30s, 72°C 1 min), 72°C 10 min, where  $N$  indicates the number of amplification cycles and  $T_A$  the annealing temperature. (see table 3). PCR products were visualized on a 1% TAE agarose gel (90 V for 36 minutes), digital images taken and analysed using Image J v1.372 software [Burger and Burge 2007].

Primer pair	Annealing temperature	# of cycles
NFκB	57°C	33
STAT3	57°C	31
SOD1	57°C	32
CD29	57°C	35
NCF1	59°C	34
NOX4	57°C	40
Bcl2	57°C	35
GAPDH	57°C	28
NOX1	56.5°C	31
NOX2	56.5°C	40
HO-1	56.5°C	40

**Table 4 Primer optimization**

#### **4.9.) Statistical analyses**

All statistical analyses were performed in Graphpad Prism Version 4.03 and p-values below 0.05 were considered to indicate significant differences. Significance was tested in repeated measures 1-way ANOVA with post-test Bonferroni (for sample sizes  $\leq 4$ ) or Newman Keuls (for  $> 4$  samples to compare) correction.



## 5.) RESULTS

### 5.1.) CD29 activation induces phosphorylation of ERK1/2 (Thr202/Tyr204), Akt (Ser473) and GSK-3 $\beta$ (Ser9) in newborn cardiomyocytes

CD29 activates the MEK/ERK and the PI3K/PKB pathways in various cell types [Clark and Brugge 1995] including cardiac cells [Ross and Borg 2001]. In NRVM, increased phosphorylation of ERK and PKB was observed upon CD29 stimulation, which peaked at 15 min and was no longer detectable at 45 min (figure. 14A and B). Phosphorylation of serine 9 of glycogen synthase kinase (GSK)-3 $\beta$ , which is inhibitory to its kinase activity, was used to measure CD29-induced pro-survival signalling, because a) it is described as an elevated pro-apoptotic target kinase in adult cardiomyocytes upon  $\beta$ -adrenergic receptor agonists and GPCR agonists such as endothelin-1 [Haq, Choukroun et al. 2000; Menon, Johnson et al. 2007] and b) it is downstream of the PI3K/PKB pathway [Cross, Alessi et al. 1995; Sugden, Fuller et al. 2008]. Using a phosphorylation site-specific GSK-3 $\beta$  (Ser9) antibody, immunoreactive bands were observed at 15 min (figure 14C). No changes in phosphorylation were detectable when NRVM were incubated with either an inhibitory  $\alpha$ -CD29 antibody or with a non-specific IgG (figure 14A-C) pointing at the effectiveness of activating  $\alpha$ -CD29.

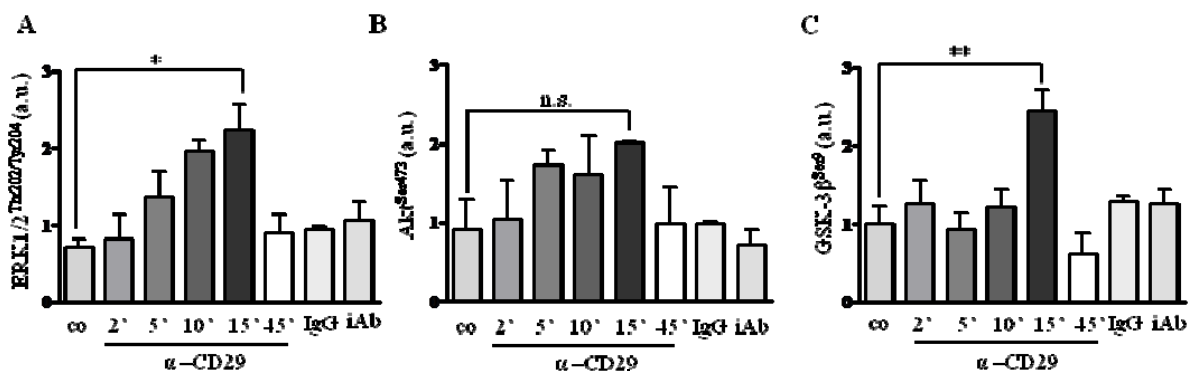


**Figure 14. CD29 induces time-dependent phosphorylation of cell-survival kinases (A) ERK1/2, (B) PKB/Akt and (C) GSK-3 $\beta$  as detected by phospho-specific antibodies (Western blot). Cardiomyocytes were treated with 5  $\mu$ g/mL activating  $\alpha$ -CD29 antibody, unspecific IgG (IgG) or inhibitory anti-CD29 (iAb) antibody. Control (co) indicates baseline phosphorylation of the respective kinase. Kinase phosphorylation of the IgG and iAb treatment was not different from control in any case. Unless indicated otherwise, comparisons were not significant. Data are presented as mean  $\pm$  s.e.m. \*  $p < 0.05$  and \*\*  $p < 0.01$  ( $n=3$  each).**

To further elucidate the pathways of kinase activation upon CD29 stimulation, the MEK inhibitor U0126 (U), the PI3K inhibitors Wortmannin (W) and LY294002 (LY), and the PKB inhibitor Akti1/2 (Akti) were used to inhibit selected parts of the signalling pathway.

Of the four inhibitors, U suppressed the  $\alpha$ -CD29-induced phosphorylation of ERK (figure 15A-D), and W, LY, and Akti (but not U) suppressed the  $\alpha$ -CD29-induced phosphorylation of PKB (figure 15E-G). No cross talk could be observed between the PI3K/PKB and the MEK/ERK signalling pathways. However, all inhibitors significantly reduced  $\alpha$ -CD29-induced GSK-3 $\beta$  (Ser9) phosphorylation (figure 15I-L). This observation places GSK-3 $\beta$  (Ser9) downstream of both the MEK/ERK and the PI3K/PKB pathways.

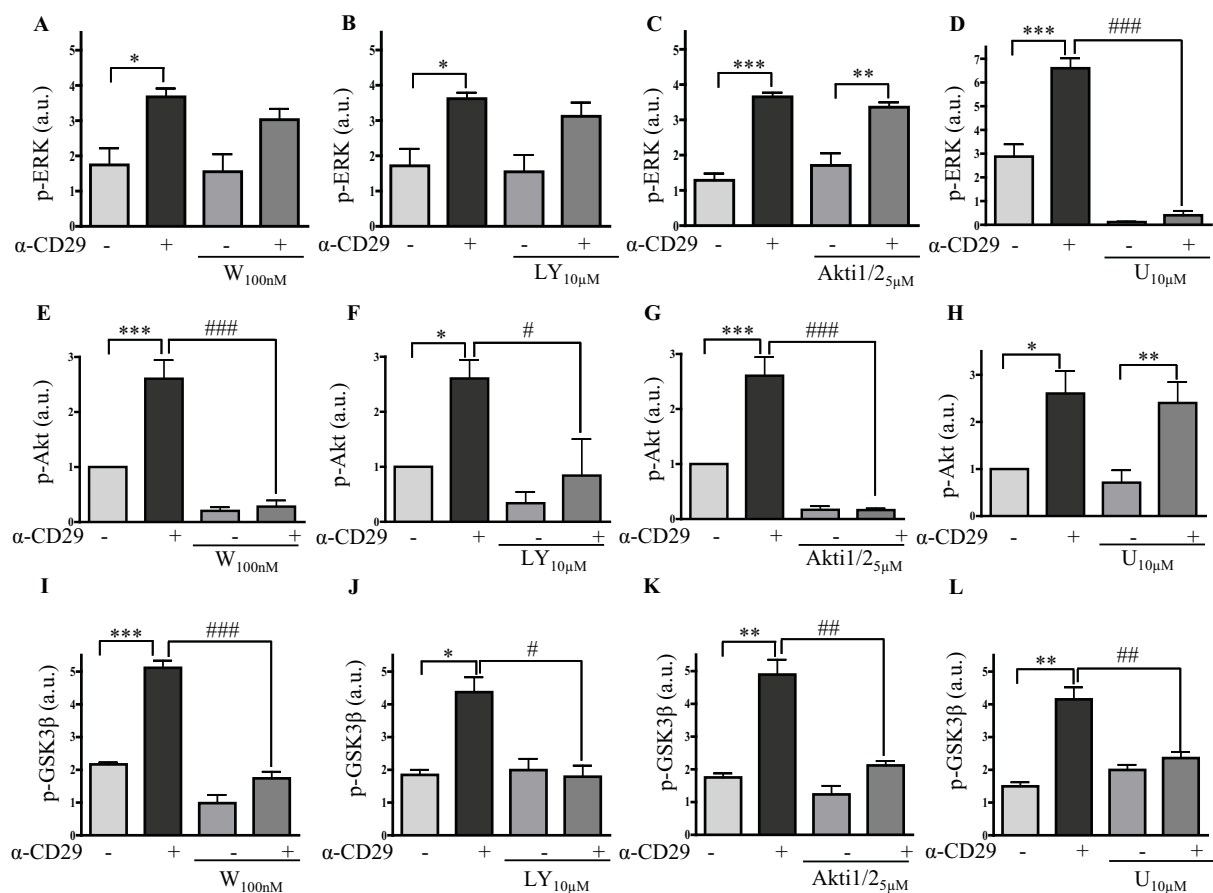


**Figure 15. GSK-3 $\beta$  is a downstream target of both, MEK/ERK and PI3K/PKB upon CD29 activation** (Western blot). Cardiomyocytes were treated with kinase inhibitors for 45 min prior to  $\alpha$ -CD29 administration (5  $\mu$ g/ml). The PI3K-inhibitors Wortmannin (W) and LY29400 (LY), the MEK1/2 inhibitor U0126 (U) and the PKB/Akt inhibitor Akti1/2 (Akti) were used. Phosphorylation-specific antibodies detected (A-D) ERK1/2 (Thr202/Tyr204), (E-H) PKB/Akt (Ser473) and (I-L) GSK-3 $\beta$  (Ser9), respectively. Data are mean  $\pm$  s.e.m. \* and #  $p < 0.05$ ; \*\* and ##  $p < 0.01$ ; \*\*\* and ###  $p < 0.001$ . (n=3 for I-L, H; n=4 for E-G, C; n=5 for A, B, D).

## 5.2.) CD29 activation induces a time-dependent oxidative burst

To assess whether CD29 activation generates ROS in NRVM, the redox-sensitive cell permeable dye DCF was used. Flow cytometry analyses demonstrated a significant increase in DCF fluorescence indicated by a shift to the right (i.e., an oxidative burst, figure 16) [Vowells, Sekhsaria et al. 1995]. After 30 min of incubation of NRVM with an activating  $\alpha$ -CD29 antibody, the oxidative burst was evident and subsided to almost control levels at the 2 hours time point (figure 16C, D). A similar increase in DCF fluorescence was observed in response to exogenous ROS ( $H_2O_2$ , 200  $\mu$ M) and to 12-phorbol 13-myristate acetate (PMA, 1  $\mu$ M), which induces endogenous ROS in other cell types [Babior 1999; Li, Mullen et al. 2002] (figure 16A, B).

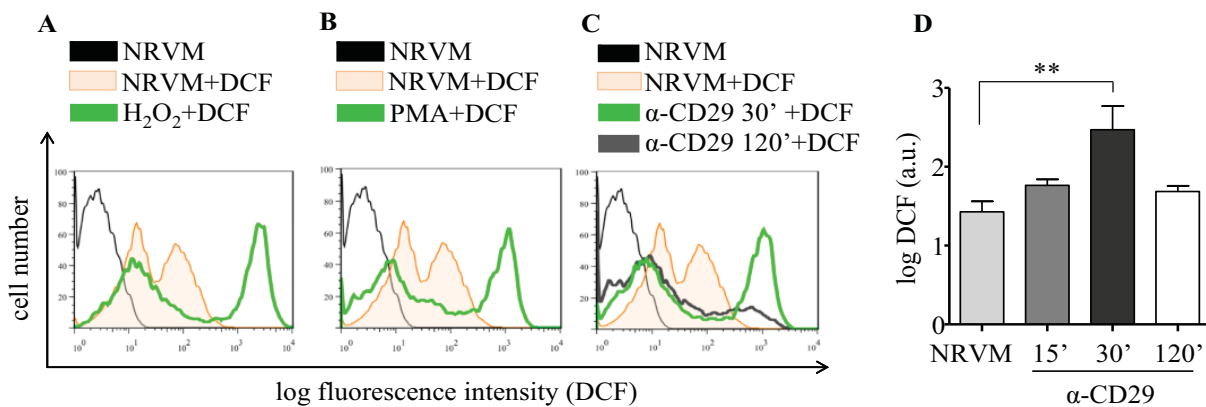


**Figure 16. CD29 activation induces an oxidative burst in NRVM.** Representative flow cytometry histograms depict NRVM loaded with the ROS indicator DCF (12.5  $\mu$ M). Unstimulated cells (NRVM) without DCF are shown in black. Fluorescence intensity is shown for unstimulated cells (NRVM+DCF, orange line) and cardiomyocytes stimulated with (A)  $H_2O_2$  (100  $\mu$ M), (B) PMA (1  $\mu$ M), or (C)  $\alpha$ -CD29 (5  $\mu$ g/mL) for 30 min (green line). The shift to the right indicates an increase in ROS. CD29 activation induced a time-dependent burst that peaked at 30 min (C and D, 30') and declined after 2 h (C, 120', grey line). Panel (D) depicts  $\alpha$ -CD29-induced fluorescence intensity at different time points. Data are mean  $\pm$  s. e. m. Unless indicated otherwise, comparisons were not significant. \*\* p < 0.001 (n=8).

**5.2.1.) The CD29-induced oxidative burst is impaired by apocynin and diphenylene iodonium in cardiomyocytes**

We further investigated a likely NOX-dependency of this burst by use of the synthetic inhibitors apo (500  $\mu$ M) and DPI (10  $\mu$ M). Apocynin has been described as a NOX inhibitor because of its ability to inhibit the regulatory NOX subunit p47<sup>phox</sup> in neutrophils. However, it is also described as an antioxidant [Heumüller, Wind et al. 2008]. Heumüller *et al.* (2008) state that it is unlikely for apo to directly act as a NOX inhibitor due to the lack of myeloperoxidase in vascular cells, myeloperoxidase activating the drug in leukocytes. DPI inhibits flavoenzymes including NOX [Lambeth, Krause et al. 2008].

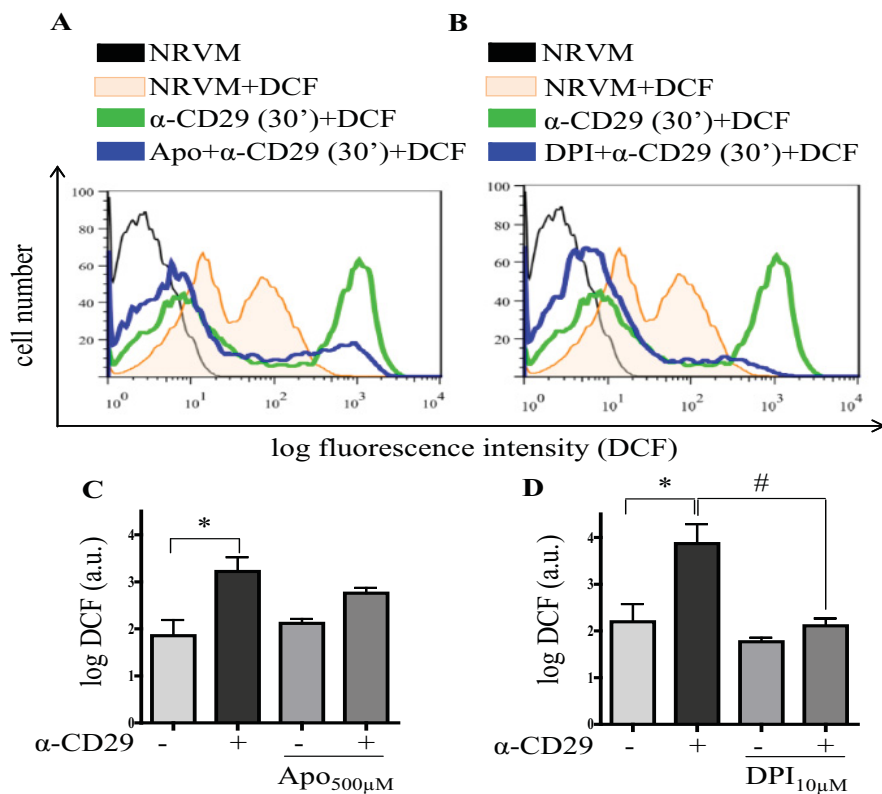


**Figure 17. The CD29-induced oxidative burst is inhibited by apocynin and DPI.** Cells were pretreated (in blue) with either apocynin (Apo; 500  $\mu$ M, 14-16 h), or DPI (10  $\mu$ M, 45 min) prior to  $\alpha$ -CD29 administration (5  $\mu$ g/mL, 30 min). (A, B) Controls and colours are as in figure 16. Pretreatment suppressed the  $\alpha$ -CD29-induced oxidative burst partially (apo, n=4) and completely (DPI, n=5) (C, D). Data are presented as mean  $\pm$  s. e. m. Unless indicated otherwise, comparisons were not significant. \* and # p < 0.05.

As shown in figure 16, CD29 engagement induced an oxidative burst (DCF-positive cells) after 30 min indicated by the green line depicted in figure 17A and B. Both apo and DPI markedly decreased DCF fluorescence intensity when administered prior to  $\alpha$ -CD29 (figure 17A-D), as shown by the blue line where DCF-positive cardiomyocytes shift to the left. In case of DPI, the respiratory burst declines to baseline levels (NRVM without treatment), whereas apo-treated cells still show residual burst activity.

### **5.3.) CD29-induced pro-survival signalling is ROS-dependent**

Newborn cardiomyocytes generated ROS upon  $\alpha$ -CD29 binding its receptor (figure 16), which raised the question whether CD29-induced signalling is ROS regulated. To test this hypothesis, MnTMPyP (MnT), a mimetic of the antioxidant enzymes SOD and cat, was used to reduce ROS levels. Pre-treatment with MnT significantly inhibited the  $\alpha$ -CD29-induced phosphorylation of ERK1/2 (figure 18A), Akt (figure 18B) and GSK-3 $\beta$  (figure 18C).

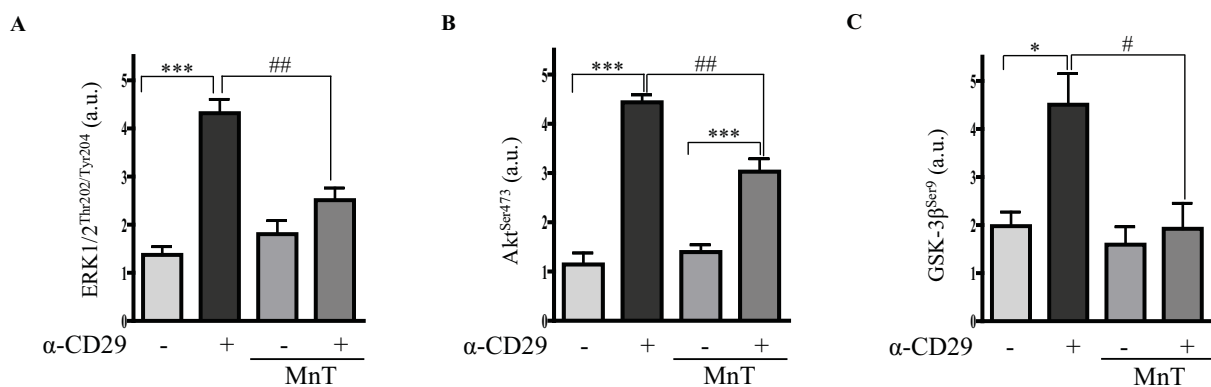


**Figure 18. MnTMPyP reduces CD29-induced pro-survival signalling.** Cells were treated with MnTMPyP (MnT, 5  $\mu$ M, 45 min) prior to  $\alpha$ -CD29 (5  $\mu$ g/mL, 15 min). Aliquots of total cell lysate were analysed with the respective rabbit  $\alpha$ -phospho-antibodies [ERK1/2 (Thr202/Tyr204), PKB/Akt (Ser473) and GSK-3 $\beta$  (Ser9)].  $\alpha$ -CD29-induced phospho-ERK1/2 (A, n=10), phospho-Akt (B, n=6) and phospho-GSK-3 $\beta$  (C, n=4) signals were blocked by the SOD/catalase mimetic MnT. Data are mean  $\pm$  s.e.m. Unless indicated otherwise, comparisons were not significant. \*\*\*  $p < 0.001$ , \*  $p < 0.05$ , ##  $p < 0.01$ , #  $p < 0.05$ .

Similarly, co-overexpression of SOD and cat using adenoviral constructs significantly reduced MEK, Akt and GSK-3 $\beta$  phosphorylation (figure 19A-C). Co-overexpression was performed by administering both SOD and cat simultaneously.

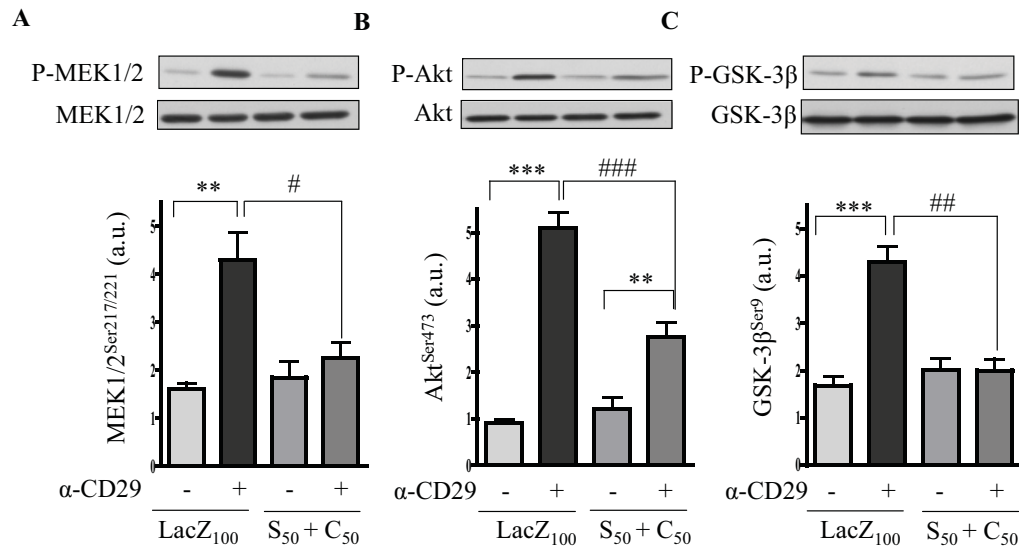


**Figure 19. CD29-induced pro-survival signalling depends on ROS.** (A-C) NRVM were infected with adenoviral constructs to express either,  $\beta$ -galactosidase (LacZ<sub>100</sub>) at 100 MOI or to co-overexpress SOD (S<sub>50</sub>) and cat (C<sub>50</sub>) at 50 MOI 36 hours prior to  $\alpha$ -CD29 administration (10  $\mu$ g/mL) for 15 minutes. Equal protein amounts were subjected to Western blotting using phosphorylation-specific antibodies for MEK1/2 (Ser217/221), PKB/Akt (Ser473) and GSK-3 $\beta$  (Ser9). Data are presented as mean  $\pm$  s. e. m. \*\*\* and ### p < 0.001, \*\* and ## p < 0.01 and # p < 0.05 (n=5 for A, B and n=3 for C). Unless indicated otherwise, comparisons were not significant.

Importantly, single-enzyme overexpression of SOD or cat was less effective than overexpression of both enzymes. Although either enzyme alone inhibited phospho-MEK1/2 (figure 20A) and phospho-GSK-3 $\beta$  (figure 20C), no inhibition of phospho-PKB (figure 20B) was observed, indicating that both enzymes are needed to attenuate CD29-induced ROS-dependent PKB signalling.

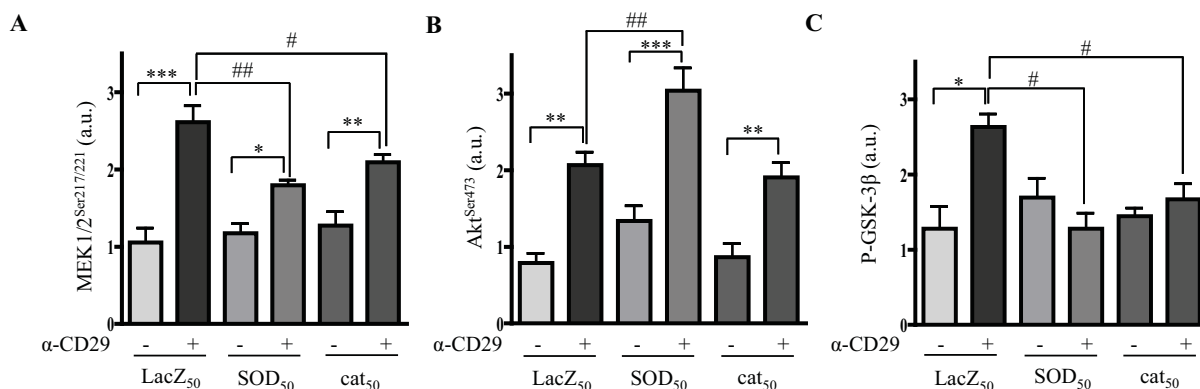


**Figure 20. Overexpression of SOD or catalase.** (A-C) CMC were transfected with adenoviral constructs to overexpress SOD (Ad.Cu/ZnSOD1; SOD<sub>50</sub>), cat (Ad.Catalase, Cat<sub>50</sub>) or  $\beta$ -galactosidase (Ad5CMVcytoLacZ; Lac<sub>50</sub>) at 50 MOI 36 hours prior to  $\alpha$ -CD29 administration (10  $\mu$ g/ml, 15 min). Single-enzyme overexpression of SOD significantly inhibited  $\alpha$ -CD29 induced phospho-MEK1/2(A) and -GSK-3 $\beta$  (C), whereas PKB/Akt phosphorylation (B) was significantly increased. In contrast, cat efficiently inhibited phosphorylation of all three kinases (A-C). Phospho-specific antibodies were rabbit  $\alpha$ -MEK1/2 (Ser217/221),  $\alpha$ -PKB (Ser473) and  $\alpha$ -GSK-3 $\beta$  (Ser9). Data are presented as mean  $\pm$  s.e.m. Unless indicated otherwise, comparisons were not significant. \* and #  $p < 0.05$ , \*\* and ##  $p < 0.01$ , \*\*\*  $p < 0.001$  (n=5 for A and B, n=3 for C).

#### **5.4.) CD29-induced pro-survival signalling is inhibited by apocynin and DPI**

To test the role of NOX in CD29-induced pro-survival signal transduction, apo and DPI were used. Both inhibitors suppressed CD29-induced ERK1/2 phosphorylation (figure. 21A, D) and PKB-phosphorylation (figure 21B, E). Although both apo and DPI also inhibited CD-29-induced GSK-3 $\beta$  phosphorylation, a reliable assessment of this inhibition is not possible, because both substances affected basal kinase phosphorylation (figure 21C, F). Nevertheless, these findings suggest that NOX might serve as the source of CD29-induced ROS that trigger ROS-dependent pro-survival signalling in cardiomyocytes.

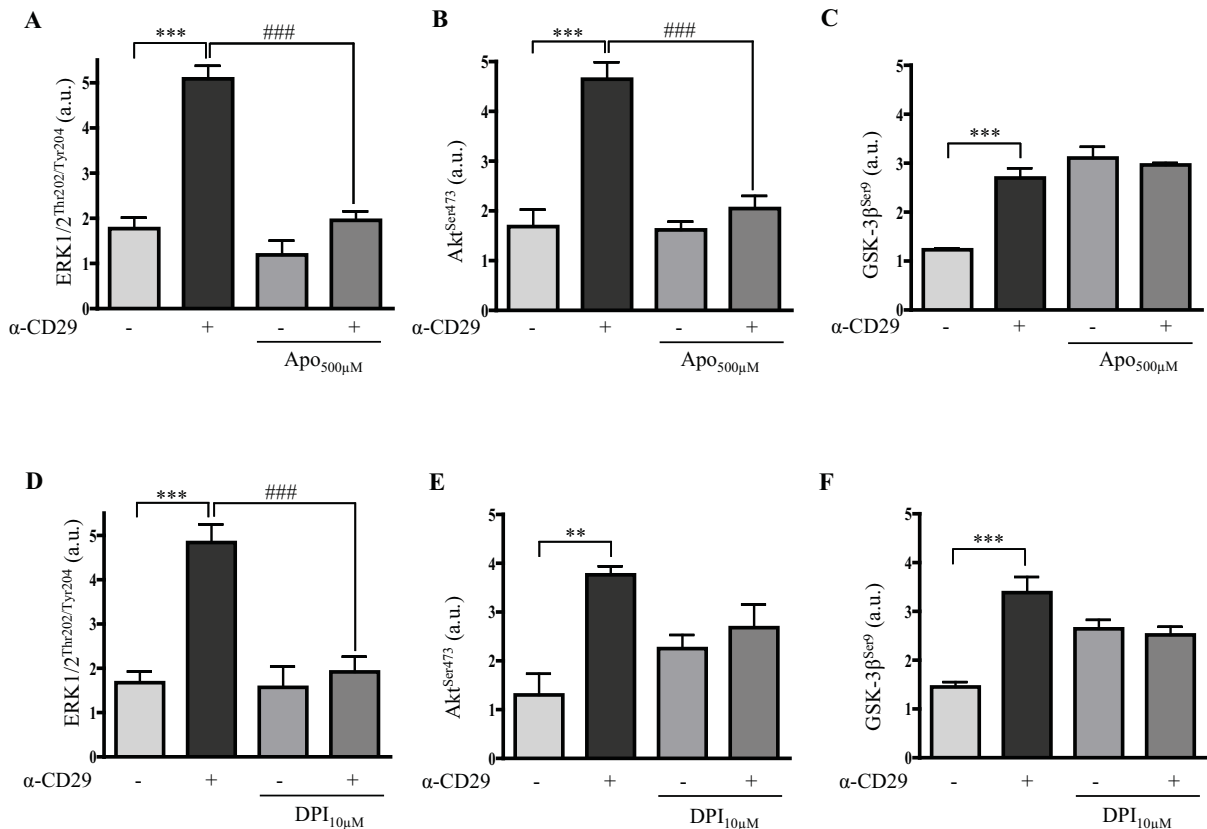


**Figure 21. Apocynin and DPI impair CD29-induced survival signalling.** Apocynin (500 µM) was administered overnight and DPI (10 µM) 45 minutes prior to α-CD29 (5 µg/ml, 15 min). The phospho-specific antibodies used were rabbit α-ERK1/2 (Thr202/Tyr204), α-PKB/Akt (Ser473) and α-GSK-3β (Ser9). Data are presented as mean ± s.e.m. Unless indicated otherwise, comparisons were not significant. \*\* p < 0.01, \*\*\* and ### p < 0.001 (n=4 for C and F; n=5 for B; n=6 for A, D and E).

### **5.5.) gp91<sup>phox</sup>- and p47<sup>phox</sup>-deficient cardiomyocytes show loss of α-CD29-induced pro-survival signals**

Another set of experiments corroborated NOX as the source of ROS; by examining α-CD29-induced signalling in NMVM isolated from gp91<sup>phox</sup> (NOX2; *CYBB*) knock-out mice and from mice lacking a functional catalytic subunit p47<sup>phox</sup> (p47<sup>phox</sup> LOF). In *CYBB* knock-out strains, a neomycin resistance gene is inserted in exon 3 so that no protein is expressed<sup>12</sup>. p47<sup>phox</sup> LOF strains were generated by a point mutation in the *Ncf1* gene. This mutation is an A to C transversion at position -2 at the 5' end of exon 8 of the *Ncf1* gene, resulting in aberrant

<sup>12</sup> <http://jaxmice.jax.org/strain/002365.html>



splicing of the *Ncf1* transcript, no intact p47<sup>phox</sup> protein being detectable by Western blotting in cells from these mice<sup>13</sup>. Upon CD29 stimulation, significantly lower levels of phospho-ERK1/2, phospho-PKB and phospho-GSK-3 $\beta$  were observed in NOX2-knock-out NMVM as compared to wild-type (wt) (figure 22A-C). In p47<sup>phox</sup> LOF NMVM, CD29 activation failed to induce phosphorylation of PKB (Ser473) (figure 22E) and GSK-3 $\beta$ (Ser9) (figure 22F). By contrast, CD29-induced phosphorylation of ERK1/2 (figure 22D), was unaffected by the loss of functional p47<sup>phox</sup>, suggesting the activation of a p47<sup>phox</sup>-independent and/or compensatory pathway.

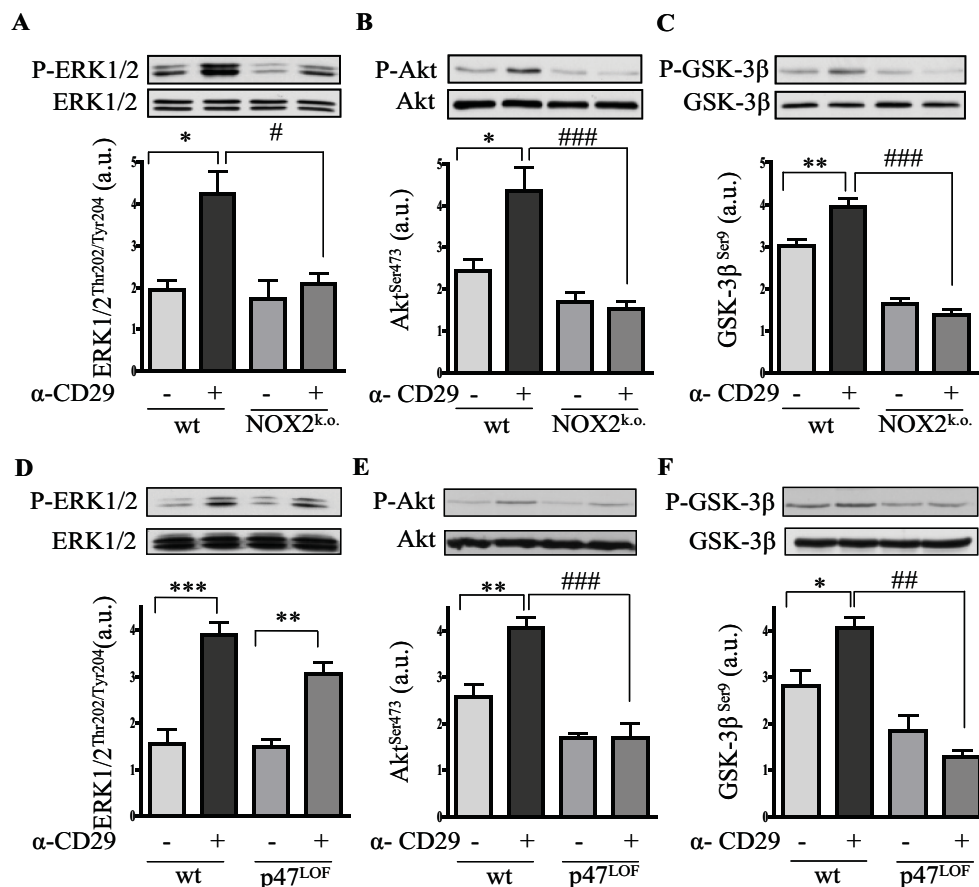


**Figure 22. CD29-induced signal transduction requires NOX2-derived ROS.**  $\alpha$ -CD29 administration (10  $\mu$ g/mL, 15 min) induced phosphorylation of ERK1/2 (p44/42), PKB/Akt and GSK-3 $\beta$  in wt NMVM (A-F).  $\alpha$ -CD29 induced phosphorylation was absent in NOX2 knock-out (NOX2<sup>k.o.</sup>) cardiomyocytes (A-C); and partially diminished in p47<sup>phox</sup> LOF (p47<sup>LOF</sup>) NMVM (D-F). Data are presented as mean  $\pm$  s. e. m. Unless indicated otherwise, comparisons were not significant. \*  $p < 0.05$ ; \*\* and ##  $p < 0.01$ ; \*\*\* and ###  $p < 0.001$  (n=5 for A, C, D-F; n=6 for B).

<sup>13</sup> <http://jaxmice.jax.org/strain/004742.html>

## 5.6.) The CD29-induced oxidative burst is impaired in p47<sup>phox</sup> LOF, but not in NOX2 knock-out cardiomyocytes

Because NOX2-derived ROS play an important role in CD29-induced pro-survival signalling in NMVM, we tested whether the CD29-induced oxidative burst was impaired in NMVM deficient in NOX2 or p47<sup>phox</sup>. Upon activation of CD29, a shift in DCF fluorescence was observed in wt NMVM, which was missing in p47<sup>phox</sup> LOF NMVM (figure 23A, C).

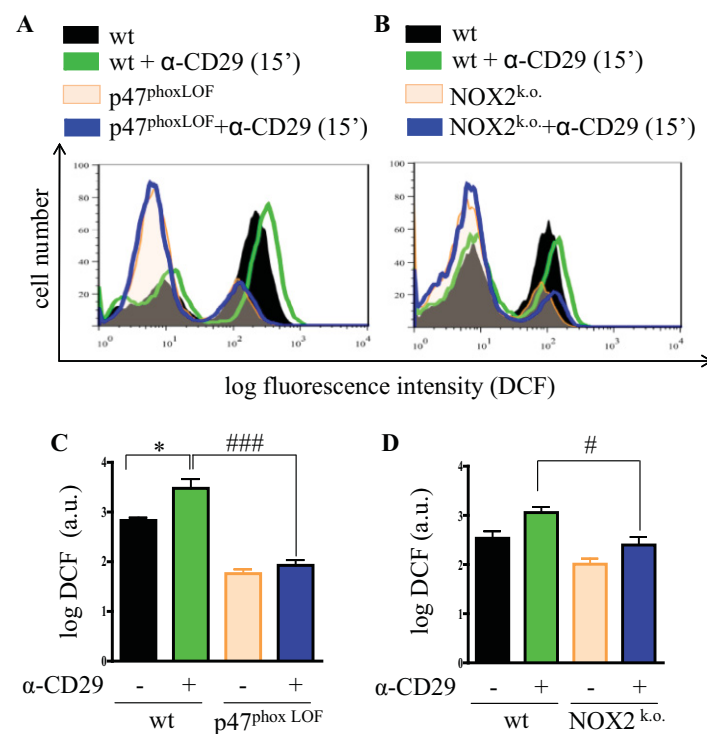


**Figure 23. Lack of CD29-induced oxidative burst in p47<sup>phox</sup> LOF cardiomyocytes.** Serum-starved NMVM were incubated with DCF (12.5  $\mu$ M, 20 min) before detaching with accutase. Wt cardiomyocytes and cells deficient in functional NOX subunits were treated with  $\alpha$ -CD29 antibody (15  $\mu$ g/mL, 15 min) and DCF intensity was measured by flow cytometry. Representative histograms of p47<sup>phox</sup> LOF (A, C) and NOX2 k.o. (B, D) NMVM depict untreated wt (black),  $\alpha$ -CD29 treated wt (green), untreated (orange) and treated (blue) (A) p47<sup>phox</sup> LOF or (B) NOX2 k.o. cardiomyocytes. Quantitative data (C, D) are presented as mean  $\pm$  s. e. m. Unless indicated otherwise, comparisons were not significant. \* and #  $p < 0.05$ ; ###  $p < 0.001$  (n=4 each).

In contrast, in NOX2 knock-out cells, CD29 activation enhanced DCF fluorescence (figure 23B), although the level of DCF fluorescence was significantly reduced compared to wt (figure 23D). Therefore, another p47<sup>phox</sup>-dependent NOX (e.g. NOX1) [Bánfi, Clark et al. 2003] might be involved in CD29-induced ROS formation in NMVM.

## **5.7.) Effects of CD29 activation on SAPK/JNK phosphorylation**

CD29 engagement induces JNK phosphorylation that peaks at 15 minutes; this signal is lost by 45 minutes. As was observed previously (section 5.1.), neither the inhibitory CD29 nor unspecific IgG indicated any activation pattern (figure 24).

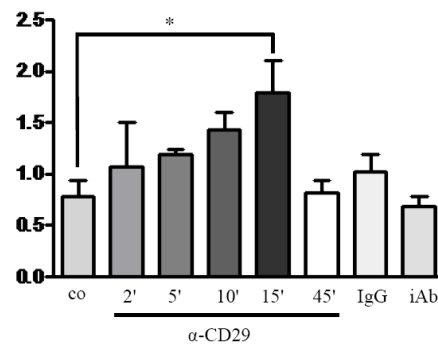


**Figure 24. CD29 engagement induced time-dependent phosphorylation of JNK1/2, as detected by Western blotting.** NRVM were treated with 5  $\mu$ g/mL activating  $\alpha$ -CD29 antibody, unspecific IgG (IgG) or inhibitory anti-CD29 (iAb) antibody. Control (co) indicates baseline phosphorylation of JNK. Kinase phosphorylation after IgG and iAb treatment was not different from control. Unless indicated otherwise, comparisons were not significant. Data are presented as mean  $\pm$  s.e.m. \*  $p < 0.05$  (n=2).

### ***5.7.1.) Localization of SAPK/JNK1/2 in CD29-induced signalling***

The use of the PI3K inhibitors (W and LY) and the PKB inhibitor (Akt1/2) revealed no cross-talk of PI3K and PKB with SAPK/JNK. By contrast, the MEK inhibitor (U) suppressed CD29-induced SAPK/JNK phosphorylation (figure 25). This places SAPK/JNK1/2 downstream of MEK/ERK.

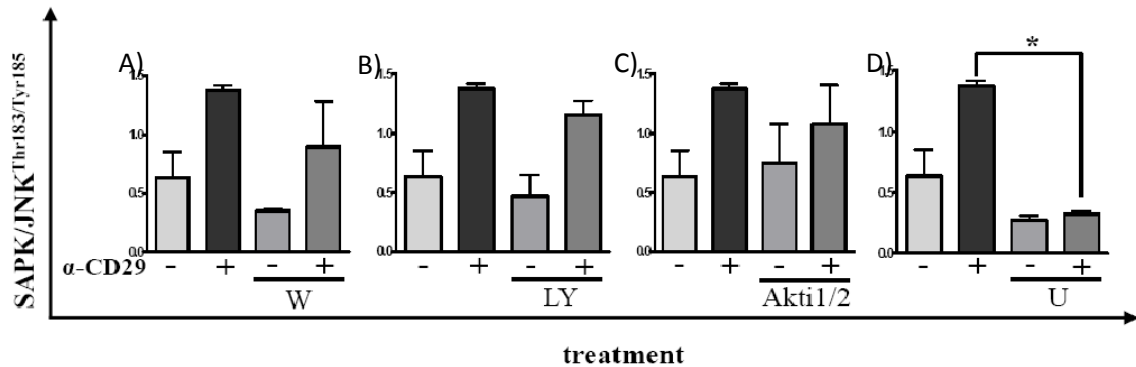


**Figure 25. Localization of SAPK/JNK in  $\alpha$ -CD29 stimulated cardiomyocytes.** SAPK/JNK is downstream of MEK/ERK. Cardiomyocytes were treated with kinase inhibitors for 45 min prior to  $\alpha$ -CD29 administration (5  $\mu$ g/mL). The PI3K-inhibitors Wortmannin (W) and LY29400 (LY), the MEK1/2 inhibitor U0126 (U) and the PKB inhibitor Akti1/2 were used. Phosphorylation-specific antibodies detected (A-D) SAPK/JNK (Thr183/Tyr185). Data are mean  $\pm$  s.e.m. \*  $p < 0.05$ ; (n=2).

### 5.7.2.) Effect of JNK inhibition on GSK-3 $\beta$ phosphorylation

Ciani & Salinas (2007) demonstrated that in Wnt Dvl (dishevelled) signalling in mouse neurons, concomitant inhibition of GSK-3 $\beta$  involves the activation of the JNK pathway that results in increased microtubule stability [Ciani and Salinas 2007]. To test whether GSK-3 $\beta$  is likely to be a downstream kinase of SAPK/JNK, the inhibitor SP60015 (SP) was used. Preliminary results in NRVM indicated that CD29-induced GSK-3 $\beta$  (Ser9) phosphorylation was inhibited by JNK inhibition (figure 26).

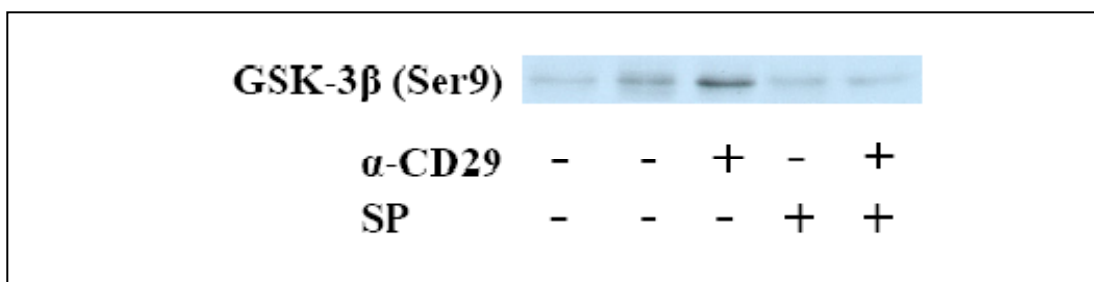


**Figure 26. CD29 induced GSK-3 $\beta$  phosphorylation is repressed by an SAPK/JNK inhibitor (SP).** (n=1).

### 5.7.3.) Effect of apocynin and the flavoenzyme inhibitor DPI on SAPK/JNK phosphorylation

As reported in section 5.4., the flavoenzyme inhibitor DPI and the antioxidant apo inhibited the survival kinases ERK1/2 and PKB. To investigate whether the SAPK/JNK signal was also induced by ROS, DPI was administered 45 min. and apo about 17 h. prior to the 15 min  $\alpha$ -CD29 treatment. Although the mean values of only 2 experiments are depicted in figure 27, it appears very likely that CD29-induced SAPK/JNK phosphorylation is dependent on ROS.

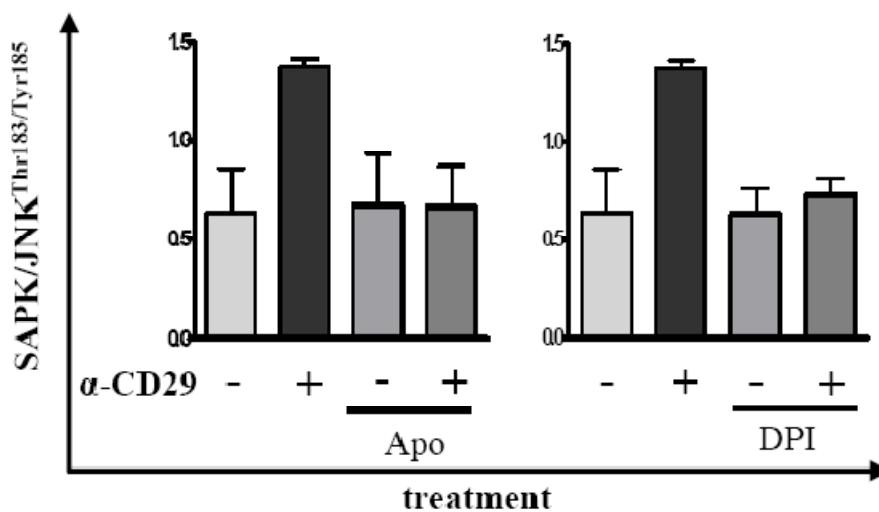


**Figure 27. Inhibition of SAPK/JNK upon treatment with synthetic compounds.** Apocynin (Apo, 500  $\mu$ M) was incubated for 14-16 h, whereas DPI (10  $\mu$ M) was applied for 45 minutes prior to CD29 treatment for 15 minutes. Data are presented as mean  $\pm$  s.e.m. (n=2).

### 5.8.) Src tyrosine kinase is upstream of both MEK/ERK and PI3K/PKB

Cardiomyocytes were treated with the Src kinase inhibitors SU6656 (SU, 10  $\mu$ M) and pyrazolopyrimidin (PP2, 10  $\mu$ M) for 45 min prior to CD29 administration (5  $\mu$ g/mL). Both SU and PP2 have been considered to be selective Src inhibitors [Hanke, Gardener et al. 1996; Blake, Broome et al. 2000], although Bain *et al.* (2007) showed that also AMP Kinase or Mammalian sterile 20-like kinase 2 (MST2) are inhibited by SU [Bain, Plater et al. 2007].

MST2 is a Ste20-like kinase that encodes a serine/threonine kinase that functions as MAPK [O'Neill, Matallanas et al. 2005] which activates JNK in response to stress and is inhibited by PKB in kidney cells [Kim, Shu et al. 2010]. SU showed no effect in inhibiting phospho-ERK (figure 28A), but the phospho-signals of PKB (figure 28B) and GSK-3 $\beta$  (figure 28C) were reduced significantly. PP2 was more efficient in inhibiting ERK1/2, PKB and GSK-3 $\beta$  kinase than SU.

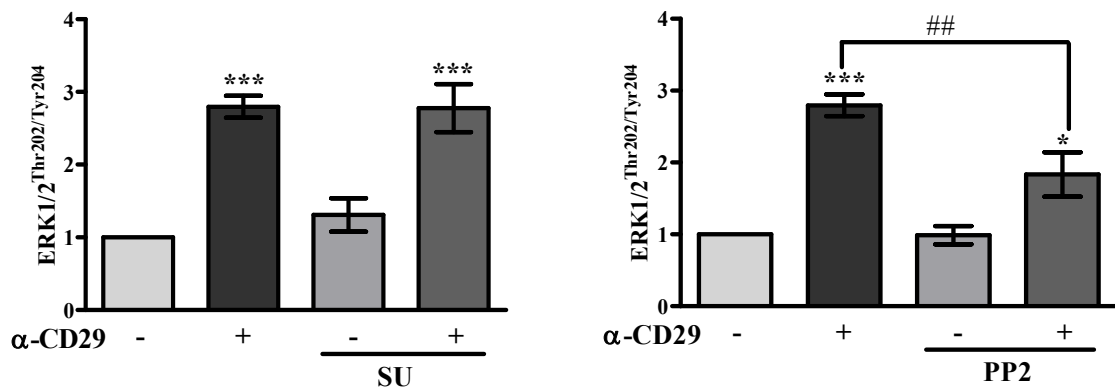


**Figure 28A.** There was no inhibition of phospho-ERK1/2 with Src kinase inhibitor, whereas PP2 diminished ERK1/2 phosphorylation in newborn cardiomyocytes. Data are mean values  $\pm$  s.e.m. \*  $p < 0.05$ , ##  $p < 0.01$ ; \*\*\*  $p < 0.001$  (n=3).

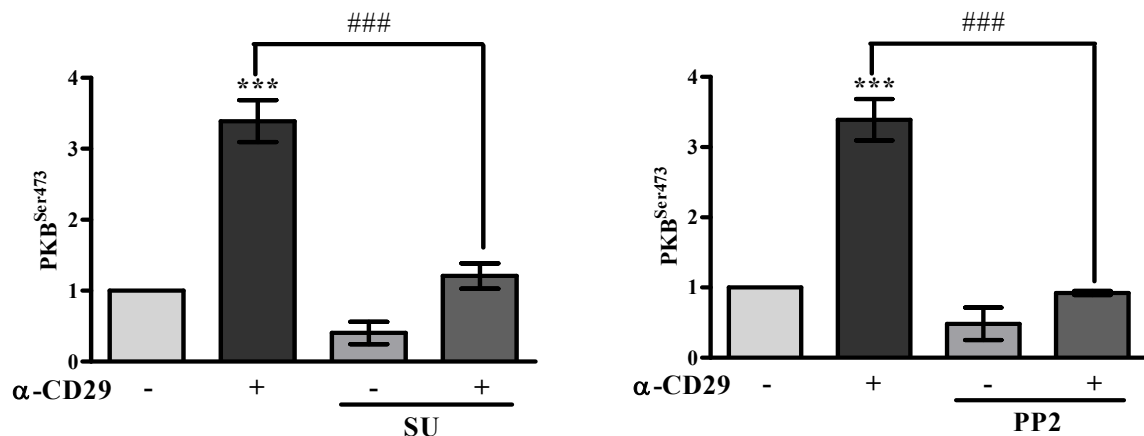


**Figure 28B.** Src kinase inhibitors SU and PP2 reduce CD29-induced PKB phosphorylation in NRVM. \*\*\* and ###  $p < 0.001$  (n=3).

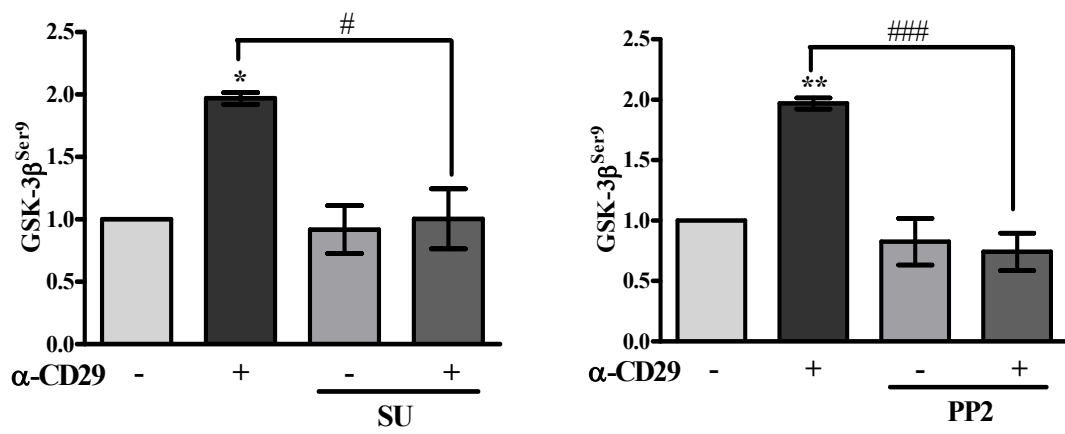


**Figure 28C.** CD29-induced GSK-3 $\beta$  Ser9 phosphorylation is reduced in the presence of both Src kinase inhibitors SU and PP2. Data are mean values  $\pm$  s.e.m. \* and #  $p < 0.05$ ; \*\*  $p < 0.01$ , ###  $p < 0.001$  ( $n=3$ ).



### 5.8.1.) Src family kinase is ROS dependent

As previously shown, pro-survival kinases were ROS dependent. To switch Src kinase activity on, a protein tyrosine phosphatase dephosphorylates Src at Tyr527, after which autophosphorylation of Tyr416 is necessary for complete activation [Cooper and Howell 1993]. A phospho-specific antibody for Src Tyr416 and antibody specific to unphosphorylated Src Tyr527 were used to determine whether Src activity depends on ROS. First, the synthetic antioxidant compound apocynin (figure 29A) was used to determine ROS involvement. Second, the enzymes catalase and SOD were applied synergistically to newborn cardiomyocytes by use of adenoviral constructs. Preliminary data indicate that Src family kinase might be ROS regulated, because apocynin inhibits Src Tyr527 signals. Further, overexpression of both constructs diminished phosphorylation of Src kinase Tyr416 as shown by Western blot analysis

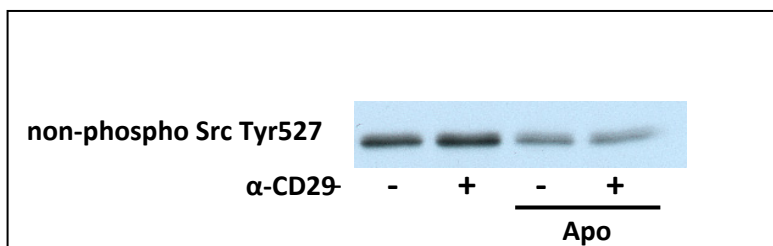


Figure 29A. Apocynin inhibits CD29-induced Src kinase signals (Western blot).

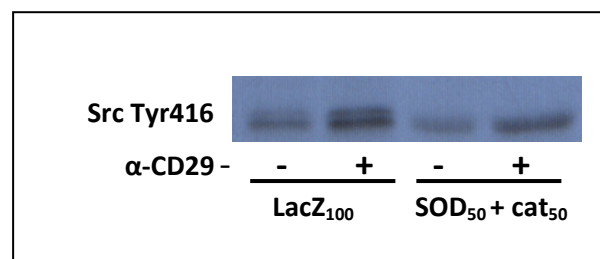
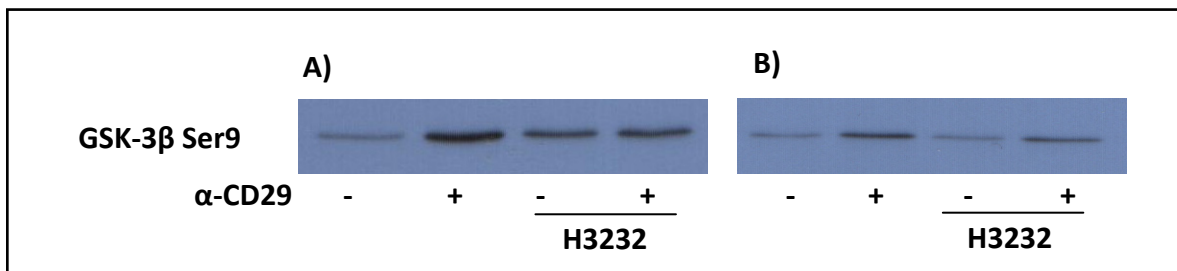


Figure 29B. Synergistic expression of SOD (SOD at 50 MOI) and catalase (cat at 50 MOI) inhibits phospho Src kinase Tyr416 signals.

### 5.8.2.) Protein kinase C inhibits CD29-induced GSK-3 $\beta$ phosphorylation

To investigate whether GSK-3 $\beta$  is a target of PKC, NRVM and rat cardiomyoblasts were treated with the PKC inhibitor H3232 for 45 minutes prior to CD29 administration (15 minutes). H3232 is a synthetic peptide which binds to the pseudosubstrate domain of PKC and inhibits its kinase activity. [Alexander, Hexham et al. 1989; Jakab, Weiger et al. 1996]. Similar patterns as in NRVM were observed in H9c2 cells, namely H3232 inhibited CD29 induced GSK-3 $\beta$  (Ser9) inactivation (figure 30).



**Figure 30.** H3232 inhibition of the GSK3 $\beta$  signal in NRVM (A) and H9c2 (B) cells is shown.

### 5.8.3.) Effects of the Src kinase inhibitor PP2, SU and PKC inhibitor on ROS generation

In cardiac myoblasts, DCF fluorescence was clearly reduced after treatment with the PKC inhibitor H3232, as compared to control NRVM. Both datasets (figure 31A and B) hint at the involvement of PKC in ROS formation (figure 31A) and at being located upstream of NOX (figure 31B).

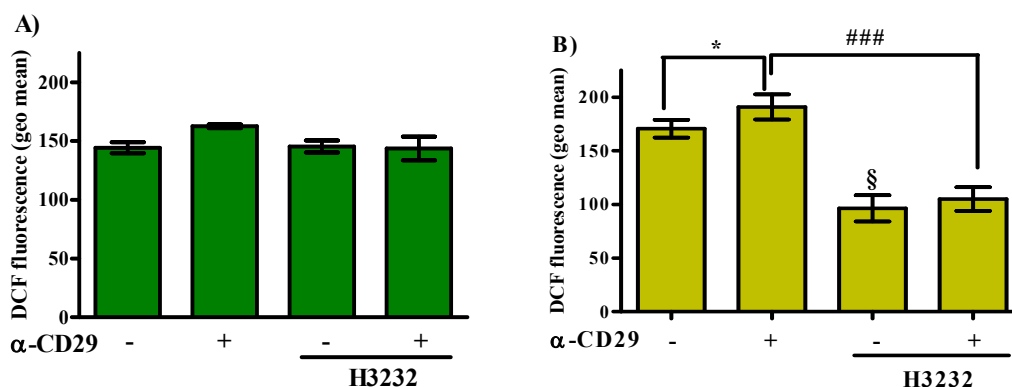


**Figure 31.** H3232 inhibits the CD29-induced burst in NRVM (A) and H9c2 (B). Data are presented as mean values  $\pm$  s.e.m. (n=2) \* p < 0.05, ### p < 0.001; § p < 0.05 vs. H9c2 without  $\alpha$ -CD29 treatment.

In H9c2 cells, the CD29-induced burst seemed to peak earlier than in cardiac myocytes. Like for CMC, H<sub>2</sub>O<sub>2</sub> and PMA served as positive controls and induced strong DCF fluorescence. Preliminary data indicated that PP2 did not inhibit the burst in CMC. However, it affected ROS generation in H9c2 cells, whereas SU inhibited the CD29-induced burst in cardiomyocytes. Some studies state that W inhibits the oxidative burst [Colavitti, Pani et al. 2002], while others implicate PKC as a regulator of NOX [Raad, Paquet et al. 2009]. Although further investigations need to be performed to test whether Src lies upstream of NOX, PKC is likely to be an upstream kinase of NOX in NRVM and H9c2, because it inhibits the production of oxygen radicals. It is noteworthy that Western blot analyses revealed almost no increase in phosphorylation of PKC $\zeta$  in wt mouse CMC, whereas in NOX2 knock-out cardiomyocytes with and without CD29 treatment an increase in PKC $\zeta$  phosphorylation was observed that was not detected in p47<sup>phox</sup> LOF cardiomyocytes (figure 32).

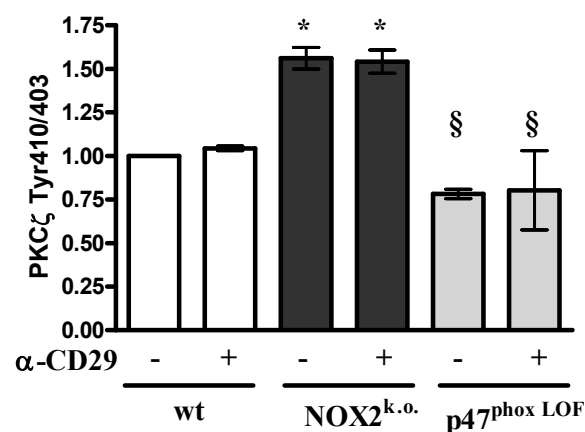


**Figure 32. Phosphorylation of PKC $\zeta$  in different mouse cardiomyocyte strains.** \*p<0.05 vs. wt CMC; § p<0.05 vs. NOX2 k.o.(n=2)

## **5.9.) Preliminary gene expression data**

### **5.9.1.) NOX expression**

Preliminary data on *NOX* gene expression suggest the presence of *NOX1*, *NOX2* and *NOX4*, although time course experiments only indicate very low levels of *NOX4*. *NOX* expression data have to be interpreted cautiously, however, because semi-quantitative PCR was used, and the expression of the control gene. *GAPDH* itself was not constant among all different samples analysed (not shown). Nevertheless, *NOX1* and *NOX2* appeared to be expressed at much higher levels than *NOX4* (figure 33A-C), and *NOX1* levels seemed higher throughout all time points (30 min to 16 h) than *NOX2* levels. This contrasts with data by Hingtgen *et al.* (2006), who showed that neonatal cardiomyocytes and adult left ventricular cardiomyocytes predominantly expressed *NOX2*, while *NOX1* was barely detectable [Hingtgen, Tian et al. 2006]. In VSMC, Ang II activates both *NOX1* mRNA and *NOX2* gene and *NOX2* protein levels [Lyle and Griendling 2006].

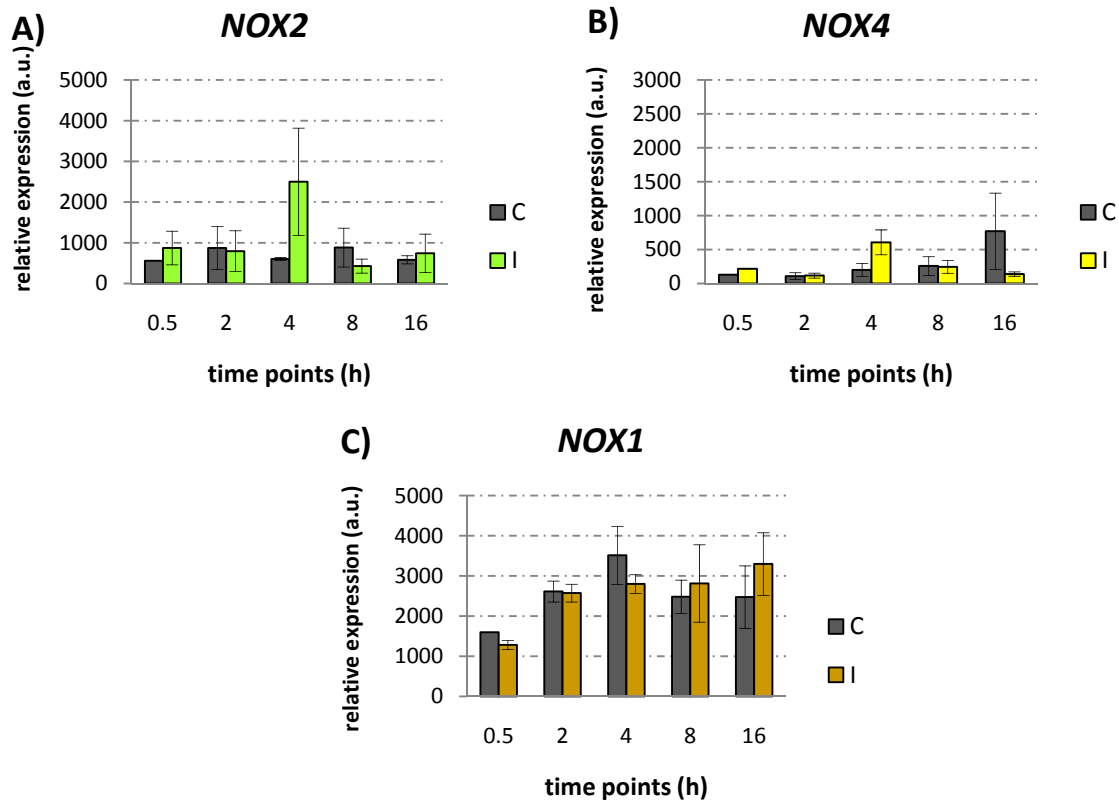


**Figure 33. Expression patterns of NOX gene copies in NRVM.** C: control without any stimulus; I represents cells treated with  $\alpha$ -CD29 antibody, measured at the indicated time points after treatment. NOX2 and NOX4 were amplified for 40 cycles, and NOX1 for 31 cycles. NOX2 and NOX4 levels are thus directly comparable because they were amplified for the same number of cycles. The bars indicate less NOX4 than NOX2. Although NOX1 was measured at a different, lower cycle number, its relative expression level is much higher compared to NOX2. These data indicate that NOX4 is less highly expressed than NOX2 and NOX1. (n=2)

It is clear that further experiments are required to establish and validate NOX gene expression patterns, ideally using a more precise quantitative method such as quantitative real-time RT-PCR.

### 5.9.2.) Expression patterns of stress responsive and anti-apoptotic genes

Preliminary investigations of Cu/Zn SOD (*SOD1*), haem oxygenase 1 (*HO-1*), NF $\kappa$ B, signal transducer and activator of transcription 3 (*STAT3*) and *Bcl2* expression were performed. NF $\kappa$ B is a redox-sensitive transcription factor implicated in cell survival [Trachootham, Lu et al. 2008], and HO-1 an inducible stress protein that is reported to be anti-apoptotic and

cardioprotective [Wang, Hamid et al. 2010]. HO-1 and SOD1 are reported to protect from oxidative stress [Matés 2000]; Bcl2 protects cells from stress-induced apoptosis [Zhang, Vuori et al. 1995]. Preliminary data on *SOD*, *HO-1*, *Bcl2* and *NFκB* gene expression are shown in figure 34A-D. *Bcl2*, *HO-1* and *SOD1* were induced upon CD29 engagement at 2 h and 4h time points.

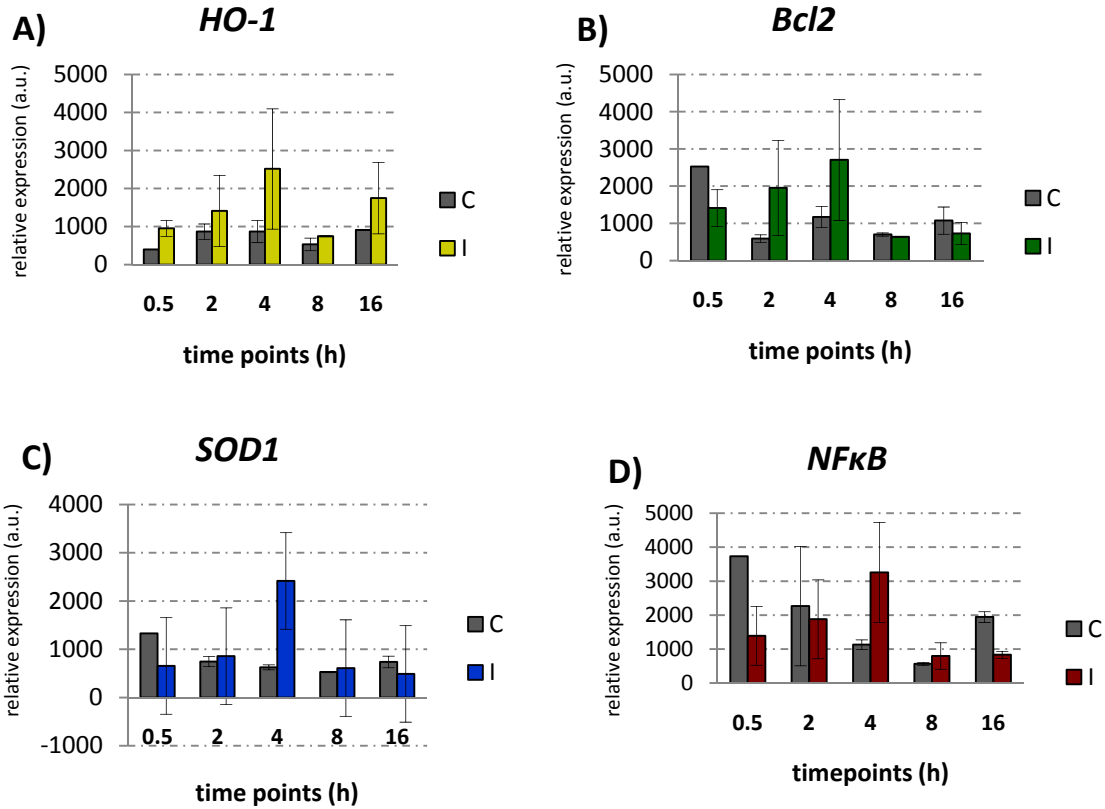


**Figure 34. Expression patterns of Cu/Zn SOD (*SOD1*), haem oxygenase (*HO-1*), *NFκB* and *Bcl2* in NRVMs.** C: control; I: CD29-treated cells, measured at the indicated time points. The expression levels cannot be compared directly among the different genes, because their expression was assayed at different cycle numbers. *SOD* (32 cycles), *HO-1* (40 cycles); *NFκB* (33 cycles) and *BCL2* (35 cycles) (n=2).

## 6.) DISCUSSION

### 6.1.) CD29 and the oxidative burst

It has become evident that moderate or low levels of ROS act as mediators in cellular signalling processes. The production and removal of ROS are tightly regulated by enzymatic (e.g., SOD, catalase) and non-enzymatic (e.g., ascorbic acid,  $\alpha$ -tocopherol) systems that ensure a balanced redox-system. While under physiological conditions, low levels of ROS act transiently and locally, excessive ROS levels are harmful to bystander cells and adjacent tissue by damaging proteins, lipids, DNA and carbohydrates, resulting in injury and pathophysiological processes.  $H_2O_2$  levels greater than 0.1 mM promote apoptosis in neonatal and adult cardiomyocytes [Aikawa, Komuro et al. 1997; Kwon, Pimentel et al. 2003]. The latter became necrotic when exposed to levels greater than 1 mM [Aikawa, Komuro et al. 1997].

However, in the experiments described in this thesis, the generated oxygen radicals and non-radicals seemed to be present at low levels rather than in excessive amounts. We showed that CD29-induced ROS generation occurred within a one-hour time interval. This burst was impaired by DPI and apo. Interestingly, these findings are in agreement with DPI-based data implicating NOX in CD29-induced ROS production in the colic adenocarcinoma cell line (caco-2) [Honoré, Kovacic et al. 2003], but not with findings from mouse embryonic FB (NIH-3T3), where growth factors and integrin-derived ROS were mostly 5-lipoxygenase (5-LOX)-dependent [Chiarugi, Pani et al. 2003]. At 2 hours, the level of ROS declined to baseline levels, but we observed a second wave of ROS generation at three to four hours after activation of the integrin receptor. Using NOX subunit-deficient mouse strains, we showed that NOX is responsible for ROS generation in cardiomyocytes. The finding that inhibition of ROS formation is more pronounced in  $p47^{phox}$  LOF than in NOX2 knock-out cells implies the involvement of another functional NOX member (i.e., not NOX2). NOX4 differs from NOX2 and NOX1 by being independent of regulatory subunits like  $p47^{phox}$ , only requiring the transmembrane  $p22^{phox}$  subunit [Ambasta, Kumar et al. 2004] for activity. The most likely candidate therefore is NOX1, since its activity also depends on phagocytic  $p47^{phox}$  regulatory subunits in certain tissues [Chen, Craige et al. 2009]. In general, NOX1 functions with the

p47<sup>phox</sup> homologue NOXO1 [Bánfi, Clark et al. 2003], which is dispensable where p47<sup>phox</sup> is present, as e.g. in HEK293 cells [Gianni, Diaz et al. 2009].

Our findings clearly implicate NOX as the source of ROS upon CD29 activation. However, Taddei *et al.* (2007) showed that in NIH 3T3 (mouse embryonic FB), integrin engagement through FN binding induced an initial, mitochondria-derived burst, followed by a second ROS release attributed to 5-LOX [Taddei, Parri et al. 2007]. O'Donnell & Azzi (1996) also addressed LOX as potential source of ROS in human skin FB upon nicotinamide nucleotide stimulation [O'Donnell and Azzi 1996]. Touyz & Schiffrin (1999) showed ang II-mediated phospholipase D-dependent and NOX-sensitive, ROS formation in VSMC [Touyz and Schiffrin 1999]. Of particular importance are the findings of Bonizzi *et al.* (1999), who showed distinct ROS involvement in IL-1 $\beta$  induced NF $\kappa$ B activation [Bonizzi, Piette et al. 1999]. In lymphoid cells, ROS formation depends on LOX, whereas in epithelial cells, IL-1 $\beta$  did not generate ROS and NF $\kappa$ B activation was independent of 5-LOX. Interestingly, IL-1 $\beta$  treatment of monocytes led to NOX-dependent ROS production. Taken together, these findings highlight that the contribution of different ROS sources to overall ROS levels depends on the cell type upon IL-1 $\beta$  treatment. The notion that the same stimulus activates different ROS sources depending on cell type and/or tissue may explain the distinct findings between Chiarugi and colleagues and ours. Chiarugi and colleagues implicate 5-LOX as the main source of ROS in FB upon integrin engagement, whereas our results indicate NOX as the predominant source of ROS in cardiomyocytes.

## **6.2.) CD29-induced signalling depends on NOX2-derived ROS**

Pathways that are related to pro-survival cascades typically involve PI3K/PKB and/or MAPK/ERK1/2 in cardiomyocytes [Matsui, Nagoshi et al. 2003]. A prominent target of PKB is the GSK3 [Cross, Alessi et al. 1995], of which two isoforms, GSK3 $\alpha$  and GSK3 $\beta$ , are expressed in cardiomyocytes. Phosphorylation of the regulatory serine residues Ser21 or Ser9 is inhibitory to GSK-3 $\alpha$  or GSK-3 $\beta$  activity, respectively. Inhibition of GSK-3 via the PI3K pathway promotes cell survival in Rat-1 cells (a fibroblast cell line), PC12 cells or chicken neurons [Frame and Cohen 2001]. Additionally, CD29-dependent, PI3K-mediated phosphorylation of the inhibitory GSK-3 $\beta$  Ser9 protects adult rat CMC from  $\beta$ -adrenergic



receptor-induced apoptosis [Menon, Johnson et al. 2007]. We showed that in NRVM the PI3K/PKB and MEK/ERK pathways are both activated by CD29; here, GSK3 $\beta$  was uncovered as a target of both pathways. Even though GSK3 $\beta$  is reportedly directly phosphorylated by PKB, several other kinases such as S6K or RSK (a kinase target of ERK1/2) have been implicated in GSK3 $\beta$  inhibition in the heart [Sugden, Fuller et al. 2008]. Furthermore, we showed that CD29 induced the stress responsive kinase JNK, which acts upstream of GSK-3 $\beta$ , although JNK activation occurred at a much lower level than for the other investigated kinases. JNK activation has been demonstrated to mediate cytoprotection in NRVM after oxidative stress (hypoxia reoxygenation) [Dougherty, Kubasiak et al. 2002] and in nitric oxide-induced apoptosis [Andreka, Zang et al. 2001]. In conclusion, we found that CD29-induced survival signalling in cardiomyocytes includes the phosphorylation of ERK1/2, PKB, JNK and GSK-3 $\beta$ , all of which were further examined for their ROS dependency.

At moderate levels, ROS may serve as signalling molecules participating in the regulation of cell survival [Finkel 1998; Chiarugi 2009; Groeger, Quiney et al. 2009], because of their ability to activate pro-survival related cascades, including PI3K/PKB in VSMC upon Ang II treatment [Ushio-Fukai, Alexander et al. 1999] and/or ERK1/2 in various cell types [Dröge 2002; Forman and Torres 2002], including neonatal cardiomyocytes [Aikawa, Komuro et al. 1997]. We showed the aforementioned survival kinases to be ROS-dependent by the combined use of the enzymes Cu/Zn SOD and catalase, both of which were investigated pharmacologically (MnTMPyP) and by adenoviral overexpression. In the presence of both SOD and catalase, ROS is cleared and  $\alpha$ -CD29-induced MEK1/2-phosphorylation, ERK1/2-phosphorylation, PKB phosphorylation, and GSK-3 $\beta$  phosphorylation were inhibited (see also figure 35). Siwik *et al.* (1999) showed that in neonatal rat cardiomyocytes, the inhibition of Cu/Zn SOD with diethyldithiocarbamic acid (DDC) resulted in apoptosis when DDC was applied at higher concentrations, whereas lower concentrations of DDC mediated cell growth [Siwik, Tzortzis et al. 1999]. High DDC levels led to high intracellular superoxide anion levels that were cleared by Euk8, a SOD/cat mimetic. In this respect, our experiments showed that single-enzyme overexpression of either enzyme was not as efficient as the combination of both in inhibiting CD29-induced signalling in NRVM. Therefore, both O<sub>2</sub><sup>•-</sup> and H<sub>2</sub>O<sub>2</sub> are implicated as second messengers in CD29-induced pro-survival signal transduction in NRVM. Recently, beneficial effects of ROS were shown *in vitro* and also in humans. In particular, Groeger *et al.* (2009) indicated the necessity of H<sub>2</sub>O<sub>2</sub> for cell survival in retina cells [Groeger, Quiney et al.

2009]. Also, recent studies showed that the health promoting effects of ROS during physical exercise were prevented by the application of antioxidants [Gomez, Domenech et al. 2008; Ristow, Zarse et al. 2009].

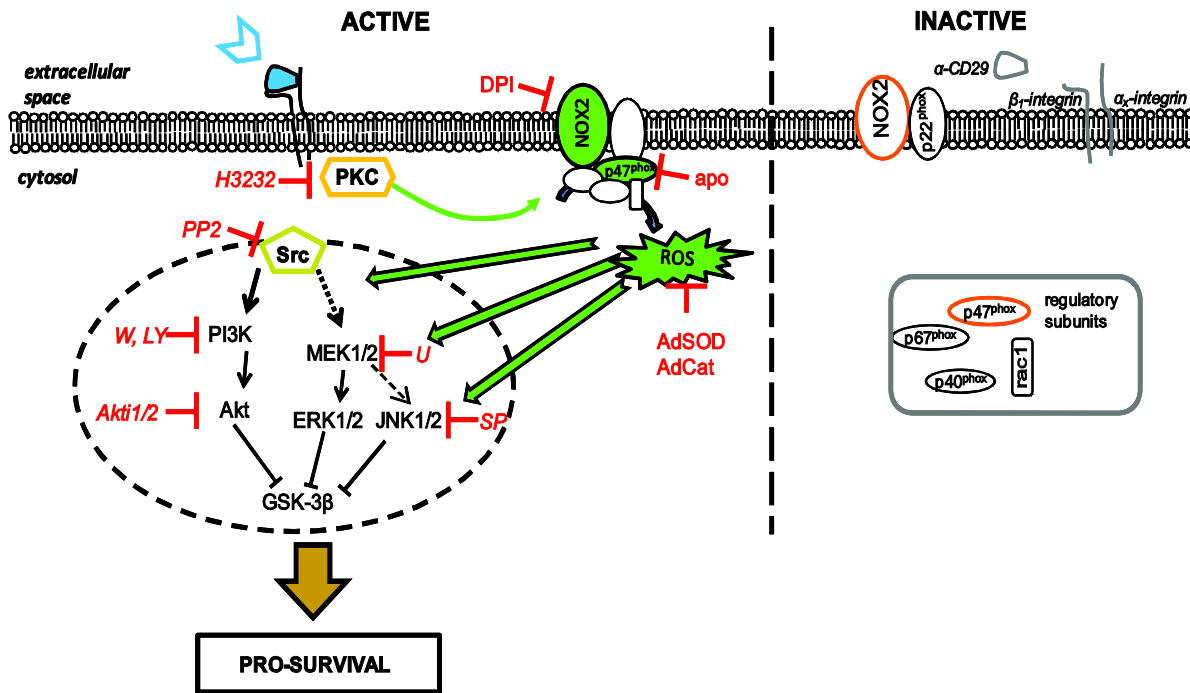


**Figure 35. CD29-induced intracellular signalling events in NRVM.** Inactive CD29 and NOX are depicted on the right. CD29 forms a heterodimeric transmembrane receptor (light grey) with different  $\alpha$ -integrin subunits. The transmembrane NOX subunit NOX2 (gp91<sup>phox</sup>, orange) together with p22<sup>phox</sup> form the catalytic part of NOX. Upon activation (on the left), the regulatory NOX subunits p47<sup>phox</sup> (orange) and p67<sup>phox</sup>, located in the cytosol, are phosphorylated and – together with rac1 and p40<sup>phox</sup> – translocate to the catalytic subunits. CD29 activation (blue chevron) induces NOX subunit assembly and ROS production. These ROS (green notched arrow, black outline) activate the pro-survival signalling cascades (black dashed circle). Using the indicated kinase inhibitors for Src (PP2), MEK (U), PI3K (W and LY), PKB/Akt (Akti1/2) and JNK (SP), the pro-apoptotic kinase GSK3 $\beta$  was located downstream of both, the MEK/ERK and PI3K/PKB pathways. It is of note that U is also reported to inhibit other protein kinases than MEK1/2 [Bain, Plater et al. 2007]. Inhibition (apo, DPI, H3232; red blunted arrow) or loss of NOX function (due to non-functional p47<sup>phox</sup> or NOX2 knock-out), or scavenging of NOX-derived ROS (adenoviral overexpression of SOD and cat; AdSOD, AdCat, red blunted arrow), resulted in impaired ROS formation and loss of survival signal transduction in neonatal cardiomyocytes.

Finally the role of NOX in CD29-activated cells was investigated. DPI and apocynin both abolished CD29-induced ERK1/2 phosphorylation, PKB phosphorylation, and JNK phosphorylation, whereas the evaluation of GSK-3 $\beta$  phosphorylation is hampered because DPI and apo induced kinase phosphorylation. In any event, these findings suggest an involvement of NOX. Subsequently, mice carrying either a knock-out of the transmembrane NOX subunit NOX2, or a LOF of the regulatory subunit p47<sup>phox</sup> were used to assess whether NOX2 determines CD29-activation-mediated survival signal transduction in NMVM. As expected, NOX2 knock-out mouse cardiomyocytes showed reduced levels of CD29-induced ERK1/2 phosphorylation. Similarly, the levels of phosphorylation of PKB and GSK-3 $\beta$  were significantly reduced in both NOX2- and p47<sup>phox</sup>-LOF cardiomyocytes, highlighting the central role of NOX2- and p47<sup>phox</sup>-derived ROS in CD29-induced survival signalling. The remaining phospho-ERK1/2 signal in p47<sup>phox</sup> LOF NMVM indicates a NOX independent and/or compensatory pathway. As discussed before (section 6.1), p47<sup>phox</sup> can be replaced by its homologue NOXO1 in the NOX homologue NOX1, which might signal through ERK1/2 in p47<sup>phox</sup> LOF cardiomyocytes. Taken together these data clearly indicate that CD29-induced survival signalling depends on NOX-derived ROS.

### **6.3.) Kinases potentially up- and downstream of NOX**

We sought for likely upstream kinases of the PI3K/PKB and the MEK/ERK pathway and/ or of NOX. Primarily, Src family kinase involvement was investigated by use of the inhibitors SU and PP2, both of which did place Src family kinase upstream of both PI3K/PKB and MEK/ERK signalling pathways. Preliminary data on the inhibition of Src family kinase by the antioxidant apo and the combined SOD/cat overexpression point at Src being ROS-regulated. Giannoni *et al.* (2005) reported that ROS activated Src tyrosine kinase through redox regulation during cell adhesion and anchorage-dependent cell growth [Giannoni, Buricchi et al. 2005]. Src was oxidized and activated in response to ECM attachment and thus following integrin activation. In detail, Giannoni and co-workers proposed that in cell suspension, Src kinase is inactive and in a reduced state with only Tyr527 phosphorylated. Upon contact to the ECM in “early adhesion”, Tyr527 is dephosphorylated and Tyr416 autophosphorylated. Src kinase is still reduced, but partially active. In the following “late adhesion/spreading” phase, Tyr527 is still dephosphorylated due to ECM binding and LOX-derived ROS production. Tyr416 is still

phosphorylated, and then Src kinase is oxidized and becomes completely active. After the application of reducing agents, ROS formation is diminished, Src kinase becomes reduced and inactive, Tyr416 is dephosphorylated and Tyr527 phosphorylated. Three years later, the same research group presented a model in which integrin engagement due to cell attachment induced Src activity via oxidation of the kinase [Giannoni, Buricchi et al. 2008]. In that study, this led to inhibition of the pro-apoptotic kinase Bim through EGFR activation followed by ERK and PKB activation, and protected against anoikis in a human endothelial cell line derived from the bladder (ECV304). Also, another study demonstrated Src kinase activation upon Ang II treatment, which transactivated EGFR, Rac and NOX1 [Lyle and Griendling 2006]. Thus in short, our data indicate that Src activity is impaired upon ROS removal and it appears very likely that NOX2 promotes Src's activity through redox-regulation.

Secondly, we explored whether PKC could be involved in the investigated signalling cascade(s), hypothesizing an involvement upstream of NOX. In neutrophils, PKC has been suggested to activate the regulatory NOX subunit p47<sup>phox</sup> by phosphorylation [Fontayne, Dang et al. 2002]. In VSMC the effectiveness of NOX activation depends on PKC (among other kinases). By administering the PKC inhibitor H3232 to newborn cardiomyocytes or to cardiac myoblasts, ROS formation was attenuated, indicating that PKC might indeed regulate NOX. Interestingly, in the NOX2 knock-out strain, PKC $\zeta$  is highly phosphorylated compared to wild type or the p47<sup>phox</sup> LOF strain. It is of note that a CD29-induced increase in PKC $\zeta$ -phosphorylation is absent in wild-type CMC, which leaves the possibility that PKC $\zeta$  is not inducible by CD29. Nevertheless, we showed that PKC lies upstream of NOX, and highly activated PKC $\zeta$  could be suggestive of the activity of another NOX homologue.

#### **6.4.) NOX and NOX-derived ROS in the heart**

Data on the involvement of NOX in different processes in the cardiovascular system, including cell survival and apoptosis, is partly contradictory. Findings suggesting beneficial roles of NOX in physiological processes are scarce. Such findings include NOX participating in

oxygen sensing or regulating the vascular muscle tone [Cave, Brewer et al. 2006]. However, in the myocardium, NOX and NOX-derived ROS have previously mainly been implicated in pathophysiological processes [Akki, Zhang et al. 2009].

Peng *et al.* (2005) showed that NOX2 contributed to myocardial dysfunction when endotoxins (lipopolysaccharides) were present in the blood [Peng, Lu et al. 2005]. Increased NOX2 protein expression was shown in human CMC after acute myocardial infarction (AMI) [Krijnen, Meischl et al. 2003]. In that study, infarcted myocardial tissue of patients who died of AMI was investigated. High levels of NOX2 were detected, localized at the plasma membrane and in the cytosol of cardiomyocytes. NOX2 was expressed in both, normal and diseased human cardiomyocytes, but was increased in sections after AMI. Similarly, Looi *et al.* (2008) demonstrated the involvement of NOX2 in adverse cardiac remodelling after myocardial infarction in NOX2 knock-out mice [Looi, Grieve et al. 2008]. In contrast, NOX2-derived ROS have been also implicated as mediators of cardiomyocyte protection against ischaemia/reperfusion injury conferred by ischaemic preconditioning [Bell, Cave et al. 2005]. NOX2 is involved in the hypertrophic response to Ang II [Bendall, Cave et al. 2002], and ROS production was increased in wild-type cardiomyocytes upon Ang II treatment compared to the basal level in knock-out mice. The hypertrophic markers ANF (atrial natriuretic factor; inhibits maladaptive hypertrophy),  $\beta$ -MHC, were significantly induced in wild type cardiomyocytes but not in knock-out CMC, as was the heart to body weight ratio in wild-type animals. These findings indicate a pathophysiological role of NOX2 in Ang II-induced hypertrophy. A follow-up study by the same group investigated the role of NOX upon pressure overload in left ventricular hypertrophy in NOX2 knock-out mice [Byrne, Grieve et al. 2003]. Byrne *et al.* used chronic Ang II infusion or aortic constriction as a study system; while Ang II failed to induce an increase in NOX activity, ANF expression and cardiac mass in NOX2 knock-out mice, aortic constriction did induce NOX activity. Furthermore, expression of NOX4 was upregulated at both protein and gene levels, hinting at contrasting roles of NOX isoforms in response to different stimuli. Whereas these findings in the literature mainly point to damaging functions of NOX2 in the heart under pathophysiological conditions, our data indicate that under physiological conditions, NOX2 is essential for survival.

NOX4 has been reported to be important during cardiac differentiation, in regulating MAPK activation, and several transcription factors [Li, Stouffs et al. 2006]. NOX4 knock-down

impairs cardiac differentiation, which can be rescued by application of exogenous H<sub>2</sub>O<sub>2</sub> in the nM range. Recently, NOX4 has been implicated as major source of mitochondrial oxidative stress causing cardiac dysfunction upon pressure overload in the mouse heart, as shown by use of a cardiac specific NOX4 knock-out [Kuroda, Ago et al. 2010]. They also showed that NOX4 overexpression promotes the proliferation of cardiac FB. Although other NOX isoforms were not upregulated in cardiac-specific NOX4 knock-out mice, its catalytic partner subunit p22<sup>phox</sup> was dramatically downregulated at the protein but not at the mRNA level [Kuroda, Ago et al. 2010]. Similar observations were made in systemic NOX2 knock-outs. NOX4 is particularly interesting with respect to its ROS formation: While it can generate H<sub>2</sub>O<sub>2</sub> without regulatory NOX subunits, it depends on p22<sup>phox</sup> in HEK293, Hela, H292 and COS cells [Martyn, Frederick et al. 2006]. Additionally, it has been emphasized that NOX4 activity is regulated at the gene expression level [Serrander, Cartier et al. 2007]. Interestingly, Zhang *et al.* (2010) showed that NOX4 protects the heart from failure [Zhang, Brewer et al. 2010]. In that study, NOX4 null mice were generated by targeted deletion of the translation initiation site and exon 1 and 2 of NOX4, which resulted in total loss of NOX4 protein without affecting myocardial protein levels of NOX2 or p22<sup>phox</sup>. Upon pressure overload, NOX4 knock-out animals developed contractile impairment, ventricular dilation, as well as exaggerated cardiac hypertrophy and increased interstitial fibrosis as compared to NOX4 competent litter mates [Zhang, Brewer et al. 2010]. These findings demonstrate that NOX4 protects against pressure overload-induced heart failure. Secondly, Zhang *et al.* generated a cardiomyocyte-specific NOX4 transgenic mouse to increase NOX4 protein levels. These mice showed increased NOX4 gene- and p22<sup>phox</sup> protein expression whereas NOX2 levels remained constant between strains. NOX4 transgenic mouse hearts did not show basal dysfunction, and they showed less hypertrophy and interstitial fibrosis in response to pressure overload. Additionally, upon pressure overload these transgenic mice exhibited an enhanced myocardial capillary density and release of angiogenic factors promoting angiogenesis [Zhang, Brewer et al. 2010]. In conclusion, contrasting roles have been attributed to NOX4 in the literature. NOX4 seems mandatory in cardiac differentiation but also in the failing heart, whereas it is also a cause of cardiac dysfunction. Since the effect of NOX4 appears to depend on context, this raises the possibility that NOX2 may display a similar context dependency. Therefore, its study in different laboratory model systems may be fruitful and lead to the elucidation of further protective effects of NOX2.

## **6.5.) The physiological relevance of NOX and ROS**

$O_2^{\bullet-}$  and  $H_2O_2$  are the prevalent oxygen-derived molecules implicated in redox signalling. More than a decade ago, these ROS were implicated in a range of cellular outcomes including apoptosis, senescence, and survival. Several cell surface receptors, transmembrane agonists, and extracellular signals, including peptide growth factors, cytokines, cell attachment or phorbol esters mediate ROS generation [Rhee 1999; Mehdi, Azar et al. 2007].  $H_2O_2$  modulates protein tyrosine kinases and phosphatases by reduction or oxidation, all of which are essential in cell signalling [Rhee 2006].  $H_2O_2$  acts locally and within a defined time-frame [Mishina, Tyurin-Kuzmin et al. 2011]. A number of studies suggest NOX as the source of ROS involved in physiological processes (see comprehensive review by [Bedard and Krause 2007]).

In particular, NOX2-derived ROS are essential in neutrophils, in host defence and cellular signalling. Conversely, the lack or loss of function of NOX2 has been implicated in the severe disease CGD, which is accompanied by infections and inflammations [Lambeth 2004]. NOX2-derived ROS are also anti-inflammatory and prevent autoimmune disease [Hultqvist, Olsson et al. 2009]. Accumulating evidence implies NOX2-derived ROS in cell survival, as shown by the studies of Maraldi *et al.* (2009) and Groeger *et al.* (2009). In the human leukaemic megacaryocytic cell line M07e, NOX2 was implicated as the source of ROS in response to interleukin (IL) 3 treatment [Maraldi, Prata et al. 2009]. In that study, NOX2-mediated survival was mainly validated by use of DPI and apocynin, although NOX2 siRNA was also used in initial experiments. DCF fluorescence and viability were significantly reduced compared to IL3-treated cells and cell death markers such as caspase 3 or apoptotic nuclei were studied with the synthetic inhibitors apocynin and DPI [Maraldi, Prata et al. 2009]. In a previous study by the same group, ROS were shown to be anti-apoptotic by use of several ROS scavenging compounds such as EUK-134 [Maraldi, Prata et al. 2009]. EUK-134 is a SOD/catalase mimetic and inhibited phosphorylation of PKB, ERK, and Src, but did not affect JNK phosphorylation. Based on their study, suggesting that transient  $H_2O_2$  generation induces survival [Mackey, Sanvicens et al. 2008], Groeger *et al.* (2009) later showed that NOX2 and NOX4 are the source of these ROS in a retina-derived photoreceptor cell line (661W) [Groeger, Mackey et al. 2009]. A possible physiological relevance was examined in

mouse retinal explants by use of DCF fluorescence-based time-lapse imaging to detect H<sub>2</sub>O<sub>2</sub> generation. Knock-down of *NOX2* and *NOX4* by siRNA decreased oxidative burst activity by 70%. These findings indicate pro-survival roles of NOX outside of the heart and thus make pro-survival roles of NOX in the heart appear more plausible.

### **6.6.) The spatiotemporal distribution and subcellular localization of NOX**

Although several ROS sources besides NOX are present in each cell, recent reports demonstrated NOX acting in a spatio-temporally defined manner. NOX is distributed in several compartments including endosomes, the endoplasmic reticulum, lipid rafts, nuclei, or at cell migrations sites [Ushio-Fukai 2006; Ushio-Fukai 2009]. Oakley *et al.* (2009) also suggested that so-called redoxosomes exist. These redox-active endosomes contain NOX, as well as other ROS processing proteins such as SOD1. In response to stimuli such as IL-1 or TNF $\alpha$ , superoxide anions are produced in the endosomal lumen facilitated by NOX1 and/or NOX2 [Oakley, Abbott *et al.* 2009]. The different localizations of NOX reviewed above might explain that NOX isoforms such as NOX2 and NOX4 can participate either in distinct [Byrne, Grieve *et al.* 2003; Anilkumar, Weber *et al.* 2008] or similar processes [Petry, Djordevjević *et al.* 2006; Pendayala, Gorshkova *et al.* 2009; Kim, Choi *et al.* 2010].

In a model of specialized microdomains (caveolae), angiotensin II receptor type I (AT<sub>1</sub>R) stimulation by ang II resulted in partial internalization of the receptor. This was accompanied with activation of NOX1 and recruitment of caveolin 1 to the receptor, which promoted transactivation of EGFR through ROS-dependent Src activation. Both, tyrosine-phosphorylated EGFR and caveolin 1, are subsequently released to the site of focal adhesion. There they colocalize with another NOX family member, namely NOX4, as well as paxillin and integrin, resulting in redox signalling leading to VSMC hypertrophy [Ushio-Fukai 2009]. Pendayala *et al.* (2009) localized NOX4 in the nucleus under normoxia. In response to hyperoxia, NOX4 translocates to the cytosol and endoplasmic reticulum. They also described the reciprocal compensation of NOX2 and NOX4 in lung endothelial cells: They showed increased expression and regulation of NOX2 proteins and transcripts, in siRNA-mediated *NOX4*-deficient lung endothelial cells. *Vice Versa*, NOX4 proteins and transcripts are



upregulated in *NOX2* knock-down cells [Pendayala, Gorshkova et al. 2009]. In rat and human VSMC, Hilenski *et al.* (2004) investigated the subcellular localization of *NOX1* and *NOX4* [Hilenski, Clempus et al. 2004]. Laser scanning confocal microscopy revealed that *NOX1* was localized to the surface and at cellular margins, whereas *NOX4* was found at focal adhesions, i.e. where cells contact the underlying matrix. *NOX4* co-localized with vinculin, a marker for focal adhesions and *NOX1* was co-localized with caveolin in VSMC. Distinct cellular redox responses due to different responses were also assigned to *NOX2*- and *NOX4*-transfected HEK293 cells [Anilkumar, Weber et al. 2008]. Anilkumar *et al.* showed *NOX2* was localized at the plasma membrane, while *NOX4* was found at the endoplasmic reticulum, co-localizing with calnexin. Under non-treated conditions, *NOX4* overexpression increased superoxide production – which was not the case when *NOX2* was overexpressed [Anilkumar, Weber et al. 2008]. Likewise, phospho-JNK and ERK1/2 levels were elevated in *NOX4* but not in *NOX2* expressing cells. Constant phospho-PKB and phospho-GSK-3 $\beta$  signals were observed in both *NOX2*- and *NOX4*-expressing HEK293 cells. Interestingly however, p38 phosphorylation was increased in *NOX2* expressing cells. Ang II-induced  $O_2^{\bullet-}$  generation was driven by *NOX2* and not by *NOX4*. Insulin-induced  $O_2^{\bullet-}$  production was both *NOX2*- and *NOX4*-driven, whereas TNF $\alpha$ -treated cells only induced ROS in *NOX2*-transfected cells [Anilkumar, Weber et al. 2008].

Due to the distinct spatiotemporal NOX distributions [Oakley2009, Ushio-Fukai2006], it is clear that NOX-derived ROS may act in a context-dependent fashion, and may also contribute to cell survival. This also implies that a) at the same time, several NOX isoforms may be activated in response to one defined stimulus; b) the activated NOX isoform may act either in close proximity or at distant compartments relative to the stimulus, and c) one stimulus may activate different NOX isoforms in different physiological states. For example, under pathological conditions in the heart, *NOX2* activity may be harmful while *NOX4* activity is not. However, our data implicate *NOX2* in cell survival processes, while *NOX4* is hardly expressed in the cardiomyocytes we investigated. Also, another functional NOX homologue dependent on p47<sup>phox</sup> is activated under conditions when *NOX2* activity is impaired. Therefore, it appears very likely that several NOX homologues are activated depending on the physiological conditions, the stimulus, tissue and the cell type.

## **6.7.) Conclusions**

In my thesis, I have provided novel insights into the mechanisms of CD29 induced pro-survival signalling in primary cardiomyocytes (see figure 35). The pro-survival-related pathways PI3K/PKB and MEK/ERK were activated upon CD29 engagement. Src family kinase was placed upstream of the aforementioned survival pathways and PKC was placed upstream of NOX. With the exception of PKC, all signalling kinases investigated were regulated by ROS. GSK3 $\beta$  was identified as a common anti-apoptotic kinase when phosphorylated upon PKB/Akt, MEK/ERK, JNK and PKC activation. NOX2 was identified as the source of the regulatory ROS involved. Furthermore CD29 was shown to induce a transient oxidative burst that is mediated by a p47<sup>phox</sup>-dependent NOX. Thus, NOX1 could serve as an additional oxidase involved in generating ROS. Preliminary expression data hint at the availability of this NOX isoform in ventricular cardiomyocytes. These data clearly add to the growing body of evidence that NOX-derived ROS (also) have a protective function in the heart.

## 7.) REFERENCES

- Aikawa, R., I. Komuro, et al. (1997). "Oxidative stress activates extracellular signal-regulated kinases through Src and Ras in cultured cardiac myocytes of neonatal rats." Journal of Clinical Investigation **100**: 1813-1821.
- Aikawa, R., M. Nawano, et al. (2000). "Insulin prevents cardiomyocytes from oxidative stress-induced apoptosis through activation of PI3 Kinase/Akt." Circulation **102**: 2873-2879.
- Akki, A., M. Zhang, et al. (2009). "NADPH oxidase signaling and cardiac myocyte function." Journal of Molecular and Cellular Cardiology **47**: 15-22.
- Alexander, D. R., J. M. Hexham, et al. (1989). "A protein kinase C pseudosubstrate peptide inhibits phosphorylation of the CD3 antigen in streptolysin-O-permeabilized human T lymphocytes." Biochem J. **260**: 893-901.
- Almeida, E. A. C., D. Ilić, et al. (2000). "Matrix survival signaling: from fibronectin via focal adhesion kinase to c-Jun NH<sub>2</sub>-terminal kinase." The Journal of Cell Biology **149**: 741-754.
- Ambasta, R. K., P. Kumar, et al. (2004). "Direct interaction of the novel Nox proteins with p22phox is required for the formation of a functionally active NADPH oxidase." The Journal of Biological Chemistry **279**: 45935-45941.
- Amin, J. K., L. Xiao, et al. (2001). "Reactive oxygen species mediate alpha-adrenergic receptor-stimulated hypertrophy in adult ventricular myocytes." Journal of Molecular & Cellular Cardiology **33**: 131-139.
- Andreka, P., J. Zang, et al. (2001). "Cytoprotection by Jun kinase during nitric oxide-induced cardiac myocyte apoptosis." Circulation Research **88**: 305-312.
- Anilkumar, N., R. Weber, et al. (2008). "Nox4 and Nox2 NADPH oxidases mediate distinct cellular redox signaling responses to agonist stimulation." Arteriosclerosis, Thrombosis and Vascular Biology **28**: 1347-1354.
- Aplin, A. E., A. Howe, et al. (1998). "Signal transduction and signal modulation by cell adhesion receptors: the role of integrins, cadherins, immunoglobulin-cell adhesion molecules and selectins." Pharmacological Reviews **50**: 197-263.
- Arnaout, M. A., S. L. Goodman, et al. (2007). "Structure and mechanics of integrin-based cell adhesion." Current Opinion in Cell Biology **19**: 495-507.
- Arnaout, M. A., B. Mahalingam, et al. (2005). "Integrin structure, allostery, and bidirectional signaling." Annual Reviews of Cell and Developmental Biology **21**: 381-410.
- Askari, J. A., C. J. Tynan, et al. (2010). "Focal adhesions are sites of integrin extension." The Journal of Cell Biology **188**: 891-903.
- Aumailley, M. and B. Gayraud (1998). "Structure and biological activity of the extracellular matrix." Journal of Molecular Medicine **76**: 253-265.
- Babior, B. M. (1999). "NADPH oxidase: an update." Blood **93**: 1464-1476.
- Babior, B. M., J. T. Curnutte, et al. (1976). "The particulate superoxide-forming system from human neutrophils." The Journal of Clinical Investigation **58**: 989-996.
- Bain, J., L. Plater, et al. (2007). "The selectivity of protein kinase inhibitors: a further update." Biochemical Journal **408**: 297-315.
- Banerjee, I., J. W. Fuseler, et al. (2007). "Determination of cell types and numbers during cardiac development in the neonatal and adult rat and mouse." American Journal of Physiology-Heart & Circulatory Physiology **293**: H1883-H1891.
- Banerjee, I., K. Yekkala, et al. (2006). "Dynamic interactions between myocytes, fibroblasts, and extracellular matrix." Annals of New York Academy of Sciences. **1080**: 76-84.
- Bánfi, B., R. A. Clark, et al. (2003). "Two novel proteins activate superoxide generation by the NADPH oxidase NOX1." Journal of Biological Chemistry **278**: 3510-3513.
- Barczyk, M., S. Carracedo, et al. (2010). "Integrins." Cell and Tissue Research **339**: 269-280.

- Bass, D., J. Parce, et al. (1983). "Flow cytometric studies of oxidative product formation by neutrophils: a graded response to membrane stimulation." The Journal of Immunology **130**: 1910-1917.
- Baudino, T. A., W. Carver, et al. (2006). "Cardiac fibroblasts: friend or foe?" American Journal of Physiology- Heart & Circulatory Physiology **291**: H1015-H1026.
- Baudoin, C., M.-J. Goumans, et al. (1998). "Knockout and knockin of the  $\beta$ 1 exon D define distinct roles of integrin splice variants in heart function and embryonic development." Genes & Development **12**: 1202-1216.
- Bazzoni, G., L. Ma, et al. (1998). "Divalent cations and ligands induce conformational changes that are highly divergent among  $\beta$ <sub>1</sub> integrins." The Journal of Biological Chemistry **273**: 6670-6678.
- Bedard, K. and K.-H. Krause (2007). "The NOX family of ROS-generating NADPH oxidases: physiology and pathophysiology." Physiological Review **87**: 245-313.
- Bell, R. M., A. C. Cave, et al. (2005). "Pivotal role of NOX2-containing NADPH oxidase in early ischemic preconditioning." The FASEB Journal **19**: 2037-2039.
- Bendall, J. K., A. C. Cave, et al. (2002). "Pivotal role of gp91phox-containing NADPH oxidase in angiotensin II-induced cardiac hypertrophy in mice." Circulation **105**: 293-296.
- Blake, R. A., M. A. Broome, et al. (2000). "SU6656, a selective Src family kinase inhibitor, used to probe growth factor signaling." Molecular and Cellular Biology **20**: 9018-9027.
- Blüml, S., B. Rosc, et al. (2008). "The oxidation state of phospholipids controls the oxidative burst in neutrophil granulocytes." The Journal of Immunology **181**: 4347-4353.
- Bochkov, V. N., A. Kadl, et al. (2002). "Protective role of phospholipid oxidation products in endotoxin induces tissue damage." Nature **419**: 77-81.
- Bonizzi, G., J. Piette, et al. (1999). "Reactive oxygen intermediate-dependent NF- $\kappa$ B activation by interleukin-1 $\beta$  requires 5-lipoxygenase or NADPH oxidase activity." Molecular and Cellular Biology **19**: 1950-1960.
- Borg, T. K., K. Rubin, et al. (1984). "Recognition of extracellular matrix components by neonatal and adult cardiac myocytes." Developmental Biology **104**: 86-96.
- Bowers, S., I. Banerjee, et al. (2010). "The extracellular matrix: at the center of it all." Journal of Molecular and Cellular Cardiology **48**: 474-482.
- Brakebusch, C., E. Hirsch, et al. (1997). "Genetic analysis of  $\beta$ 1 integrin function: confirmed, new and revised roles for a crucial family of cell adhesion molecules." Journal of Cell Science **110**: 2895-2904.
- Brown, D. I. and K. K. Griendling (2009). "NOX proteins in signal transduction." Free Radical Biology & Medicine **47**: 1239-1253.
- Burger, W. and M. Burge (2007). Digital imaging processing: An algorithmic introduction using Java, Springer-Verlag New York.
- Byrne, J. A., D. J. Grieve, et al. (2003). "Contrasting roles of NADPH oxidase isoforms in pressure overload versus angiotensin II - induced cardiac hypertrophy." Circulation Research **93**: 802-805.
- Byron, A., J. D. Humphries, et al. (2009). "Anti-integrin monoclonal antibodies." Journal of Cell Science **122**: 4009-4011.
- Cao, X., X. Dai, et al. (2007). "Differential regulation of NADPH oxidase in sympathetic and sensory ganglia in deoxycorticosterone acetate salt hypertension." Hypertension **50**: 663-671.
- Carver, W., R. L. Price, et al. (1994). "Disruption of  $\beta$ -1 integrin in the developing heart." The Journal of Histochemistry and Cytochemistry **42**: 167-175.
- Cave, A. C., A. C. Brewer, et al. (2006). "NADPH oxidases in cardiovascular health and disease." Antioxidants & Redox Signaling **8**: 691-728.
- Chen, K., S. E. Craige, et al. (2009). "Downstream targets and intracellular compartmentalizations in Nox signaling." Antioxidants & Redox Signaling **11**: 2467-2480.
- Chen, Q., D. W. Powell, et al. (2003). "Akt phosphorylates p47<sup>phox</sup> and mediates respiratory burst activity in human neutrophils." The Journal of Immunology **170**: 5302-5308.

- Chiarugi, P. (2009). "Survival or death: the redox paradox." Antioxidants & Redox Signaling **11**: 2651-2654.
- Chiarugi, P. and T. Fiaschi (2007). "Redox signalling in anchorage-dependent cell growth." Cellular Signalling **19**: 672-682.
- Chiarugi, P., G. Pani, et al. (2003). "Reactive oxygen species as essential mediators of cell adhesion: the oxidative inhibition of a FAK tyrosine phosphatase is required for cell adhesion." The Journal of Cell Biology **161**: 933-944.
- Ciani, L. and P. C. Salinas (2007). "c-Jun N-terminal kinase (JNK) cooperates with GSK3 $\beta$  to regulate Dishevelled-mediated microtubule stability." BMC Cell Biology **8**: 27.
- Clark, E. A. and J. S. Brugge (1995). "Integrins and signal transduction pathways: the road taken " Science **268**: 233-239.
- Colavitti, R., G. Pani, et al. (2002). "Reactive oxygen species as downstream mediators of angiogenic signaling by vascular endothelial growth factor receptor-2/KDR." The Journal of Biological Chemistry **277**: 3101-3108.
- Communal, C., M. Singh, et al. (2003). " $\beta$ 1 integrins expression in adult rat ventricular myocytes and its role in the regulation of  $\beta$ -adrenergic receptor stimulated apoptosis." Journal of Cellular Biochemistry **89**: 381-388.
- Cooper, J. A. and B. Howell (1993). "The when and how of Src regulation." Cell **73**: 1051-1054.
- Cross, D. A. E., D. R. Alessi, et al. (1995). "Inhibition of glycogen synthase-3 by insulin mediated by protein kinase B." Nature **378**: 785-789.
- D'Souza, S. E., M. H. Ginsberg, et al. (1991). "Arginyl-glycyl-aspartic acid (RGD): a cell adhesion motif." TRENDS in Biochemical Sciences **16**: 246-250.
- Dang, P. M.-C., A. Fontayne, et al. (2001). "Protein kinase C  $\zeta$  phosphorylates a subset of selective sites of the NADPH oxidase component p47<sup>phox</sup> and participates in formyl peptide-mediated neutrophil respiratory burst." The Journal of Immunology **166**: 1206-1213.
- Davidson, B., E. Allen, et al. (1993). "A model system for in vivo gene transfer into the central nervous system using an adenoviral vector." Nature Genetics **3**: 219-223.
- Davis, R. J. (2000). "Signal transduction by the JNK group of MAP kinases." Cell **103**: 239-252.
- De Leo, F. R., J. Renee, et al. (1998). "Neutrophils exposed to bacterial lipopolysaccharide upregulate NADPH oxidase assembly." The Journal of Clinical Investigation **101**: 455-463.
- De Leo, F. R., K. V. Ulman, et al. (1996). "Assembly of the human neutrophil NADPH oxidase involves binding of p67<sup>phox</sup> and flavocytochrome *b* to a common functional domain in p47<sup>phox</sup>." The Journal of Biological Chemistry **271**(29): 17013-17020.
- De Melker, A. A. and A. Sonnenberg (1999). "Integrins: alternative splicing as a mechanism to regulate ligand binding and integrin signaling events." Bio Essays **21**: 499-509.
- Dewas, C., M. Fay, et al. (2000). "The mitogen-activated protein kinase extracellular signal-regulated kinase 1/2 pathway is involved in formyl-methionyl-leucyl-phenylalanine-induced p47<sup>phox</sup> phosphorylation in human neutrophils." The Journal of Immunology **165**: 5238-5244.
- Diamond, M. S. and T. A. Springer (1994). "The dynamic regulation of integrin adhesiveness." Current Biology **4**: 506-517.
- Ding, J., C. J. Vlahos, et al. (1995). "Antagonists of phosphatidylinositol 3-kinase block activation of several protein kinases in neutrophils." The Journal of Biological Chemistry **270**: 11684-11691.
- Dorn II, G. W. and A. Diwan (2008). "The rationale for cardiomyocyte resuscitation in myocardial salvage." Journal of Molecular Medicine **86**: 1085-1095.
- Dougherty, C. J., L. A. Kubasiak, et al. (2002). "Activation of c-Jun N-terminal kinase promotes survival of cardiac myocytes after oxidative stress." Biochemical Journal **362**: 561-571.
- Dröge, W. (2002). "Free radicals in the physiological control of cell function." Physiological Review **82**: 47-95.
- Fässler, R. and M. Meyer (1995). "Consequences of lack of  $\beta$ 1 integrin gene expression in mice." Genes & Development **9**: 1896-1908.

- Fässler, R., J. Rohwedel, et al. (1996). "Differentiation and integrity of cardiac muscle cells are impaired in the absence of  $\beta 1$  integrin." Journal of Cell Science **109**: 2989-2999.
- Finkel, T. (1998). "Oxygen radicals and signaling." Current Opinion Cell Biology **10**: 248-253.
- Finkel, T. (1999). "Signal transduction by reactive oxygen species in non-phagocytic cells." Journal of Leukocyte Biology **65**: 337-340.
- Fontayne, A., P. M.-C. Dang, et al. (2002). "Phosphorylation of p47<sup>phox</sup> sites by PKC  $\alpha$ ,  $\beta$ II,  $\delta$ , and  $\zeta$ : effect on binding to p22<sup>phox</sup> and on NADPH oxidase activation." Biochemistry **41**: 7743-7750.
- Forman, H. J., M. Maiorino, et al. (2010). "Signaling functions of reactive oxygen species." Biochemistry **49**: 835-842.
- Forman, H. J. and M. Torres (2002). "Reactive oxygen species and cell signaling." American Journal of Respiratory and Critical Care Medicine **166**: S4-S8.
- Frame, S. and P. Cohen (2001). "GSK3 takes centre stage more than 20 years after its discovery." Biochemical Journal **359**: 1-16.
- Fridovich, I. (March 2009). "Oxidative stress." Encyclopedia of Life Sciences.
- Frisch, S. M. and H. Francis (1994). "Disruption of epithelial cell-matrix interaction induces apoptosis." The Journal of Cell Biology **124**: 619-626.
- Geiszt, M. and T. L. Leto (2004). "The Nox family of NADP(H) oxidases: host defense and beyond." The Journal of Biological Chemistry **279**: 51715-51718.
- George, E. L., H. S. Baldwin, et al. (1997). "Fibronectins are essential for heart and blood vessel morphogenesis but are dispensable for initial specification of precursor cells." Blood **90**: 3073-3081.
- George, E. L., E. N. George-Labouesse, et al. (1993). "Defects in mesoderm, neuronal tube and vascular development in mouse embryos lacking fibronectin." Development **119**: 1079-1091.
- Giancotti, F. G. (1997). "Integrin signaling: specificity and control of cell survival and cell cycle progression." Current Opinion in Cell Biology **9**: 691-700.
- Giancotti, F. G. and E. Ruoslahti (1999). "Integrin signaling." Science **285**: 1028-1032.
- Gianni, D., B. Diaz, et al. (2009). "Novel p47<sup>phox</sup>-related organizers regulate localized NADPH oxidase 1 (Nox1) activity." Science Signaling **2**: ra54 (1-11).
- Giannoni, E., F. Buricchi, et al. (2008). "Redox regulation of anoikis: reactive oxygen species as essential mediators of cell survival." Cell Death and Differentiation **15**: 867-878.
- Giannoni, E., F. Buricchi, et al. (2005). "Intracellular reactive oxygen species activates Src tyrosine kinase during cell adhesion and anchorage-dependent cell growth." Molecular and Cellular Biology **25**: 6391-6403.
- Goldsmith, E. C. and T. K. Borg (2002). "The dynamic interaction of the extracellular matrix in cardiac remodeling." Journal of Cardiac Failure **8**: S314-S318.
- Goldsmith, E. C., A. Hoffman, et al. (2004). "Organization of fibroblasts in the heart." Developmental Dynamics **230**: 787-794.
- Gomez, C., Mari-Carmen, E. Domenech, et al. (2008). "Oral administration of vitamin C decreases muscle mitochondrial biogenesis and hampers training-induced adaptations in endurance performance." The American Journal of Clinical Nutrition **87**: 142-149.
- Greene, L. A. and A. S. Tischler (1976). "Establishment of a noradrenergic clonal cell line of rat adrenal pheochromocytoma cells which respond to nerve growth factor." The Proceedings of the National Academy of Sciences USA **73**: 2424-2428.
- Gregory, E. M. and I. Fridovich (1973). "Induction of superoxide dismutase by molecular oxygen." Journal of Bacteriology **114**: 543-548.
- Gregory, E. M., S. A. Goscin, et al. (1974). "Superoxide dismutase and oxygen toxicity in a eukaryote." Journal of Bacteriology **117**: 456-460.
- Groeger, G., A. M. Mackey, et al. (2009). "Stress-induced activation of NOX contributes to cell survival signalling via production of hydrogen peroxide." Journal of Neurochemistry **109**: 1544-1554.
- Groeger, G., C. Quiney, et al. (2009). "Hydrogen peroxide as a cell survival signaling molecule." Antioxidants & Redox Signaling **11**: 2655-2671.

- Gschwendt, M., K. Kielbasse, et al. (1994). "Tyrosine phosphorylation and stimulation of protein kinase C $\delta$  from porcine spleen by src in vitro." FEBS Letters **347**: 85-89.
- Gupte, S. A., P. M. Kaminski, et al. (2009). "Peroxide generation by p47<sup>phox</sup>-Src activation of Nox2 has a key role in protein kinase C-induced smooth muscle contraction." American Journal of Physiology- Heart & Circulatory Physiology **296**: H1048-H1057.
- Gustafsson, E., A. Aszódi, et al. (2003). "Role of collagen type II and perlecan in skeletal development." Annals of New York Academy of Sciences **995**: 140-150.
- Halliwell, B. and J. M. Gutteridge (1985). "The importance of free radicals and catalytic metal ions in human disease." Molecular Aspects in Medicine **8**: 89-193.
- Hancock, J. T., R. Desikan, et al. (2001). "Role of reactive oxygen species in cell signalling pathways." Biochemical Society Transaction **29**: 345-350.
- Hanke, J. H., J. P. Gardener, et al. (1996). "Discovery of a novel, potent and src family-selective tyrosine kinase inhibitor." The Journal of Biological Chemistry **271**: 695-701.
- Haq, S., G. Choukroun, et al. (2000). "Glycogen Synthase Kinase-3 $\beta$  is a negative regulator of cardiomyocyte hypertrophy." The Journal of Cell Biology **151**: 117-129.
- Heidari, Y., A. M. Shah, et al. (2004). "NOX-2S is a new member of the NOX family of NADPH oxidases." Gene **335**: 133-140.
- Hemler, M. E., C. Huang, et al. (1987). "The VLA protein family." The Journal of Biological Chemistry **262**: 3300-3309.
- Hensley, K., K. A. Robinson, et al. (2000). "Reactive oxygen species, cell signaling, and cell injury." Free Radical Biology & Medicine **28**: 1456-1462.
- Hescheler, J., R. Meyer, et al. (1991). "Morphological, biochemical, and electrophysiological characterization of a clonal cell (H9C2) line from rat heart." Circulation Research **69**: 1476-1486.
- Heumüller, S., S. Wind, et al. (2008). "Apocynin is not an inhibitor of vascular NADPH oxidases but an antioxidant." Hypertension **51**: 211-217.
- Heyworth, P. G., C. F. Shrimpton, et al. (1989). "Localization of the 47 kDa phosphoprotein involved in the respiratory-burst NADPH oxidase of phagocytic cells." Biochemical Journal **260**: 243-248.
- Hilenski, L. L., R. E. Clempus, et al. (2004). "Distinct subcellular localization of Nox1 and Nox4 in vascular smooth muscle cells." Arteriosclerosis, Thrombosis and Vascular Biology **24**: 677-683.
- Hill, J. A. and E. N. Olson (2008). "Cardiac plasticity." The New England Journal of Medicine **358**: 1370-1380.
- Hingtgen, S. D., X. Tian, et al. (2006). "Nox2-containing NADPH oxidase and Akt activation play a key role in angiotensin II - induced cardiomyocyte hypertrophy." Physiological Genomics **26**: 180-191.
- Honoré, S., H. Kovacic, et al. (2003). " $\alpha$ 2 $\beta$ 1-integrin signaling by itself control G1/S transition in a human adenocarcinoma cell line (Caco-2) implication of NADPH oxidase-dependent production of ROS." Experimental Cell Research **285**: 59-71.
- Hultqvist, M., L. M. Olsson, et al. (2009). "The protective role of ROS in autoimmune disease." TRENDS in Immunology **30**: 201-208.
- Hynes, R. (1992). "Integrins: versatility, modulation, and signaling in cell adhesion." Cell **69**: 11-25.
- Hynes, R. (1996). "Targeted mutations in cell adhesion genes: what have we learned from them?" Developmental Biology **180**: 402-412.
- Hynes, R. O. (1987). "Integrins: a family of cell surface receptors." Cell **48**: 549-554.
- Hynes, R. O. (1999). "Cell adhesion: old and new questions." TRENDS in Cell Biology **9**: M33-M37.
- Hynes, R. O. (2002). "Integrins: bidirectional, allosteric signaling machines." Cell **110**: 673-687.
- Hynes, R. O. and Q. Zhao (2000). "The evolution of cell adhesion." The Journal of Cell Biology **150**: F89-F95.
- Jakab, M., T. M. Weiger, et al. (1996). "Ethanol activates maxi Ca<sup>2+</sup>-activated K<sup>+</sup> channels of clonal pituitary (GH3) cells." The Journal of Membrane Biology **157**: 237-245.

- Juliano, R. L. (2002). "Signal transduction by cell adhesion receptors and the cytoskeleton: functions of integrins, cadherins, selectins, and immunoglobulin-superfamily members." Annual Review of Pharmacology and Toxicology **42**: 283-323.
- Karnovsky, M. L. and A. J. Sbarra (1960). "Metabolic changes accompanying the ingestion of particulate matter by cells." American Journal of Clinical Nutrition **8**: 147-155.
- Kawahara, T., M. T. Quinn, et al. (2007). "Molecular evolution of the reactive oxygen-generating NADPH oxidase (NOX/DUOX) family of enzymes." BMC Evolutionary Biology **7**: 109.
- Keller, R. S., S.-Y. Shai, et al. (2001). "Disruption of integrin function in the murine myocardium leads to perinatal lethality, fibrosis, and abnormal cardiac performance." American Journal of Pathology **158**: 1079-1090.
- Kim, D., S. Shu, et al. (2010). "Regulation of proapoptotic mammalian ste20-like kinase MST2 by the IGF1-Akt pathway." PloS One **5**: e9616.
- Kim, K. S., H. W. Choi, et al. (2010). "Reactive oxygen species generated by NADPH oxidase 2 and 4 are required for chondrogenic differentiation." The Journal of Biological Chemistry **285**: 40294-40302.
- Kimes, B. W. and B. L. Brandt (1976). "Properties of a clonal muscle cell line from rat heart." Experimental Cell Research **98**: 367-381.
- Knight, C. G., L. F. Morton, et al. (1998). "Identification in collagen type I of an integrin  $\alpha 2\beta 1$ -binding site containing an essential GER sequence." The Journal of Biological Chemistry **273**: 33287-33294.
- Krijnen, P. A. J., C. Meischl, et al. (2003). "Increased Nox2 expression in human cardiomyocytes after acute myocardial infarction." Journal of Clinical Pathology **56**: 194-199.
- Krishnamurthy, P., V. Subramanian, et al. (2006). "Deficiency of  $\beta 1$ integrins results in increased myocardial dysfunction after myocardial infarction." Heart **92**: 1309-1315.
- Kuppuswamy, D. (2002). "Importance of integrin signaling in myocyte growth and survival." Circulation Research **90**: 1240-1242.
- Kurien, B. and R. Scofield (2003). "Protein blotting: a review." The Journal of Immunological Methods **274**: 1-15.
- Kurien, B. T. and R. H. Scofield (2006). "Western blotting." Methods **38**: 283-293.
- Kuroda, J., T. Ago, et al. (2010). "NADPH oxidase (NOX4) is a major source of oxidative stress in the failing heart." The Proceedings of the National Academy of Sciences USA **107**: 15565-15570.
- Kutty, R. K., G. Kutty, et al. (1995). "Induction of heme oxygenase 1 in the retina by intense visible light: suppression by the antioxidant demethylthiourea." The Proceedings of the National Academy of Sciences USA **92**: 1177-1181.
- Kwon, S. H., D. R. Pimentel, et al. (2003). "H<sub>2</sub>O<sub>2</sub> regulates cardiac myocyte phenotype via concentration-dependent activation of distinct kinase pathways." Journal of Molecular and Cellular Cardiology **35**: 615-621.
- Lam, E., R. Zwacka, et al. (1999). "Effects of antioxidant enzyme overexpression on the invasive phenotype of hamster cheek pouch carcinoma cells." Free Radicals & Biological Medicine **27**: 572-579.
- Lambeth, J. D. (2004). "NOX enzymes and the biology of reactive oxygen." Nature Reviews Immunology **4**: 181-189.
- Lambeth, J. D., G. Cheng, et al. (2000). "Novel homologs of gp91 $phox$ ." Frontlines **S 25**: 459-461.
- Lambeth, J. D., K.-H. Krause, et al. (2008). "NOX enzymes as novel targets for drug development." Semin Immunopathol **30**: 339-363.
- Legate, K. R., E. Montañez, et al. (2006). "ILK, PINCH and parvin: the tiPP of integrin signalling." Nature Reviews Molecular Cell Biology **7**: 20-31.
- Lei, L., D. Liu, et al. (2008). "Endothelial expression of  $\beta 1$  integrin is required for embryonic vascular patterning and postnatal vascular remodeling." Molecular and Cellular Biology **28**: 794-802.



- Li, J.-M., A. Mullen, et al. (2002). "Essential role of the NADPH oxidase subunit p47<sup>phox</sup> in endothelial cell superoxide production in response to phorbol esters and tumor necrosis factor- $\alpha$ ." Circulation Research **90**: 143-150.
- Li, J., M. Stouffs, et al. (2006). "The NADPH oxidase NOX4 drives cardiac differentiation: role in regulating cardiac transcription factors and MAP kinase activation." Molecular Biology of the Cell **17**: 3978-3988.
- Lim, C., C. Zuppinger, et al. (2004). "Anthracyclines induce calpain-dependent titin proteolysis and necrosis in cardiomyocytes." The Journal of Biological Chemistry **279**: 8290-8299.
- Lin, A. (2002). "Activation of the JNK signaling pathway: breaking the brake on apoptosis." Bio Essays **25**: 17-24.
- Liochev, S. I. and I. Fridovich (2000). "Copper- and Zinc-containing superoxide dismutase can act as a superoxide reductase and a superoxide oxidase." Journal of Biological Chemistry **275**: 38482-38485.
- Liochev, S. I. and I. Fridovich (2002). "Copper, zinc superoxide dismutase and H<sub>2</sub>O<sub>2</sub>." The Journal of Biological Chemistry **277**: 34674-34678.
- Lodish, H., A. Berk, et al. (2008). Integrating cells into tissues. Molecular Cell Biology: 801-846.
- Loike, J. D., B. Sodeik, et al. (1991). "CD11c/CD18 on neutrophils recognizes a domain at the N terminus of the A $\alpha$  chain of fibrinogen." The Proceedings of the National Academy of Sciences USA **88**: 1044-1048.
- Looi, Y. H., D. J. Grieve, et al. (2008). "Involvement of Nox2 NADPH oxidase in adverse cardiac remodeling after myocardial infarction." Hypertension **51**: 319-325.
- Luo, B.-H. and T. A. Springer (2006). "Integrins structures and conformational signaling." Current Opinion in Cell Biology **18**: 579-586.
- Lyle, A. N. and K. K. Griendling (2006). "Modulation of vascular smooth muscle signaling by reactive oxygen species." Physiology **21**: 269-280.
- MacKenna, D., S. R. Summerour, et al. (2000). "Role of mechanical factors in modulating cardiac fibroblast function and extracellular matrix synthesis." Cardiovascular Research **46**: 257-263.
- Mackey, A. M., N. Sanvicens, et al. (2008). "Redox survival signalling in retina-derived 661W cells." Cell Death and Differentiation **15**: 1291-1303.
- Maitra, N., I. L. Flink, et al. (2000). "Expression of  $\alpha$  and  $\beta$  integrins during terminal differentiation of cardiomyocytes." Cardiovascular Research **47**: 715-725.
- Maraldi, T., C. Prata, et al. (2009). "NAD(P)H oxidase isoform Nox2 plays a prosurvival role in human leukaemia cells." Free Radical Research **43**: 1111-1121.
- Maraldi, T., C. Prata, et al. (2009). "Induction of apoptosis in human leukemic cell line via reactive oxygen species modulation by antioxidants." Free Radical Biology & Medicine **46**: 244-252.
- Martin, G. R. and R. Timpl (1987). "Laminin and other basement membrane components." Annual Review of Cell Biology **3**: 57-85.
- Martyn, K. D., L. M. Frederick, et al. (2006). "Functional analysis of Nox4 reveals unique characteristics compared to other NADPH oxidases." Cellular Signalling **18**: 69-82.
- Masters, J. R. and G. N. Stacey (2007). "Changing medium and passaging cells." Nature Protocols **2**: 2276-2284.
- Matés, J. M. (2000). "Effects of antioxidant enzymes in the molecular control of reactive oxygen species toxicology." Toxicology **153**: 83-104.
- Matsui, T., T. Nagoshi, et al. (2003). "Akt and PI3-kinase signaling in cardiomyocyte hypertrophy and survival." Cell Cycle **2**: 220-223.
- Maytin, M., D. A. Siwik, et al. (2004). "Pressure overload-induced myocardial hypertrophy in mice does not require gp91<sup>phox</sup>." Circulation **109**: 1168-1171.
- McCord, J. M. and I. Fridovich (1969). "Superoxide dismutase." The Journal of Biological Chemistry **244**: 6049-6055.
- McDonald, J. A. (1989). "Receptors for extracellular matrix components." American Journal of Physiology **257**: L331-L337.

- Mehdi, M. Z., Z. M. Azar, et al. (2007). "Role of receptor and nonreceptor protein tyrosine kinases in H<sub>2</sub>O<sub>2</sub>-induced PKB and ERK1/2 signaling." *Cell Biochemistry and Biophysics* **47**: 1-10.
- Menon, B., J. Johnson, et al. (2007). "Glycogen synthase kinase-3 $\beta$  plays a pro-apoptotic role in  $\beta$ -adrenergic receptor-stimulated apoptosis in adult rat ventricular myocytes: role of  $\beta$ 1-integrin." *Journal of Molecular and Cellular Cardiology* **42**: 653-661.
- Menon, B., M. Singh, et al. (2005). " $\beta$ -adrenergic receptor-stimulated apoptosis in adult cardiac myocytes involves MMP2-mediated disruption of  $\beta$ 1 integrin signaling and mitochondrial pathway." *American Journal of Physiology Cell Physiology* **290**: 254-261.
- Meredith, J., B. Fazeli, et al. (1993). "The extracellular matrix as a cell survival factor." *Molecular Biology of Cell* **4**: 953-961.
- Miner, E. C. and W. L. Miller (2006). "A look between cardiomyocytes: the extracellular matrix in heart failure." *Mayo Clinic Proceedings* **81**: 71-76.
- Mishina, N. M., P. A. Tyurin-Kuzmin, et al. (2011). "Does cellular hydrogen peroxide diffuse or act locally?" *Antioxidants & Redox Signaling* **14**: 1-7.
- Mülhardt, C. (2008). *Der Experimentator: Molekularbiologie/Genomics*, Spektrum Akademischer Verlag.
- Nakano, H., A. Nakajima, et al. (2006). "Reactive oxygen species mediate crosstalk between NF $\kappa$ B and JNK." *Cell Death and Differentiation* **13**: 730-737.
- Nauseef, W. M. (2004). "Assembly of the phagocyte NADPH oxidase." *Histochemistry and Cell Biology* **122**: 277-291.
- O'Donell, V. B. and A. Azzi (1996). "High rates of extracellular superoxide generation by cultured human fibroblasts: involvement of a lipid-metabolizing enzyme." *Biochemical Journal* **318**: 805-812.
- O'Neill, E. W., D. Matallanas, et al. (2005). "Mammalian sterile 20-like kinases in tumor suppression: an emerging pathway." *Cancer Research* **65**: 5485-5487.
- Oakley, F. D., D. Abbott, et al. (2009). "Signaling components of redox active endosomes: the redoxosomes." *Antioxidants & Redox Signaling* **11**: 1313-1333.
- Okamura, N., B. M. Babior, et al. (1990). "The p67-*phox* cytosolic peptide of the respiratory burst oxidase from human neutrophils." *Journal of Clinical Investigation* **85**: 1583-1587.
- Olson, E. N. (2004). "A decade of discoveries in cardiac biology." *Nature Medicine* **10**: 467-474.
- Pendayala, S., I. Gorshkova, et al. (2009). "Role of Nox4 and Nox2 in hyperoxia-induced reactive oxygen species generation and migration of human lung endothelial cells." *Antioxidants & Redox Signaling* **11**: 747-764.
- Peng, T., X. Lu, et al. (2005). "Pivotal role of gp91<sup>phox</sup>-containing NADH oxidase in lipopolysaccharide-induced tumor necrosis factor- $\alpha$  expression and myocardial depression." *Circulation* **111**: 1637-1644.
- Petry, A., T. Djordjević, et al. (2006). "NOX2 and NOX4 mediate proliferative responses in endothelial cells." *Antioxidants & Redox Signaling* **8**: 1473-1484.
- Petry, A., M. Weitnauer, et al. (2010). "Receptor activation of NADPH oxidases." *Antioxidants & Redox Signaling* **13**: 467-487.
- Plow, E. F., T. A. Haas, et al. (2000). "Ligand binding to integrins." *Journal of Biological Chemistry* **275**: 21785-21788.
- Pope, A., G. Sands, et al. (2008). "Three-dimensional transmural organization of permysal collagen in the heart." *American Journal of Physiology Heart & Circulatory Physiology* **295**: H1243-H1252.
- Qin, F., R. Patel, et al. (2006). "NADPH oxidase is involved in angiotensin II-induced apoptosis in H9C2 cardiac muscle cells: effects of apocynin." *Free Radical Biology & Medicine* **40**: 236-246.
- Quinn, M. T., M. C. B. Ammons, et al. (2006). "The expanding role of NADPH oxidases in health and disease: no longer just agents of death and destruction." *Clinical Science* **111**: 1-20.
- Raad, H., M.-H. Paclet, et al. (2009). "Regulation of the phagocyte NADPH oxidase activity: phosphorylation of gp91<sup>phox</sup>/NOX2 by protein kinase C enhances diaphorase activity and binding to Rac2, p67<sup>phox</sup>, and p47<sup>phox</sup>." *The FASEB Journal* **23**: 1011-1022.

- Rehm, H. (2002). Der Experimentator: Proteinbiochemie/Proteomics, Spektrum-Akademischer Verlag.
- Reinhard, C., B. Shamon, et al. (1997). "Tumor necrosis factor  $\alpha$ -induced activation of c-jun N-terminal kinase is mediated by TRAF2." The EMBO Journal **16**: 1080-1092.
- Rhee, S. (2006). "H<sub>2</sub>O<sub>2</sub>, a necessary evil for cell signaling." Science **312**: 1882-1883.
- Rhee, S. G. (1999). "Redox signaling: hydrogen peroxide as intracellular messenger." Experimental and Molecular Medicine **31**: 53-59.
- Ristow, M., K. Zarse, et al. (2009). "Antioxidants prevent health-promoting effects of physical exercises in humans." The Proceedings of the National Academy of Sciences USA **106**: 8665-8670.
- Robinson, T. F., S. M. Factor, et al. (1987). "Morphology, composition, and function of struts between cardiac myocytes of rat and hamster." Cell and Tissue Research **249**: 247-255.
- Rocco, M., C. Rosano, et al. (2008). "Integrin conformational regulation: uncoupling extension/tail separation from changes in the head region by a multiresolution approach." Structure **16**: 954-964.
- Rojas, A. I. and A. R. Ahmed (1999). "Adhesion receptors in health and disease." Critical Reviews in Oral Biology & Medicine **10**: 337-358.
- Ross, R. (2002). "The extracellular connections: the role of integrins in myocardial remodeling." Journal of Cardiac Failure **8**: S326-S331.
- Ross, R., C. Pham, et al. (1998). " $\beta_1$  integrins participate in the hypertrophic response of rat ventricular myocytes." Circulation Research **82**: 1160-1172.
- Ross, R. S. and T. K. Borg (2001). "Integrins and the myocardium." Circulation Research **88**: 1112-1119.
- Rosse, C., M. Linch, et al. (2010). "PKC and the control of localized signal dynamics." Nature Reviews Molecular Cell Biology **11**: 103-112.
- Ruoslahti, E. and M. D. Pierschbacher (1987). "New perspectives in cell adhesion: RGD and integrins." Science **238**: 491-497.
- Sawyer, D., D. Siwik, et al. (2002). "Role of oxidative stress in myocardial hypertrophy and failure." Journal of Molecular and Cellular Cardiology **34**: 379-388.
- Sbarra, A. J. and M. L. Karnovsky (1959). "The biochemical basis of phagocytosis." The Journal of Biological Chemistry **234**: 1355-1362.
- Schaller, M. D., J. D. Hildebrand, et al. (1994). "Autophosphorylation of the focal adhesion kinase, pp125<sup>FAK</sup>, directs SH2-dependent binding of pp60<sup>src</sup>." Molecular and Cellular Biology **14**: 1680-1688.
- Schlessinger, J. (1997). "Direct binding and activation of receptor tyrosine kinases by collagen." Cell **91**: 869-872.
- Schwartz, M. A. (2010). "Remembrance of dead cells past: discovering that the extracellular matrix is a cell survival factor." Molecular Biology of the Cell **21**: 499-500.
- Scuteri, A., A. Galimberti, et al. (2010). "NGF protects dorsal root ganglion neurons from oxaliplatin by modulating JNK/SapK and ERK1/2." Neuroscience Letters **486**: 141-145.
- Segal, A. W. and K. P. Shatwell (1997). "The NADPH oxidase of phagocytic leukocytes." Annals of New York Academy of Sciences **832**: 215-222.
- Seibenhener, M. L., J. Roehm, et al. (1999). "Identification of Src as a novel atypical protein kinase C-interacting protein." Molecular Cell Biology Research Communications **2**: 28-31.
- Serrander, L., L. Cartier, et al. (2007). "NOX4 activity is determined by mRNA levels and reveals a unique pattern of ROS generation." Biochemical Journal **406**: 105-114.
- Shai, S.-Y., A. E. Harpf, et al. (2002). "Cardiac myocyte-specific excision of the  $\beta_1$  integrin gene results in myocardial fibrosis and cardiac failure." Circulation Research **90**: 458-464.
- Shimaoka, M., J. Takagi, et al. (2002). "Conformational regulation of integrin structure and function." Annual Reviews Biophysical and Biomolecular Structure **31**: 485-516.
- Siwik, D. A., J. D. Tzortzis, et al. (1999). "Inhibition of copper-zinc superoxide dismutase induces cell growth, hypertrophic phenotype, and apoptosis in neonatal cardiac myocytes in vitro." Circulation Research **85**: 147-153.

- Smith Jr., S. C., R. Jackson, et al. (2004). "Principles for national and regional guidelines on cardiovascular disease prevention." *Circulation* **109**: 3112-3121.
- Spinale, F. G. (2002). "Matrix metalloproteinases: regulation and dysregulation in the failing heart." *Circulation Research* **90**: 520-530.
- Springhorn, J. and W. Claycomb (1989). "Preproenkephalin mRNA expression in developing rat heart and in cultured ventricular cardiac muscle cells." *Biochemical Journal* **258**: 73-78.
- Srivastava, D. and E. N. Olson (2000). "A genetic blueprint for cardiac development." *Nature* **407**: 221-226.
- Sugden, S., S. Fuller, et al. (2008). "Glycogen synthase kinase 3 (GSK3) in the heart: a point of integration in hypertrophic signalling and a therapeutic target? A critical analysis." *British Journal of Pharmacology* **153**: S137-S153.
- Taddei, M. L., M. Parri, et al. (2007). "Integrin-mediated cell adhesion and spreading engage different sources of reactive oxygen species." *Antioxidants & Redox Signaling* **9**: 469-481.
- Takada, Y., X. Ye, et al. (2007). "The integrins." *Genome Biology* **8**: 215.1-215.9.
- Terracio, L., K. Rubin, et al. (1991). "Expression of collagen binding integrins during cardiac development and hypertrophy." *Circulation Research* **68**: 734-744.
- Thaik, C., A. Calderone, et al. (1995). "Interleukin-1b modulates the growth and phenotype of neonatal rat cardiac myocytes." *Journal of Clinical Investigation* **96**: 1093-1099.
- Toledano, M. B., A.-G. Planson, et al. (2010). "Reining in H<sub>2</sub>O<sub>2</sub> for safe signaling." *Cell* **140**: 454-456.
- Touyz, R. M. and E. L. Schiffrin (1999). "Ang II-stimulated superoxide production is mediated via phospholipase D in human vascular smooth muscle cells." *Hypertension* **34**: 976-982.
- Trachootham, D., W. Lu, et al. (2008). "Redox regulation of cell survival." *Antioxidants & Redox Signaling* **10**: 1343-1374.
- Ueyama, T., T. Kusakabe, et al. (2008). "Sequential binding of cytosolic phox complexes to phagosomes through regulated adaptor proteins: evaluation using the novel monomeric Kusabira-green system and life imaging of phagocytosis." *The Journal of Immunology* **181**: 629-640.
- Uhlinger, D. J., K. L. Taylor, et al. (1994). "p67-phox enhances the binding of p47-phox to the human neutrophil respiratory burst oxidase complex." *The Journal of Biological Chemistry* **269**: 22095-22098.
- Ushio-Fukai, M. (2006). "Localizing NADPH oxidase-derived ROS." *Science STKE* **re8**.
- Ushio-Fukai, M. (2009). "Compartmentalization of redox signaling through NADPH oxidase-derived ROS." *Antioxidants & Redox Signaling* **11**: 1289-1299.
- Ushio-Fukai, M., R. W. Alexander, et al. (1999). "Reactive oxygen species mediate the activation of Akt/protein kinase B by angiotensin II in vascular smooth muscle cells." *The Journal of Biological Chemistry* **274**: 22699-22704.
- Van der Flier, A., A. C. Gaspar, et al. (1997). "Spatial and temporal expression of the  $\beta$ 1D integrin during mouse development." *Developmental Dynamics* **210**: 472-486.
- Van der Flier, A. and A. Sonnenberg (2001). "Function and interactions of integrins." *Cell Tissue Research* **305**: 285-298.
- Velling, T., S. Nilsson, et al. (2004). " $\beta$ 1-integrins induce phosphorylation of Akt on serine 473 independently of focal adhesion kinase and Src family kinases." *EMBO reports* **5**: 901-905.
- Vignais, P. V. (2002). "The superoxide-generating NADPH oxidase: structural aspects and activation mechanism." *Cellular and Molecular Life Sciences* **59**: 1428-1459.
- Vowells, S. J., S. Sekhsaria, et al. (1995). "Flow cytometric analysis of the granulocyte respiratory burst: a comparison study of fluorescent probes." *Journal of Immunological Methods* **178**: 89-97.
- Wang, G., T. Hamid, et al. (2010). "Cardioprotective and antapoptotic effects of heme oxygenase-1 in the failing heart." *Circulation* **121**: 1912-1925.
- Wang, L., H.-J. Yang, et al. (2010). "Insulin like growth factor 1 protects human neuroblastoma cells SH-EP1 against MPP+-induced apoptosis by Akt/GSK-3 $\beta$ /JNK signaling." *Apoptosis* **15**: 1470-1479.

- Weber, K. (1989). "Cardiac interstitium in health and disease: the fibrillar collagen network." Journal of the American College of Cardiology **13**: 1637-1652.
- Weber, K. and C. Brilla (1991). "Pathological hypertrophy and cardiac interstitium." Circulation **83**: 1849-1865.
- Weber, K., Y. Sun, et al. (1994). "Collagen network of the myocardium: function, structural remodeling and regulatory mechanisms." Journal of Molecular & Cellular Cardiology **26**: 279-292.
- Wegener, K. L. and I. D. Campbell (2008). "Transmembrane and cytoplasmic domains in integrin activation and protein-protein interactions." Molecular Membrane Biology **25**: 376-387.
- Xiang, F., Y. Sakata, et al. (2006). "Transcription factor CHF1/Hey2 suppresses cardiac hypertrophy through an inhibitory interaction with GATA4." American Journal of Physiology- Heart & Circulatory Physiology **290**: 1997-2006.
- Xiao, L., D. Pimentel, et al. (2002). "Role of reactive oxygen species and NAD(P)H oxidase in  $\alpha_1$ -adrenoreceptor signaling in adult rat cardiac myocytes." American Journal of Physiology Cell Physiology **282**: C926-C934.
- Xiong, J.-P., T. Stehle, et al. (2003). "New insights into the structural basis of integrin activation." Blood **102**: 1155-1159.
- Zaidel-Bar, R., S. Itzkovitz, et al. (2007). "Functional atlas of the integrin adhesome." Nature Cell Biology **9**: 858-867.
- Zhang, M., A. C. Brewer, et al. (2010). "NADPH oxidase-4 mediates protection against chronic load induced stress in mouse hearts by enhancing angiogenesis." The Proceedings of the National Academy of Sciences USA **107**: 18121-18126.
- Zhang, Z., K. Vuori, et al. (1995). "The  $\alpha_5\beta_1$  integrin supports survival of cells on fibronectin and up-regulates Bcl-2 expression." The Proceedings of the National Academy of Sciences USA **92**: 6161-6165.
- Zwacka, R., W. Zhou, et al. (1998). "Redox gene therapy for ischemic/reperfusion of the liver reduces AP1 and NF $\kappa$ B activation." Nature Medicine **4**: 698-704.

## 8.) ACKNOWLEDGEMENTS

I thank Dr Gabriela Kuster Pfister for the great experience and the challenge to work in the field of cardiac cell biology. I would like thank Prof. Markus Rüegg and Prof. Karl Hofbauer for taking part in the thesis committee and their critical comments and questions. Likewise, I thank Prof. Ruth Chiquet-Ehrismann for chairing my thesis committee.

Furthermore I thank Prof. Marijke Brink for asking stimulating and critical questions at meetings.

I also would like to thank the following people (in alphabetical order) for a helping hand, stopping the elevator, a smile for the day, apéros, a PC, good discussions, critical thoughts and scientific help, providing antibodies or primers as well as all kinds of chemicals or tools, for the help with FlowJo, the flow cytometer, the knock-out mice, support in talks, joint meetings, stopping by for a coffee or lunch together, for cake or a glass of wine, being listener in phases when experiments did not work at all and when the challenges seemed too much to take.

Lena Angmann, Roberto Brera, Kathrin Bühler , Kaethi Dembinski, Frederique Doublouz; Federica Facciotti, Maria Filippova, Steffi Fritz, Jean Grisouard, Stéphanie Häuselmann, Heike Himmelreich, Heidi Hoyer mann, Roc Humar, Vreni Jäggin, Linde John, Vera Lorenz; Silvia Meili Butz, Karolin Möller; Christian Morandi, Lucia Mori De Liebero; Ottmar Pfister, Isabelle Plaisance, Tanja Radimerski; Pankaj Shende; Gaby Zenhäusern; Ueli Schneider and team, Kseniya Maslova, Emanuelle Traunecker, and all those I probably forgot to mention here.

I specially want to thank Hiroko Asano, Alex Boyko, Alok Gupta, Ueli Grosniklaus, Monica and Skip Schauer; Meret Huber and Shuqing Xu, Sara Manafzadeh and Yannick Städler, Simone & Florian Schiestl for sophisticated and motivating chats, for having a good time at apéros, BBQ, fondue (meat), dinner parties or simply sitting together; and for always being welcome at Ueli's partys and lab outings.

Furthermore, I would like to thank my parents, who from childhood on thought me to ask difficult questions and for encouraging me in my interest in natural sciences. Right from the beginning, they challenged me as a biologist, having to identify *Picea* and *Abies*.

Finally I would like to express my gratitude to my greatly beloved Philipp, who always supported me in every situation, personally and scientifically. He always encouraged me to follow my way in times I thought I would lose it. I thank him for his critical advice, for keeping the “Schmäh”, picking me from the station whenever experiments ran very late, and for making it possible to work out scientific questions.

## 9.) CURRICULUM VITAE

### PERSONAL DATA:

Name: Berit Ines Rosc-Schlüter  
Academic degree: Mag. rer. nat. (Graz, 2006)  
Date of birth: 23. 09. 1977  
Place of birth: Graz, Austria  
Nationality: Austrian  
Marital status: Married

### EDUCATION:

1992-1996: BORG (grammar school; natural sciences) in Deutschlandsberg, Austria  
June 1996: University entrance qualification (Matura)  
1996-2000: Studies of Biology in Graz with intermission  
2000-2006: Studies of Microbiology at the University and Technical University in Graz with intermission  
2003-2006: Advanced courses and practicals in immunology, oncology and genetics at the Medical University of Vienna and at the University of Vienna  
04 2004-04 2005: Diploma thesis in immunology (funded via a BMT research grant) at the Medical University of Vienna: *Induction and regulation of innate, antimicrobial defence mechanisms in phagocytes*. Advisor: Prof. Johannes Stöckl  
02.2007-01.2011 PhD studies at the Department of Biomedicine at the University and University Hospital of Basel: *NADPH oxidase (NOX) in the heart: The interplay of NOX-derived ROS and  $\beta_1$ -integrin-induced survival signalling in the heart*. Advisor: Dr. med. Gabriela M. Kuster



### PUBLICATIONS:

S. Blüml, **B. Rosc**, A. Lorincz, M. Seyerl, S. Kirchberger, O. Oskolkova, V. N. Bochkov, O. Majdic, E. Ligeti, J. Stöckl; *The oxidation state of phospholipids controls the oxidative burst in neutrophil granulocytes*; *The Journal of Immunology*, 2008, 181; 4347-4353

Gabriela M. Kuster, Stéphanie P. Häuselmann, **Berit I. Rosc-Schlüter**, Vera Lorenz, and Otmar Pfister; *Reactive oxygen/ nitrogen species and the myocardial cell homeostasis: an ambiguous relationship*; *Antioxidants & Research Signaling*, 2010, 13; 1899-1910

### MANUSCRIPTS SUBMITTED AND IN PREPARATION:

**B. I. Rosc-Schlüter**, S. P. Häuselmann, V. Lorenz, F. Facciotti, O. Pfister; G. M. Kuster; *NOX2-derived reactive oxygen species are crucial for CD29-induced pro-survival signaling in cardiomyocytes. in prep.*

S. P. Häuselmann, **B. I. Rosc-Schlüter**, V. Lorenz, I. Plaisance, M. Brink, O. Pfister and G. M. Kuster;  *$\beta$ 1-Integrin is up-regulated via Rac1-dependent reactive oxygen species as part of the hypertrophic cardiomyocyte response*; submitted to *Free Radical Biology and Medicine*.

### ORAL PRESENTATIONS:

**B. I. Rosc-Schlüter**, S. P. Häuselmann, V. Lorenz, F. Facciotti, L. Mori De Libero, O. Pfister, G. M. Kuster; **SGK-Lausanne (freie Mitteilungen) June 2009**; *Beta1-integrin-mediated pro-survival signalling depends on NOX2-derived reactive oxygen species*;

**B. I. Rosc-Schlüter**, S. P. Häuselmann, V. Lorenz, F. Facciotti, L. Mori De Libero, O. Pfister and G. M. Kuster; **Cardiovascular Biology and Clinical Implications Meeting, Muntelier October 2009**; *Beta1-integrin-mediated anti-apoptotic signalling depends on NOX2-derived reactive oxygen species*;

**B. I. Rosc-Schlüter**, S. P. Häuselmann, V. Lorenz, F. Facciotti, O. Pfister, G. M. Kuster; **Kardiologie Assistenten Journal Club, University Hospital Basel, September 2010**; *Reactive Oxygen Species: Getting to the heart of the matter*;

### POSTER PRESENTATIONS:

**B. I. Rosc**, S. Blüml, V. Bochkov, O. Majdic, J. Stöckl; *Phospholipids novel regulators of human phagocyte functions*; Annual Meeting of the Austrian Society for Allergy and Immunology (ÖGAI), Graz, Austria, **2005**

**B. I. Rosc-Schlüter**, S. P. Häuselmann, V. Lorenz, F. Facciotti, L. Mori De Libero, O. Pfister, G. M. Kuster; *Beta 1 integrin induced anti-apoptotic signalling requires NOX2 derived reactive oxygen species*; Heart Failure Congress, Nice, France, **2009**

**B. I. Rosc-Schlüter**, S. P. Häuselmann, V. Lorenz, F. Facciotti, L. Mori De Libero, O. Pfister, G.M Kuster;  
*NOX2-derived ROS play a key role in beta1-integrin-induced pro-survival signalling*; Biovalley Life  
Science Week 2009; Basel, 13<sup>th</sup> - 16<sup>th</sup> October **2009**

